

8-29-2010

Size optimization of an off-grid hybrid renewable energy system for different amounts of resources and demands

Alvaro Zanon Alonso
Santa Clara University

Follow this and additional works at: https://scholarcommons.scu.edu/mech_mstr

Recommended Citation

Alonso, Alvaro Zanon, "Size optimization of an off-grid hybrid renewable energy system for different amounts of resources and demands" (2010). *Mechanical Engineering Master's Theses*. 29.
https://scholarcommons.scu.edu/mech_mstr/29

This Thesis is brought to you for free and open access by the Engineering Master's Theses at Scholar Commons. It has been accepted for inclusion in Mechanical Engineering Master's Theses by an authorized administrator of Scholar Commons. For more information, please contact rscroggin@scu.edu.

**Size optimization of an off-grid hybrid renewable energy
system for different amounts of resources and demands**

By

Alvaro Zanon Alonso

MASTERS THESIS

Submitted in Partial Fulfillment of the Requirements

for the Degree of Masters of Science

in Mechanical Engineering

School of Engineering

Santa Clara University

Santa Clara, California

August 29, 2010

Dedicated To My Nephew, Jesus Mozas Zanon

Born March 11, 2010

Acknowledgements

First, I would like to thank my advisor, Professor Lee, for his guidance and advice throughout not only this thesis, but also throughout my last year at Santa Clara University, both on the academic and personal level. Also I'd like to thank Professor Ayoubi for introducing me to the optimization techniques applied to renewable systems.

Thanks to Kyle Pistor for his advice and suggestions during some parts of my thesis, and for attending my presentations.

The success of this work would not have been possible without the love and support of my family and girlfriend. They were the inspiration and motivation that helped me carry on throughout my thesis

Size optimization of an off-grid hybrid renewable energy system for different amounts of resources and demands

Alvaro Zanon Alonso

Department of Mechanical Engineering

Santa Clara University

Santa Clara, California

2010

ABSTRACT

Hybrid renewable systems represent a very reliable and economical solution to the energy supply problem for stand-alone applications. The purpose of this thesis is to analyze the relationship between the size of such systems and the amount of renewable resources available to them. Moreover, the results will identify which components of the system have a greater energy contribution as the amount of resources change.

The optimum size of a stand-alone hybrid renewable energy system was investigated over the possible ranges of insolation and wind speed in the United States. This system includes an array of photovoltaic (PV) panels, a set of wind turbines, an AC diesel generator, a bank of lead-acid batteries and an inverter. In order to evaluate the performance of this system, an AC electricity demand ranging from 10 to 100 kW peak power demand was modeled. This range was selected to describe the energy needs of most residential communities, businesses and small industrial applications. The system was optimized in HOMER by finding its minimum lifecycle cost for every combination of insolation, wind speed and peak electricity demand values.

The first results served as a validation of the expected outcome; an increase in either insolation or wind speed translated into a larger amount of energy produced by the PV array or the wind park, respectively. However, the increase in solar energy is achieved through an increase of the PV array size, whereas the increase in wind energy is accomplished using less wind turbines. The reason is that the power produced by the PV panels has a nearly proportional dependence on the amount of insolation striking them and thus, more PV panels are required to produce a larger amount of energy as insolation increases. On the other hand, the power produced by the wind turbines is directly proportional to the cube of the wind speed. This explains why as the wind speed increases, a smaller number of wind turbines will produce a larger amount of energy.

Another important result was derived by evaluating the system under very high or very low renewable resources. When very low insolation and wind speed values are available, the contribution of PV panels is greater than that of wind turbines. Conversely, with very high insolation and wind speed values, the main contribution to the system is provided by the wind turbines. The reason is that below 3.5 – 4 m/s wind speed, turbines will not typically start moving, and the only active renewable components of the system are the solar panels. With high insolation and wind speed values, the first results showed an increased performance of the wind turbines versus the PV panels.

The results for the lowest insolation and wind speed values also showed that neither PV panels nor wind turbines are capable of producing a great amount of energy. A small inverter size revealed that most of the energy was delivered in AC by the diesel generator, which works as the main source of energy for the system. The diesel generator produces electricity only when demanded by the loads. Therefore, when the generator is being used extensively, very little energy needs to be stored in the batteries for a later use. This explains the small size of the battery bank in the optimum system. Under very high insolation and wind speed values, wind turbines have a bigger contribution than PV panels in the optimum system. In fact, since wind is available during the most part of the day, more energy is readily available and a large diesel generator is not required to cover peaks in the electricity demand. In this case, the diesel generator acts as a back-up source of energy for the system.

Finally, an estimate of the optimal lifecycle and initial costs of system was provided. It was observed that as the amount of insolation and wind speed increases, both costs decrease following an almost linear trend for most of the cases.

Keywords: Hybrid renewable energy systems; Optimum system size; Stand-alone system; Renewable resources dependency; Lifecycle cost; Initial cost.

TABLE OF CONTENTS

Chapter 1

INTRODUCTION	1
<hr/>	
1.1 The Need for Hybrid Renewable Systems	1
1.2 Project Statement	4
1.3 Reader's Guide	6

Chapter 2

AVAILABILITY OF ENERGY RESOURCES	9
<hr/>	
2.1 The Solar Resource	9
2.2 The Wind Resource	13
2.3 The Diesel Resource	19
2.4 Parameters Used in the Calculations	20

Chapter 3

COMPONENTS OF THE HYBRID RENEWABLE SYSTEM	24
<hr/>	
3.1 Solar Photovoltaic Panels	24
3.2 Wind Turbines	29
3.3 Diesel Generator	34
3.4 Batteries	37
3.5 Inverter	39
3.6 Parameters Used in the Calculations	38

Chapter 4

DESCRIPTION OF THE ELECTRIC DEMAND	49
---	-----------

Chapter 5

THE OPTIMIZATION METHOD	53
--------------------------------	-----------

Chapter 6

GENERATION AND ANALYSIS OF RESULTS	61
---	-----------

6.1	System Size Dependence on the Insolation Intensity	62
-----	---	-----------

6.2	System Size Dependence on the Wind Speed Intensity	68
-----	---	-----------

6.3	System Size Dependence on the Electricity Demand	71
-----	---	-----------

6.4	Annual Energy Production by Each Component	77
-----	---	-----------

6.5	System Size Costs	87
-----	--------------------------	-----------

Chapter 7

CONCLUSIONS	91
--------------------	-----------

REFERENCES	95
-------------------	-----------

Appendix A

U.S. SOLAR AND WIND RESOURCE MAPS	98
--	-----------

Appendix B

ECONOMIC DESCRIPTION OF THE COMPONENTS

102

Appendix C

OPTIMIZATION RESULTS

107

LIST OF FIGURES

- Figure 1.1** Diagram of a hybrid energy system consisting of solar PV panels, wind turbines, a diesel generator and batteries.
- Figure 2.1** Spectral power density of sunlight outside the atmosphere. Plot obtained with the software SMARTS provided by NREL using the Gueymard 2004 method.
- Figure 2.2** Diagram representing the types of energy conversions which take place in a wind turbine.
- Figure 2.3** Probability density function of a Weibull distribution for different values of the shape parameter, k .
- Figure 2.4** Probability density function of a Weibull distribution with $k = 2$ for different values of the average wind speed, v_{avg} .
- Figure 2.5** A typical distribution of the average monthly values of wind speed for a given location.
- Figure 2.6** Diesel fuel price predictions by the U.S. Energy Information Administration (EIA) for the next 25 years.
- Figure 3.1** The band gap model used to describe the photovoltaic effect.
- Figure 3.2** Electrical circuit of a single real cell including parallel and series resistances.
- Figure 3.3** Effect on the I-V curve of changing either the series resistance (R_s) or the parallel resistance (R_p). Plot obtained for $I_0 = 10^{-10} A/cm^2$ and $I_{SC} = 0.045 A/cm^2$.
- Figure 3.4** Module I-V curve, Maximum Power Point (MPP) and Load curve for maximum power output.
- Figure 3.5** The main parts of a horizontal axis wind turbine (a) and a closer look-up to the mechanical elements inside the nacelle (b).

- Figure 3.6** Available power in the wind for a 10 m rotor diameter wind turbine and an air density of 1.25 kg/m³.
- Figure 3.7** Control volume used in the calculation of the Betz limit in a wind turbine.
- Figure 3.8** Fuel consumption curve of the diesel generator modeled in this thesis.
- Figure 3.9** Efficiency curve of the diesel generator modeled in this thesis.
- Figure 3.10** Lifetime curve. Effect of the Depth-of-Discharge on a deep-cycle, lead-acid battery lifetime.
- Figure 3.11** Battery capacity curve for a typical deep-cycle, lead-acid battery.
- Figure 3.12** Power curve of the Southwest Whisper 500 wind turbine.
- Figure 3.13** Slope curve of the diesel generator.
- Figure 3.14** Intercept coefficient curve of the diesel generator.
- Figure 4.1** Energy consumption by sectors in the United States. Transportation sector not included.
- Figure 4.2** Hourly electric demand modeled in this work for weekdays (a) and weekends (b).
- Figure 5.1** Simulation flow diagram used to compute the optimum size of the hybrid renewable system.
- Figure 5.2** Average annual insolation distribution considered in this thesis.
- Figure 5.3** Average annual wind speed distribution considered in this thesis.
- Figure 6.1** Diagram of the optimization technique followed in the generation of results.
- Figure 6.2** The results window displayed in HOMER after each simulation.
- Figure 6.3** PV array size versus insolation intensity for different wind speeds and for a 50 kW peak electricity demand.

- Figure 6.4** Number of wind turbines versus insolation values for different wind speeds and for a 50 kW peak electricity demand.
- Figure 6.5** Number of batteries versus wind speed for different insolation values and for a 50 kW peak electricity demand.
- Figure 6.6** PV array size versus wind speed for different insolation values and for a 50 kW peak electricity demand.
- Figure 6.7** Number of wind turbines versus wind speed for different insolation values and for a 50 kW peak electricity demand.
- Figure 6.8** PV array size versus peak electricity demand for different insolation values and for a 6 m/s wind speed location.
- Figure 6.9** Number of wind turbines versus peak electricity demand for different insolation values and for a 6 m/s wind speed location.
- Figure 6.10** Generator size versus peak electricity demand for different insolation values and for a 6 m/s wind speed location.
- Figure 6.11** PV array size versus peak electricity demand for different wind speeds and for a 5.5 kWh/m²/day insolation intensity location.
- Figure 6.12** Number of wind turbines versus peak electricity demand for different insolation values and for a 6 m/s wind speed location.
- Figure 6.13** Annual energy generation versus availability of wind speed. Results shown for a 50 kW peak demand system under an average insolation of 5.5 kWh/m²/day.
- Figure 6.14** Quantitative and percentage of annual energy production by component versus availability of wind. Results shown for a 50 kW peak demand system with an average insolation of 5.5 kWh/m²/day.
- Figure 6.15** Annual energy stored in the batteries versus wind speed values.
- Figure 6.16** Annual energy generation versus the available insolation. Results shown for a 50 kW peak demand system under an average wind speed of 6 m/s.

- Figure 6.17** Quantitative and percentage of annual energy production by component versus availability of insolation. Results shown for a 50 kW peak demand system with an average wind speed of 6 m/s.
- Figure 6.18** Annual energy stored in the batteries versus insolation values.
- Figure 6.19** Relationship between the annual energy generated by wind turbines and solar panels as a function of the amount of available resources.
- Figure 6.20** Net present value dependence on the amount of renewable resources available for the 50 kW peak electricity demand system.
- Figure 6.21** Initial costs dependence on the amount of renewable resources available for the 50 kW peak electricity demand system.

LIST OF TABLES

- Table 2.1** Roughness length values for different terrain types.
- Table 2.2** Average geographical parameters of the United States.
- Table 2.3** Parameters used in the calculation of the hourly distribution of the wind speed.
- Table 3.1** Parameters used in the description of the PV panels.
- Table 3.2** Technical specifications of the Southwest Whisper 500 wind turbine.
- Table 3.3** Parameters of the Trojan L16P battery used in this work.
- Table 3.4** Parameters of the true sine wave inverter.
- Table 4.1** Evaluation of the energy supply capacity for the described 50 kW peak demand load profile in the United States with the same total consumption of 627 kWh/day.
- Table 6.1** Optimization results for the 50 kW peak demand system. Results shorted by insolation values for each wind speed.
- Table 6.2** Optimization results for the 50 kW peak demand system. Results shorted by wind speed values for each insolation intensity value.
- Table 6.3** Optimization results for a 6 m/s fixed wind speed. Results shorted by peak electricity demand for each insolation intensity value.
- Table 6.4** Optimization results for a 5.5 kWh/m²/day fixed insolation value. Results shorted by peak electricity demand for each wind speed.
- Table 6.5** Annual energy production of each component for the 50 kW peak demand system. Results sorted to show their dependency on the availability of renewable resources.
- Table 6.6** Relevant costs of the 50 kW peak electricity demand system versus the amount of available resources.

1. INTRODUCTION

According to Paul Davidson [1], there were around 180,000 families living off-grid in the United States as of April 2006. This number may not seem alarmingly high, but the author also reported that a 33% yearly increase was observed during the last decade. Assuming the same growth rate, there would be more than half a million households living off-grid as of 2010 in the United States. The switch to an off-grid lifestyle can be explained by several reasons including environmental, political and/or financial as the predominant ones. While the residential sector only represents about $\frac{1}{4}$ of the overall energy consumption in the United States, the commercial and industrial sectors are also susceptible of benefiting from an off-grid energy system. This fact calls for the design of efficient and economic off-grid energy systems. A relatively new approach to this problem is the use of hybrid renewable systems, a system combining two or more energy generation systems. The characteristics of such systems and their optimum configuration represent the focus of this thesis.

1.1. THE NEED FOR HYBRID RENEWABLE SYSTEMS

General principle of holism:

“The whole is more than the sum of its parts” (Aristotle, “Metaphysics”)

The traditional approach to the energy supply in stand-alone systems using renewable sources of energy is the use of solar photovoltaic (PV) panels. An array of PV panels is used to collect and/or store the energy from the sun during the day time. When the solar installation is connected to the utility grid, peaks in electricity demand can be covered by using grid electricity. For an off-grid system, however, peaks in electricity demand need to be covered by the batteries and thus, the battery bank needs to be oversized, which increases the system cost significantly.

Other popular alternatives are wind turbines or fuel generators. Most wind turbines will not start generating electricity until the wind speed reaches a minimum value (usually around 3 – 5 m/s). Moreover, wind is quite variable and does not always blow with the same intensity. Therefore, they share the same problem with solar panels: wind turbines need an additional energy storage system. Fuel generators represent an economical alternative for stand-alone systems with a low to medium usage. When these systems are expected to be used in a regular basis, i.e. as the main source of energy, the operating costs increase significantly due to the cost of the fuels. In this case, the economical viability of installing a fuel generator needs to be further studied by predicting the future price of the fuel over the expected lifetime of the project.

In most part of the United States, the wind is stronger during the night time than during the day time, whereas the solar insolation reaches its peak in the middle of the day and it is inexistent at night. Furthermore, wind speeds are usually a bit higher during the winter and lower during the summer, just the opposite to the solar insolation. Therefore, because the peak operating times for PV panels and wind turbine systems occur at different times of the day and year, a PV/wind hybrid system represents a more reliable and economic alternative option than systems with only one of these renewable energy systems.

A hybrid energy system combines two or more energy conversion technologies, or two or more fuels for the same device. An example of a hybrid system consisting of solar photovoltaic panels, wind turbines, a diesel generator and batteries is shown in Fig. 1.1.

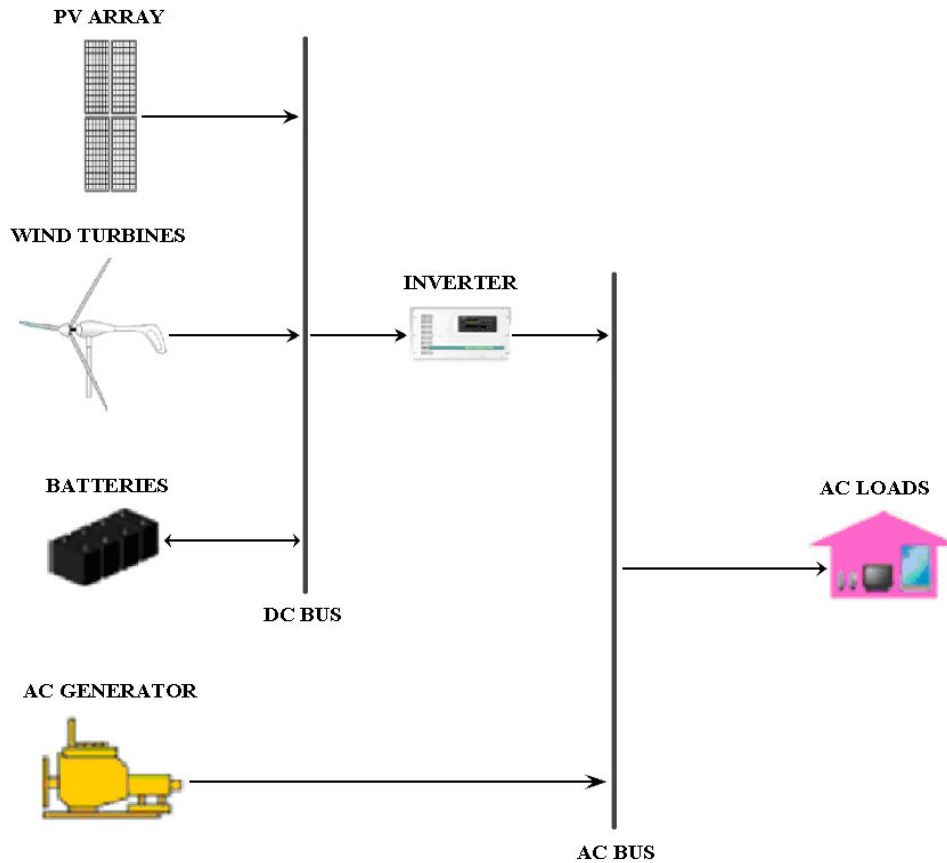


Figure 1.1 Diagram of a hybrid energy system consisting of solar PV panels, wind turbines, a diesel generator and batteries.

Compared to renewable energy systems consisting only of solar PV panels or wind turbines, hybrid systems provide enhanced advantages such as:

- 1) *Flexibility*: the peak operating times for solar panels and wind turbines are combined for a greater balance in energy supply.
- 2) *Efficiency*: the system is designed to maximize its overall performance. If the efficiency of one system decreases, the efficiency of another system would typically increase. For example, low solar radiation at night would decrease the efficiency of solar panels, but since a high wind speed is expected at night, the efficiency of the wind turbines would increase due to higher wind speeds.

- 3) *High reliability*: the quality and availability of energy is achieved through the use of redundant technologies.
- 4) *Lower emissions*: since the use of renewable sources is prioritized over fossil fuels.
- 5) *Economics*: lower system costs over the entire lifetime of the project, called the Net Present Cost (NPC).
- 6) *Entrepreneurial*: hybrid systems represent outstanding entry market strategies for emerging technologies that cannot compete with the traditional low-cost options.

1.2. PROJECT STATEMENT

The goal of this work is to evaluate the dependencies of the optimal size of a hybrid system on the electricity demands and the amount of renewable resources in the United States. An AC electricity demand was modeled to meet the energy requirements of most residential, commercial and industrial applications. For practical purposes, the insolation range was divided in 0.5 kWh/m²/day increments, and the wind speed range was divided in 1 m/s increments. For different values of the electricity demand, the system will be optimized over the range of insolation and wind speed values in the United States. This will allow studying how the optimal configuration of the hybrid system changes with the amount of renewable resources. Moreover, in the case of a change in the electricity demand, this study will predict the configuration of the new optimal system.

Due to the high availability of sun and wind, and the popularity of solar panels and wind turbines, these are the two only renewable technologies that would be considered in this study. Therefore, each location would be characterized by its average annual amount of insolation and wind speed intensity. In most part of the United States, the value of the average annual amount of insolation ranges between 4.5 and 6.5 kWh/m²/day whereas the average annual wind speed ranges between 4 and 8 m/s [2]

Additionally, this system will be provided with a bank of lead-acid batteries and/or a diesel generator for the times when neither the wind turbines nor the solar panels

can cover the electricity demand. Adding a diesel generator increases the complexity of the system because it is highly desirable to operate it close to their nominal capacity. Otherwise the generator would not burn the fuel efficiently and some unburned residue will remain in the combustion chamber, thus reducing its lifetime. Furthermore, the diesel generator can be used to provide power and simultaneously recharge the batteries when these are running low. To deal with the complexity, modern electronic controllers are used that can operate the system automatically. Most commercial diesel generators include these electronic controllers.

The electricity demand will be modeled in this project as an AC load since most small/medium systems and appliances run in AC. The range of electricity demands studied in this work was chosen to be 10 – 100 kW to account for the electricity needs of small residential communities, most businesses and commercial establishments, and small industry. Four specific electricity demands were considered in this work, 10, 20, 50 and 100 kW. Since the power generated by the PV panels and the wind turbines considered in this work is in DC, an inverter needs to be added to the system. An inverter converts DC power into AC power and thus, serves as a connector between the DC and AC buses of the system, as shown in Fig. 1.1.

In summary, the hybrid energy system studied in this work consists of a combination of photovoltaic panels, wind turbines and/or a diesel AC generator as the sources of energy, a bank of lead-acid batteries as energy storage systems, and a DC to AC. This study was performed in three different steps.

The first step was to find the optimum size of the hybrid system, defined in this project as the optimum number of components and their size that minimizes the net present value, NPV, of the project. The NPV represents the overall system costs such as installation, components replacement and operation & maintenance over its entire life cycle. For each combination of annual insolation, annual wind speed and peak electricity demand values, the system was optimized using the program HOMER [3]. This software was developed by the National Renewable Energy Laboratory (NREL).

The total number of optimized systems is given by the number of combinations:

$$\text{Nr. of combinations} = (5 \text{ insolation values}) \times (5 \text{ wind speed values}) \times (4 \text{ electricity demands}) = 100$$

Thus, the optimum PV array size, number of wind turbines, diesel generator size and number of batteries was obtained for each of these combinations.

The second step was to analyze the dependencies of the optimum system size with varying values of insolation, wind speed and peak electricity demand. This was done by keeping fixed one of these input parameters at a time and studying the effects of the other two parameters on the optimum system size.

Finally, an estimate of the initial costs and the life cycle costs over the entire project lifetime were provided and evaluated to analyze their relationship with the optimal system size.

1.3. READER'S GUIDE

Chapter 2 describes the energy resources used by the hybrid system studied in this work. The main concepts pertaining the solar, wind and diesel fuel resources are described to a big extent. Different methods for examining the availability of these resources are also provided.

The description of the main components of the hybrid renewable system considered in this work is given in Chapter 3. For each of these components, the physical concepts governing their working principles are covered in detail. Finally, different optimization methods for each of these individual systems are discussed.

In Chapter 4, the AC electricity demand used in the optimization of the hybrid system is modeled. An overview of the main energy sectors in the United States is first given and then considered for the description of a very representative and accurate electricity demand which covers a wide spectrum of those sectors.

Chapter 5 begins with a discussion of the complexities encountered in developing a suitable optimization method for this work. The inputs and outputs used in the method are then described, followed by an example showing how the program HOMER works.

Finally, a detailed description of the optimization method developed for this thesis is given, breaking out the method into three different stages.

The results of the optimization process are given in Chapter 6, sorted accordingly to show the dependencies between different input parameters. The optimum system size is thoroughly analyzed by keeping constant one of the three input parameters at a time, and a discussion based on the results of this analysis is then provided. An estimate of the net present value of the optimum system is provided and discussed at the end of this chapter.

In Chapter 7, conclusions are drawn from the results of the optimization analysis carried out throughout the entire thesis.

2. AVAILABILITY OF ENERGY RESOURCES

In order to evaluate the performance of the energy generation components of the hybrid system, it is necessary to determine the availability of the resources. Recall that for the system considered in this thesis, the energy generation components are three: photovoltaic panels, wind turbines and a diesel generator.

The energy resources that will be studied in this section are the intensity of the solar radiation, the intensity of the wind speed and the price of the diesel fuel. Notice that sun and wind are renewable resources and thus, their price is not a concern. However, their intensity is not constant with time and therefore needs to be further studied. On the other hand, the diesel fuel is not a renewable source of energy and has to be purchased; thus its price over the entire lifetime of the project will be studied.

2.1. THE SOLAR RESOURCE

In the design of renewable energy systems comprising solar PV panels, a key factor that would justify their usage in the installation is the amount of solar energy from the sun available at that particular site. For this purpose, two terms need to be introduced: irradiance and insolation.

Irradiance is the power density from the sun at some site, usually expressed in photovoltaics in W/m^2 . Because power is the rate at which energy is transformed, the term irradiance refers to an instantaneous quantity [4].

Insolation (also known as irradiation) is the incident energy density from the sun at some site, usually given in photovoltaics in kWh/m^2 . Since this is not an instantaneous quantity, it is convenient to express it over a time frame. Because the intensity of sunlight at a certain location changes significantly over the 24 hours of the day whereas the variation is very small between consecutive days, the chosen time frame is normally one day. Thus, insolation is most of the times expressed in $\text{kWh/m}^2/\text{day}$.

Noticing that irradiance has units of power and insolation has units of energy, and that power is energy integrated over time, the following relationship can be found:

$$Insolation = \int_{1 \text{ day}} Irradiance dt \quad (2.1)$$

In order to calculate insolation incident on the PV panels, it is first necessary to determine the amount of irradiance from the sun that reaches the earth's surface. Sunlight gets reflected back and /or absorbed in the atmosphere due to two main effects. The first one is the scattering by molecules, particles and aerosols present in the atmosphere; and the second one is the absorption by atmospheric gases such as CO₂, O₂, O₃ or water vapor. Therefore, the sun's irradiance outside the earth's atmosphere needs to be determined, and then corrected by subtracting the portion of it reflected back and/or absorbed in the atmosphere.

To calculate the amount of irradiance outside the earth's atmosphere the spectral power density of sunlight outside the earth's atmosphere has to be obtained. This is done by using SMARTS [5], a free software developed by NREL, using the Gueymard 2004 method [6] (Fig. 2.1).

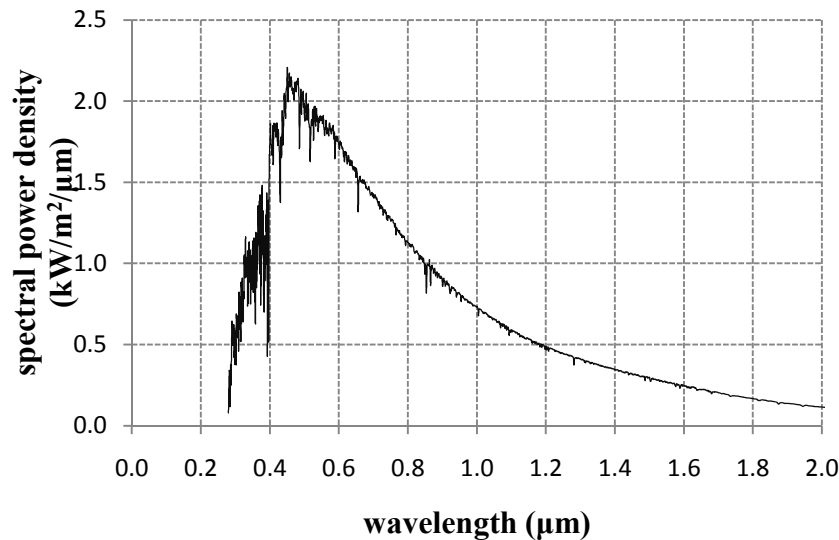


Figure 2.1 Spectral power density of sunlight outside the atmosphere. Plot obtained with the software SMARTS provided by NREL using the Gueymard 2004 method.

Integrating the spectral power density over the wavelength gives the solar irradiance perceived outside the earth's atmosphere. This value is usually referred as the Solar Constant (SC) and has a commonly accepted value [7] of,

$$SC = 1366.1 \text{ W/m}^2$$

However, the amount of radiation that reaches the top of the earth's atmosphere is usually smaller than this value. The reason is that the solar rays reach the top of the atmosphere with a different angle depending on the time of the year. To account for this deviation, the zenith angle is used, which is the angle between an outward normal from the earth and the sun rays. When the solar constant is corrected by the zenith angle, the extraterrestrial horizontal radiation is (I_0) obtained. Therefore, this term represents the radiation on a horizontal surface at the top of the earth's atmosphere [$\text{kWh/m}^2/\text{day}$]. A method to calculate I_0 is given in Duffie and Beckman [8]. In order to apply this method the latitude of the solar panels needs to be known to calculate the zenith angle.

As mentioned above, the value of the extraterrestrial horizontal radiation may get attenuated significantly in the atmosphere by the effects of scattering and absorption, thus reducing the irradiance at the earth's surface. According to Masters, G.M. [9] “[...] less than half of the radiation that hits the top of the atmosphere reaches the earth's surface as direct beam”. The portion of the extraterrestrial radiation that reaches the earth's surface without suffering any scattering and /or absorption by the atmosphere is called direct beam solar radiation (I_B). The rest of the extraterrestrial radiation reaching the earth's surface is called diffuse solar radiation (I_D). This is the portion of solar radiation whose direction, and therefore intensity, gets changed by the earth's atmosphere.

Unfortunately, these two components of the solar radiation are difficult to measure separately. The reason is that the diffuse solar radiation reaches the solar panels from all parts of the sky, whereas the direct beam solar radiation only comes from a direction aligned with the sun's path. For practical purposes, it is easier to measure the incident global irradiation on a horizontal surface (I_G), which is the sum of the direct beam and diffuse solar radiation values,

$$I_G = I_B + I_D \tag{2.2}$$

and then use the Erbs correlation [10]. This correlation gives the diffuse solar radiation as follows,

$$\frac{I_D}{I_G} = \begin{cases} 1.0 - 0.09K_T & \text{for } K_T \leq 0.22 \\ 0.9511 - 0.1604K_T + 4.388K_T^2 - 16.638K_T^3 + 12 & \text{for } 0.22 < K_T < 0.80 \\ 0.165 & \text{for } K_T \geq 0.80 \end{cases} \quad (2.3)$$

where K_T is the clearness index, which is the fraction of the solar extraterrestrial radiation striking the top of the atmosphere that reaches the earth's surface,

$$K_T = \frac{I_G}{I_0} \quad (2.4)$$

The global irradiation on a horizontal surface (I_G) is the main source of energy that solar PV panels use to generate electricity. The last component of irradiation is called reflected solar radiation (I_R). This portion of irradiation shall be accounted for especially when the PV panels are to be installed in the surroundings of highly reflective materials, such as metals, water or snow. In this case, the fraction of global irradiation on a horizontal surface that gets reflected from the ground to the solar panels should be specified. The factor that accounts for this effect is called ground reflectance or albedo (ρ). Its value ranges between 0.8 for fresh snow and 0.1 for bituminous-and-gravel roof, with a typical value of 0.2 for grass-covered areas [9]. Once this factor is defined, the reflected solar radiation can be calculated from,

$$I_R = \rho I_G \quad (2.5)$$

Therefore, the total amount of irradiation striking a solar PV panel (I_T) is the sum of these three components,

$$I_T = I_B + I_D + I_R \quad (2.6)$$

Considering these three effects together, I_T commonly takes a maximum value around 1000 W/m². This value is sometimes referred to as 1-sun, and is used as the standard for rating the performance of photovoltaic panels. The total insolation at a certain site can then be calculated with Eq. 2.1, giving an average annual insolation value in the United States between 4.5 and 6.5 kWh/m²/day [2] (Appendix A).

The method shown above is used by HOMER to evaluate the availability of the solar resource at a given location. Other popular methods exist such as the method developed by the *American Society of Heating, Refrigerating and Air-Conditioning Engineers* [11]. Additionally, there exist databases created by a number of organizations providing values of the global solar radiation on a horizontal surface for different locations on the earth. For the present work, the “*NASA Surface meteorology and Solar Energy Data Set*” [12] was used to estimate monthly insolation values for several location in the United States.

2.2. THE WIND RESOURCE

The performance of wind turbines is characterized by their ability to convert the kinetic energy in the wind first into rotating mechanical energy in a shaft and ultimately into electric energy in a generator (Fig. 2.2).

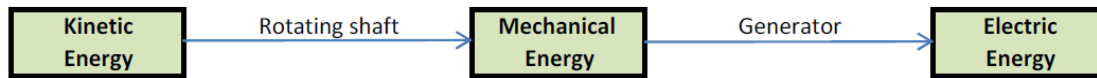


Figure 2.2 Diagram representing the types of energy conversions which take place in a wind turbine.

Thus, a limiting factor to determine whether it is feasible or not to use wind turbines in a project is the speed of the wind at the location of that particular project. This is especially important since the power in the wind varies with the cube of the wind speed (Eq. 2.7).

$$P_w = \frac{1}{2} \rho A v^3 \quad (2.7)$$

where P_w is the power in the wind (W), ρ is the density of the air (kg/m^3), A is the cross-sectional area of the wind turbine (m^2) and v is the component of the wind speed normal to A (m/s)

Another important factor to consider when selecting a suitable site to install wind turbines is the nature of the wind. Excessive air turbulences may introduce undesired vibrations in the mechanical components of the wind turbine, thus reducing significantly its lifetime. Furthermore, wind turbines typically operate in wind speed ranges around 4 and 25 m/s, reaching their peak power between approximately 10 and 25 m/s. This implies that it would be highly desirable to have winds blowing most of the time at 10-25 m/s so the potential of installing wind turbines is maximized.

But due to the random nature of the wind, this is sometimes hard to achieve and a thorough wind analysis should be carried out before taking the decision to install wind turbines. The wind speed distribution has a very random behavior along the 24 hours of the day and also between consecutive days. On the other hand, the wind speed variation is not so significant in a monthly basis. Although the average wind speed tends to be slightly higher in the winter than in the summer, the deviation with respect to the average yearly wind speed is very small. In a daily basis this deviation cannot be ignored. The reason is that there may be some times of the day in which the wind either does not blow at all or it blows very fast.

Therefore the hourly and daily wind speed distributions need to be studied in detail whereas the monthly wind speed distribution will be considered to be constant in the present work.

Hourly and Daily Variability of Wind Speeds

Several statistical methods have been developed to predict the wind speed distribution over the 24-hours of the day for the 365 days of a year. The most widely used is called the Weibull distribution, which represents the probability density function of the wind speed over the 24-hours of the day [9] [13]:

$$f(v) = \frac{k}{c} \left(\frac{v}{c}\right)^{k-1} \exp\left[-\left(\frac{v}{c}\right)^k\right] \quad (2.8)$$

where $f(v)$ is the probability density function of the wind speed, k is called the Weibull/shape parameter, c is the scale parameter and v is the wind speed (m/s). Even

though the values of k and c are chosen to fit a given set of wind data points (i.e. using an anemometer), an initial estimation can be done as follows. The value of k is closely related to the variability of wind speeds with respect to the average value. Setting the scale parameter to $c = 7$, and varying the shape parameter k gives an idea of what its range should be (Fig. 2.3).

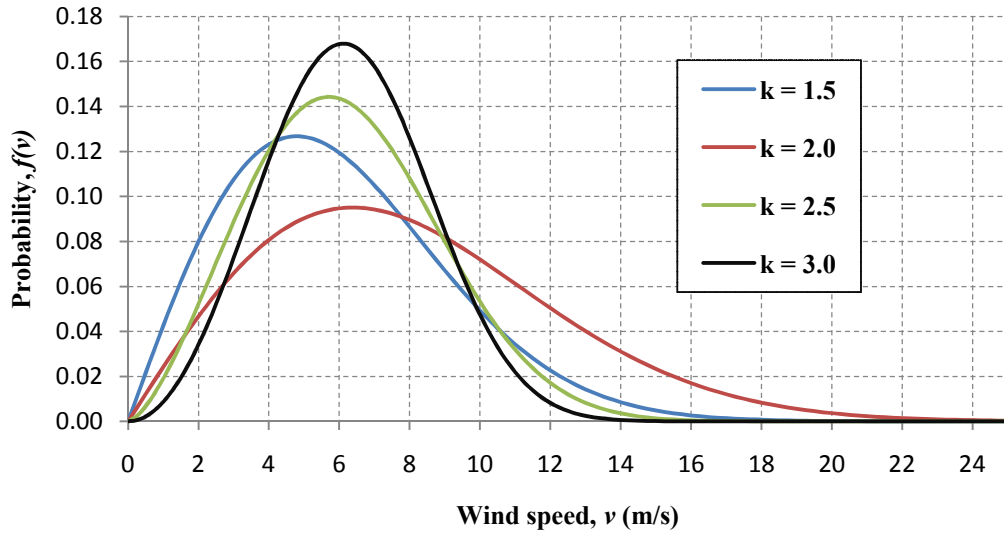


Figure 2.3 Probability density function of a Weibull distribution for different values of the shape parameter, k .

A fairly accurate value of the shape parameter that fits most experimental wind speed distributions would be close to $k = 2$. This approximation was done by using the measured data from the 239 weather stations in the United States [14].

The value of the scale parameter c can be calculated as follows if the daily average wind speed v_{avg} is known. The average of a probability density function (known as the expectation of the design variable) can be found from,

$$E(X) = \int_{-\infty}^{\infty} xf(x)dx \tag{2.9}$$

where $f(x)$ is the probability density function of the variable x . Thus, substituting the Weibull density function given in Eq. 2.8 into Eq. 2.9 allows for the calculation of the average daily wind speed,

$$v_{avg} = \int_0^{\infty} v f(v) dv = \frac{\sqrt{\pi}}{2} c \quad (2.10)$$

Therefore, the scale parameter can be calculated for $k = 2$ as,

$$c = \frac{2v_{avg}}{\sqrt{\pi}} \quad (2.11)$$

A plot of different wind speed distributions is given in Fig. 2.4 for several values of the average wind speed,

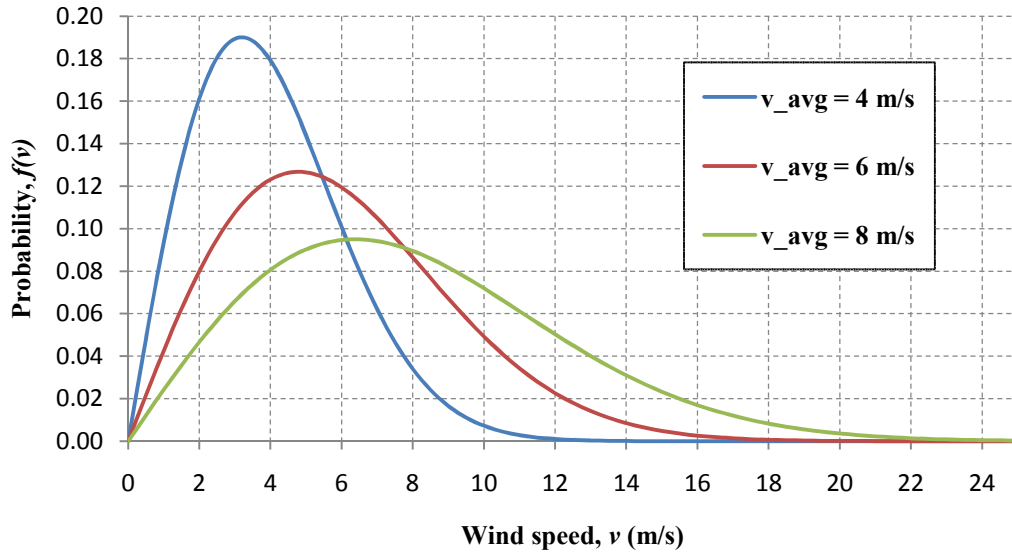


Figure 2.4 Probability density function of a Weibull distribution with $k = 2$ for different values of the average wind speed, v_{avg}

In order to fit a Weibull distribution to measured wind data, HOMER uses the maximum likelihood method [15]. To apply this method, the Weibull parameter (k) needs to be defined, as well as the following parameters:

Autocorrelation factor (r_1): factor that accounts for the dependence of the wind speed strength in one hour with respect to the previous hours. It is highly dependent on the topography, ranging from 0.70 in areas for very complex topographies to 0.97 to open air areas.

Diurnal pattern strength (δ): factor that accounts for the dependence of the wind speed strength with the time of day. The value ranges from 0.4 in areas where this dependence is high to 0.05 when the dependence is very small.

Hour of peak wind speed (Φ): represents the windiest hour of the day, on average. Based on the data of the 239 weather stations in the TMY3 data set [14], the value of this factor was estimated to be between 12 and 14.

Monthly Variability of Wind Speeds

The maximum likelihood method is a good estimate of the hourly wind speed distribution over the 8,760 hours of the year. To apply this method it is required to define the four parameters described above as well as the average monthly values of the wind speed.

Due to the random nature of wind speed and its importance in determining the feasibility of using wind turbines in an energy system, the commonly used method of evaluating the yearly availability of winds is collecting wind data with on-site weather stations. These weather stations are installed at the expected location of the wind farm and measure, among others, the speed, direction, temperature and humidity of the wind in one or a few minute's intervals to be further analyzed.

The measuring equipment is installed on top of a tower at a height matching the height of the wind turbines hub. In the present work, the monthly average values of wind speed obtained with the “*NASA Surface meteorology and Solar Energy Data Set*” database were used. An example of what a typical monthly average wind speed distribution looks like in Fig. 2.5 shown below.

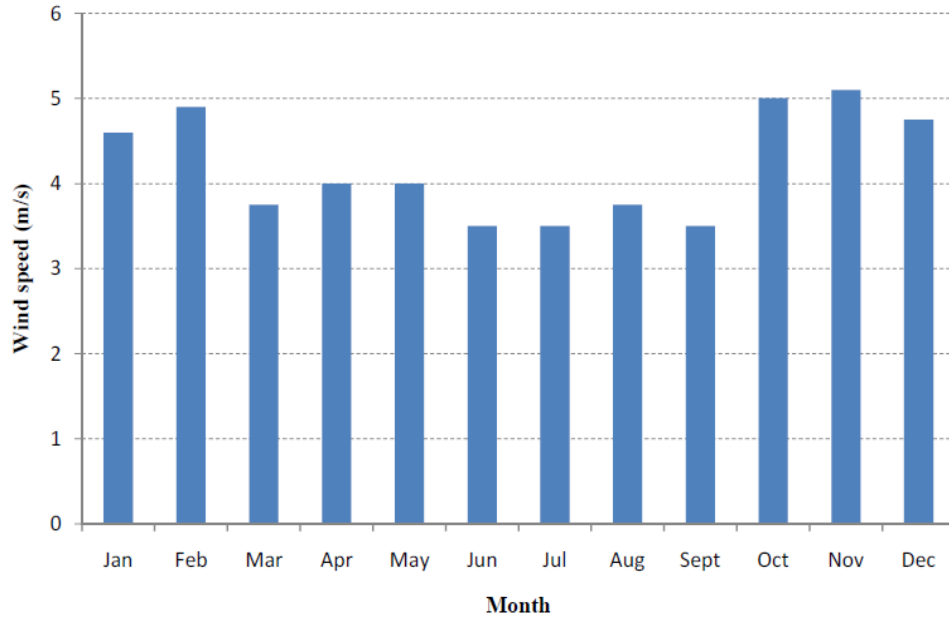


Figure 2.5 A typical distribution of the average monthly values of wind speed for a given location.

The wind speed data provided in this database is given at a height of 50 m over the ground level, and was later corrected to account for the effect of ground roughness and different hub heights. For this purpose, the following equation was used,

$$\left(\frac{v}{v_0}\right) = \frac{\ln(H/z)}{\ln(H_0/z)} \quad (2.12)$$

where v_0 (m/s) and H_0 (m) are the reference windspeed and height, v (m/s) and H (m) are the target wind speed and height, and z (m) is the roughness length coefficient provided in [9] and given in Table 2.1.

Description	Roughness Length z (m)
Water surface	0.0002
Open areas with a few windbreaks	0.03
Farm land with some windbreaks more than 1 km apart	0.1
Urban districts and farm land with many windbreaks	0.4
Dense urban or forest	1.6

Table 2.1 Roughness length values for different terrain types

2.3. THE DIESEL RESOURCE

Fuel generators are usually installed in off-grid energy systems as a back-up source of energy when the energy supply from the renewable sources fails to satisfy all the electric demand. The installation is typically provided of batteries as the main energy storage system, which delivers the remaining energy to the loads when solar PV panels, wind turbines and other renewable energy components are insufficient to cover the electric demand.

But the cost of batteries is quite high, and sizing the battery bank to be able to cover all the peaks in electric demand is cost-prohibitive and thus, fuel generators turn out to be a good alternative for these situations. The most widely used of all fuel generators are the diesel generators. Some reasons are the high availability of the diesel fuel, the reduced size and the high effectiveness as compared to other generators using fuel such as natural gas or biomass.

One of the biggest issues with diesel generators is that they do not use a renewable source of energy and consequently they release some contamination into the environment and require the diesel fuel to be purchased. Therefore, in order to economically justify the usage of diesel generators in energy systems, the diesel price needs to be somehow predicted for the entire life cycle of the system.

The difficulty in forecasting the diesel price lies in its dependency with several factors such as the political stability and relationship with the oil producers, the world economic situation, the oil's availability in the existing reservoirs, the discovery of new reservoirs and environmental reasons among others.

Based on these factors, the U.S. Energy Information Administration [16] provides a prediction of the diesel price in the United States for the next 25 years (Fig. 2.6) which coincides with the project lifetime considered in the present work.

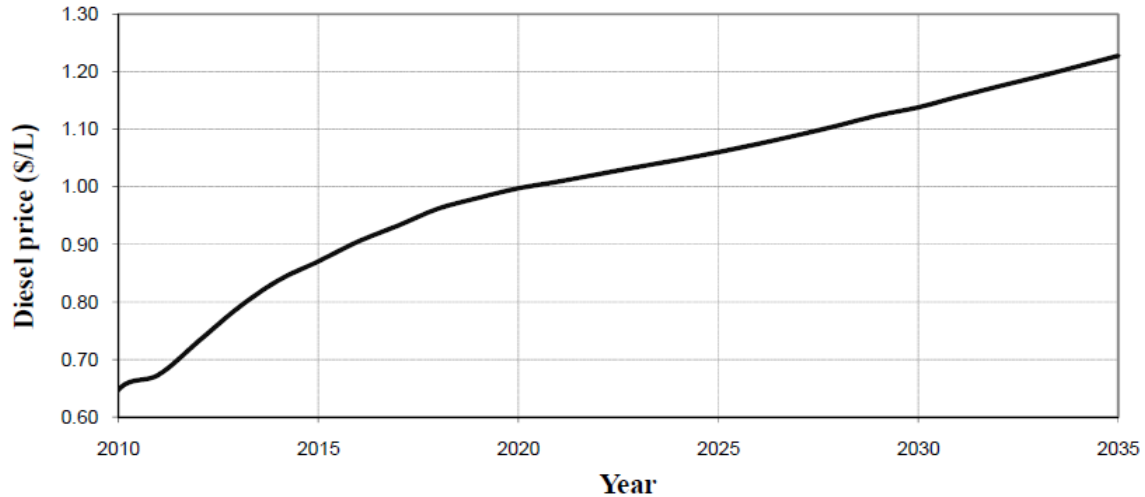


Figure 2.6 Diesel fuel price predictions by the U.S. Energy Information Administration (EIA) for the next 25 years.

Using the information given in the above figure, the predicted annual average value of the diesel price was calculated to be \$1/liter. This result was used in the economic description of the diesel fuel resource to assess the performance of the diesel generator installed in the hybrid energy system studied in this thesis.

2.4. PARAMETERS USED IN THE CALCULATIONS

In order to obtain satisfactory results in the optimization of the hybrid system, the availability of the energy resources needs to be described accurately. The parameters used in the calculation of the solar, wind and diesel resources are given below.

The solar resource

To describe the solar resource, three parameters need to be determined: the latitude in which the solar panels are to be installed (L), the global insolation on a horizontal surface (I_G) and the ground reflectance or albedo (ρ).

The data in the “*NASA Surface meteorology and Solar Energy Data Set*” [12] will be used to estimate the values of the global insolation on a horizontal surface. These insolation values range between 4.5 and 6.5 kWh/m²/day in the United States, as it can be

seen in Appendix A [2]. For the calculations in this work, this range was divided in 0.5 kWh/m²/day increments.

The location of the hybrid system will be characterized by its average annual insolation and wind speed values, and not by its latitude. The latitude of the hybrid system will be assumed to be the average latitude of the United States (Table 2.2). This simplification is necessary in order to reduce the number of calculations. The validity of this assumption is justified by considering the range of latitudes in which the United States is located. Since the United States is located within 10 degrees north and south of the average latitude of the country, and a 10 degrees deviation with respect to the average implies small variations in the results, this assumption can be made.

Latitude	38 North
Longitude	98 West
Time zone	GMT - 06:00

Table 2.2 Average geographical parameters of the United States

The average latitude is used to compute the extraterrestrial horizontal radiation (I_0) employing the method described in Duffie and Beckman [9]. Using this value and the value of the global insolation on a horizontal surface in Eq. 2.4, the clearness index can be calculated. With this value of the clearness index, the diffuse and direct beam solar radiation can be found combining Eq. 2.2 and 2.3.

The global insolation on a horizontal surface (ρ) is needed to define the reflected solar radiation according to Eq. 2.5. This value was chosen to be $\rho = 0.2$ for representing a typical value used for grass-covered areas.

The wind resource

The behavior of wind is quite random and more unpredictable than the solar radiation. Thus, the description of the wind resource requires the determination of a larger number of parameters than the solar resource. These parameters can be organized in three groups: parameters required to describe the hourly wind speed distribution, average monthly wind speed values and topographical parameters.

The maximum likelihood method [15] is used to predict the hourly wind speed distribution. To apply this method, four parameters need to be determined: the Weibull parameter, the autocorrelation factor, the diurnal pattern strength and the hour of peak wind speed. The average value of these parameters in the United States, shown in Table 2.3, was obtained from the 239 weather stations in the TMY3 data set [14], shown in Table 2.3.

Weibull parameter	2
Autocorrelation factor	0.85
Diurnal pattern strength	0.25
Hour of peak wind speed	15

Table 2.3 Parameters used in the calculation of the hourly distribution of the wind speed.

Using the data in the “*NASA Surface meteorology and Solar Energy Data Set*” [12], the average value of the annual wind speed distribution was predicted. These wind speed values range between 4.0 and 8.0 m/s in the United States, as it can be seen in Appendix A [2]. For the calculations in this work, this range was divided in 1 m/s increments.

The wind speed data in this data base was obtained at a height of 50 m above ground level. This value is used in Eq. 2.12 as the reference point at which wind speed

was measured. Also, the hybrid system will be assumed to be installed on a grass-covered area, for which the roughness length has a value close to $z = 0.01 \text{ m}$.

The diesel resource

For the description of the diesel resource only one parameter needs to be determined: the diesel fuel price. This parameter was estimated to have an average value of \$1/liter over the entire 25-year lifetime of the hybrid system.

3. COMPONENTS OF THE HYBRID RENEWABLE SYSTEM

In this chapter, the main components of the hybrid renewable energy system are explained. In order to understand the role of these components in the system, their operating principle needs to be explained, defining the main parameters used to evaluate their performance.

Since the end goal of this work is to optimize this system, a method to maximize the performance of each of the components is also provided.

3.1. SOLAR PHOTOVOLTAIC (PV) PANELS

A solar PV panel/module is a device that converts sunlight into electricity using the photovoltaic effect. The photovoltaic effect is a physical phenomenon discovered in 1839 by Becquerel [17] in which free electrons within the matter are emitted when they absorb electromagnetic radiation.

The photovoltaic effect is observed in semiconductor materials; that is, a material that behaves as an insulator at low temperatures, but that conducts electricity when energy is applied [7]. The most widely used semiconductor material in the manufacturing of solar cells is silicon due to its high abundance in the Earth's crust (26 % in weight, [18]). Other semiconductor materials such as gallium, germanium or arsenide represent different alternatives for solar cells. The type of semiconductor material used in PV panels leads to the different solar cell technologies, the most dominant of which being the crystalline silicon cell technology, holding about 90 percent of the solar cell demand [19]. Because of this, the description of PV panels provided in this section will be referred to silicon-based solar cells.

The photovoltaic effect can be described by the band gap model in terms of the energy levels of the electrons within the material (Fig. 3.1). Silicon is a tetravalent material; that is, its outer orbit contains four valence electrons. The energy level in which the valence electrons are present is called the valence band, and the next allowable energy level in which electrons are free to move within the atomic lattice is called the

conduction band. The gap between the valence band and the conduction band is called the forbidden band, and the energy that an electron must acquire to migrate across the forbidden band is called the band-gap energy (E_g). For silicon, this value is around 1.12 eV and this is the amount of energy that the incoming photons from the sun must transmit to a silicon electron for it to jump into the conduction band.

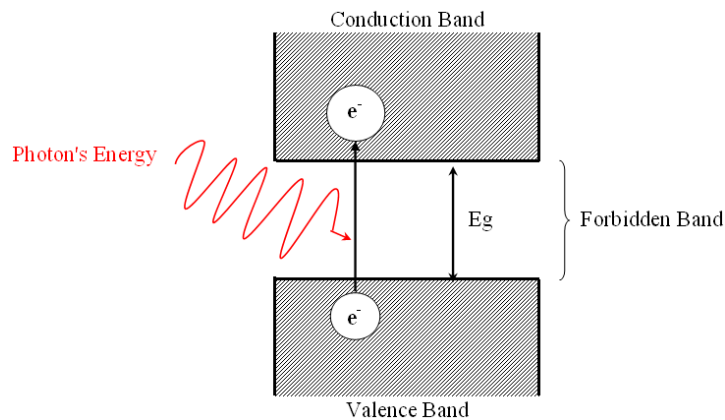


Figure 3.1 The band gap model used to describe the photovoltaic effect.

At normal temperatures the conductivity of silicon is very low, but it can be significantly increased by adding small quantities of other materials [7], usually boron and phosphorus. The process of introducing contaminant atoms into another material is called doping. By doping each side of the crystal with very small amounts of contaminant atoms, two regions are formed within the same material with different electron concentration. This originates an electric field in the junction of the two dissimilar regions, which is commonly referred to as the depletion region.

When sunlight is present, the electrons in the valence band receive energy to be placed in the conduction band. The electrons in the region of the material with higher electron concentration are 'pushed' by the electric field, drifting into the other region of the material. The drifted electron leaves an empty space, called a hole, in its original position. However, the energy state of the drifted electron in the neighbor region is highly unstable and thus it tends to bounce back to its original position. If an electric circuit is

attached to both regions of the material, these drifted electrons can be collected creating a voltage that can be used to deliver current to a load.

A solar module typically has 36 or 72 cells connected in series, although sometimes 72-cell modules are wired in two strings of 36 cells each. By connecting the cells in series, the output voltage of the module increases by a number of times of cells wired in series, whereas connecting the cells forming parallel strings increases the output current proportionally to the number of strings. The equivalent electric circuit of a single real cell is shown in Fig. 3.2, which leads to the following equation applying the Kirchhoff's Law,

$$I = I_{sc} - I_d - I_p \quad (3.1)$$

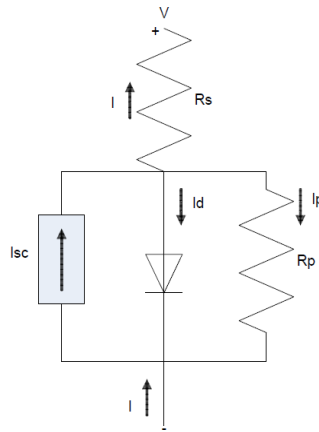


Figure 3.2 Electrical circuit of a single real cell including parallel and series resistances.

where I is the current across the cell,

I_{sc} is the short-circuit current. This is the maximum current that a solar cell can generate (when the terminals are shorted together).

I_p is the current drop due to the losses in the bulk of the material, which can be represented as a parallel resistance,

$$I_p = \frac{V_p}{R_p} = \frac{V + IR_s}{R_p} \quad (3.2)$$

I_d is the current across the cell junction, which behaves as a diode and can be characterized by the Shockley diode equation (at 25 °C) as:

$$I_d = I_0(e^{38.9V_d} - 1) = I_0(e^{38.9(V+IR_s)} - 1) \quad (3.3)$$

with I_0 being the dark saturation current ($I_0 \approx 10^{-10} - 10^{-12} \text{ A/cm}^2$) which is a measure of the electrons-holes recombination rate in the junction.

Thus, combining Eq. 3.1 through Eq. 3.3 yields the characteristic equation of a solar cell,

$$I = I_{SC} - I_0(e^{38.9(V+IR_s)} - 1) - \frac{V + IR_s}{R_p} \quad (3.4)$$

A theoretical model, called the ideal solar cell model, is used in photovoltaics to assess the performance of real cells by comparing them to the ideal case. In the ideal case, no parallel or series resistances are considered. The parallel resistance depends on the quality of the manufacturing process of the cell and the series resistance depends on the electrical connection losses in the wires. The upper efficiency limit of an ideal silicon-based solar cell was calculated in 1960 by Shockley and Queisser [20] to be 30%. Fig 3.3 shows the I-V curve obtained from Eq. 3.4 for different values of the series and the parallel resistance.

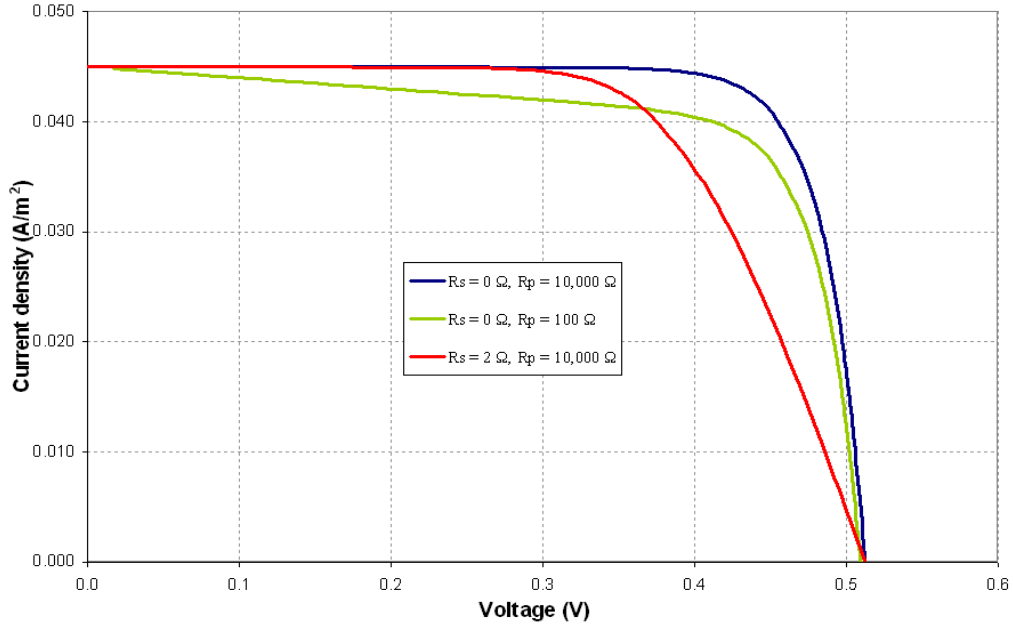


Figure 3.3. Effect on the I-V curve of changing either the series resistance (R_s) or the parallel resistance (R_p). Plot obtained for $I_0 = 10^{-10} A/cm^2$ and $I_{SC} = 0.045 A/cm^2$.

As mentioned before, solar cells are wired in a series – parallel configuration forming a solar module so as to obtain the desired output current and voltage. The maximum power that a module can generate is determined by the maximum product of current – voltage pairs that the module can generate (points along the I-V curve),

$$P_{max} = \max_i (I_i \times V_i) \quad (3.5)$$

The point at which this maximum occurs is called the Maximum Power Point (MPP), and for optimization purposes it is highly desirable to have all the loads of the system operating at this point. This is shown in Fig. 3.4 for a module consisting of 36-cells connected in series.

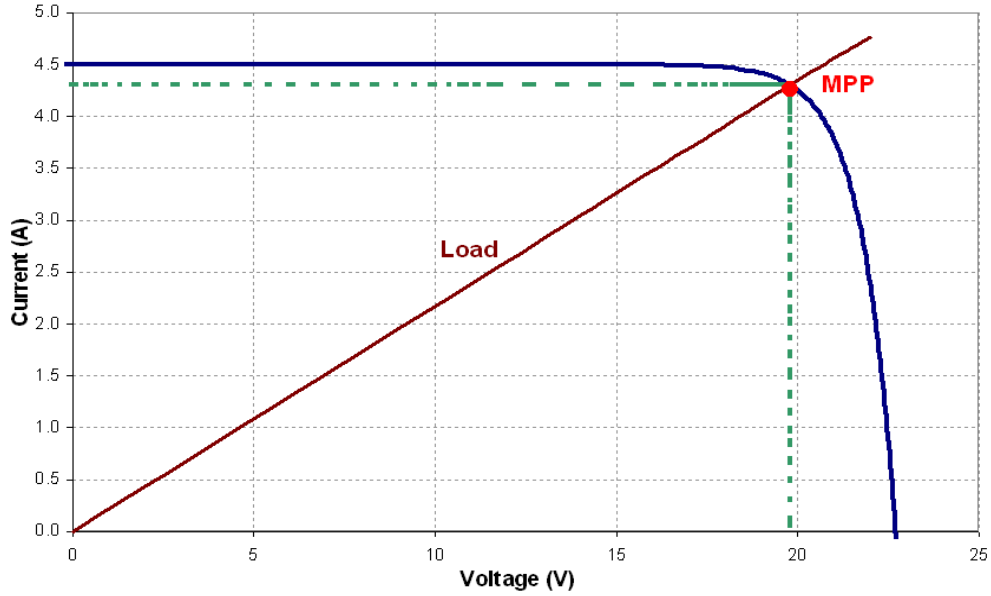


Figure 3.4 Module I-V curve, Maximum Power Point (MPP) and Load curve for maximum power output.

Solar panels are typically rated by their efficiency to convert the power available in the sun, P_{sun} [W], into usable power, P [W]. The power available in the sun is determined by the product of the available irradiance at a particular and the area of the solar panel,

$$P_{sun} [W] = Irradiance [W/m^2] \times Area[m^2]$$

Thus, the efficiency of solar panels is determined by,

$$\eta_{panel} = \frac{P}{Insolation \times Area} \quad (3.6)$$

3.2. WIND TURBINES

A wind turbine converts the kinetic energy of a mass of air into rotational mechanical energy in a shaft, which in turn drives a generator that converts this rotation into electricity. When air flows past the wind turbine blades, a surface force is exerted on them, causing them to rotate. The design of the blades should be such that maximizes lift,

which is the component of this force perpendicular to the air flow direction, to produce a higher torque. This torque is transmitted to the shaft thanks to the hub, a conical piece which connects the blades to the shaft and holds (in the case of big turbines) all the hydraulic components to spin the blades to maximize lift. Finally, the low-speed, high-torque rotation in the shaft is converted by means of a gear box into high-speed and low-torque rotation in another shaft in order to generate electricity in the generator. A diagram of the main components of a horizontal axis wind turbine, HAWT, is given in Fig. 3.5.

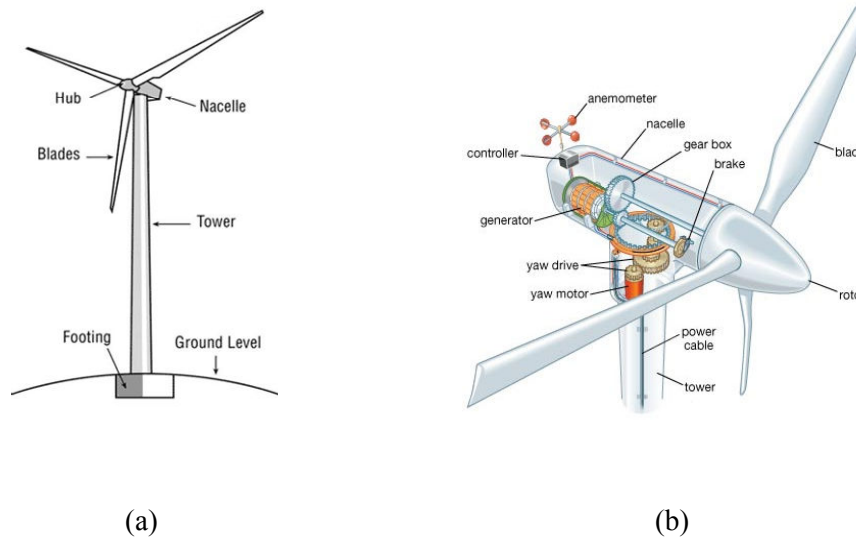


Figure 3.5 The main parts of a horizontal axis wind turbine (a) and a closer look-up to the mechanical elements inside the nacelle (b).

To evaluate the aerodynamic performance of HAWT, it is necessary to calculate the maximum power available in a mass of air, which is proportional to the cube of the wind speed by,

$$P = \frac{1}{2} \rho S v^3 \quad (3.7)$$

where ρ is the density of air [kg/m^3], S is the cross-sectional area of the wind turbine rotor [m^2] and v is the component of the wind speed normal to S [m/s]. Considering an air density of 1.25 kg/m^3 and a rotor diameter of 10 m, the power in the wind was graphed to show its dependency with the wind speed (Fig. 3.7).

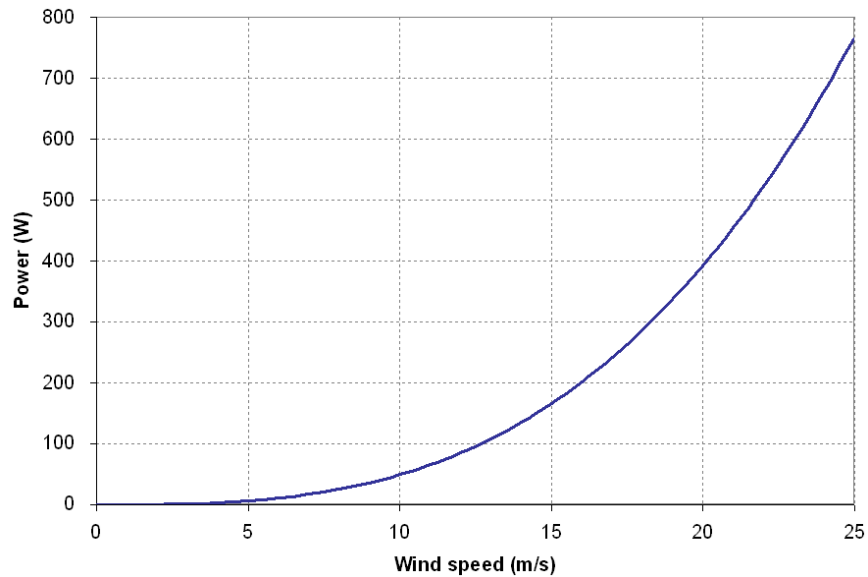


Figure 3.6 Available power in the wind for a 10 m rotor diameter wind turbine and an air density of 1.25 kg/m³.

It should be noted that the density of air is not constant since gas properties are susceptible to other parameters such as pressure or temperature. A close approximation to the air density for different temperatures can be done if air is considered to behave as an ideal gas and the air pressure is assumed to be constant and equal to 1 atm. Under these conditions the air density can be approximated with equation 3.8.

$$\rho = \frac{353.05}{T(K)} \quad (3.8)$$

The most well-known measure of the performance of a wind turbine is the power coefficient (C_p) developed by the German physicist Albert Betz [21]. In summary, the Betz's law is a theoretical proof for the maximum power in the wind that can be extracted from a wind turbine. By drawing a control volume of undisturbed air upwind and downwind of the wind turbine (Fig. 3.7), it is possible to calculate this theoretical limit as the ratio of maximum power extracted by the rotor to the power available in the wind.

$$Cp = \frac{P_{extracted_rotor}}{P_{available_wind}} \quad (3.9)$$

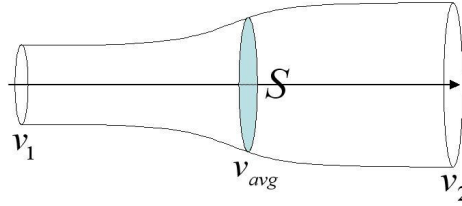


Figure 3.7 Control volume used in the calculation of the Betz limit in a wind turbine.

The maximum power extracted by the rotor, $P_{extracted_rotor}$, is given by the difference in time change in kinetic energy between the upwind and downwind flows,

$$P_{extracted_rotor} = \frac{1}{2} \dot{m} (v_1^2 - v_2^2) \quad (3.10)$$

where v_1 and v_2 are the wind speeds upwind and downwind of the wind turbine, respectively (m/s), \dot{m} is the mass flow rate through the control volume (kg/s) and S is the rotor area (m²).

Eq. 3.7 provides an expression for the power available in the wind, $P_{available_wind}$. Combining equations 3.7, 3.9 and 3.10, the power coefficient of a HAWT can be expressed as,

$$Cp = \frac{P_{extracted_rotor}}{P_{available_wind}} = \frac{\frac{1}{2} \dot{m} (v_1^2 - v_2^2)}{\frac{1}{2} \rho S v_1^3} \quad (3.11)$$

Applying conservation of mass to this control volume, the mass flow rate can be calculated as,

$$\dot{m} = \rho S v_{avg} = \rho S \left(\frac{v_1 + v_2}{2} \right) \quad (3.12)$$

Substituting Eq. 3.12 into Eq. 3.11 gives an expression of the power coefficient of a HAWT in terms of the upwind and downwind wind speeds,

$$C_p = \frac{\frac{1}{2} \rho S \left(\frac{v_1 + v_2}{2} \right) (v_1^2 - v_2^2)}{\frac{1}{2} \rho S v_1^3} \quad (3.13)$$

Since the wind speed from the upwind side of the wind turbine cannot be changed, the only design parameter in the system is the wind speed downwind the rotor. Thus, calculating the derivative of the power coefficient (Eq. 3.13) with respect to v_2 gives,

$$\frac{dC_p}{dv_2} = 0 \Rightarrow v_2 = \frac{v_1}{3} \quad (3.14)$$

Most modern horizontal axis wind turbines include a control system that constantly checks the incoming wind speed and rotates the blades such that Eq. 3.14 is satisfied at all times. Other smaller wind turbines which lack of this control system include blades with profiles designed to reach this relationship at high wind speeds.

Combining equations 3.13 and 3.14 gives the maximum power coefficient,

$$(C_p)_{\max} = 59.3\% \quad (3.15)$$

This means that the maximum power that a wind turbine can extract from the wind is 59.3 percent. However, real wind turbines under optimal operating conditions can reach values around 50 percent.

In practice, the best way to maximize the efficiency of wind turbines is to install them in the highest tower as possible, increase the area swept by the rotor, place the turbines in areas free of turbulences (i.e. away from buildings, mountains and rough terrains) and with good wind conditions, and leave enough separation between near wind turbines. Most times this is a complex task, and wind farms are designed using simulation programs specifically developed for this purpose. Some examples of these programs are WAsP, WindPro, WindFarm and OpenWind.

3.3. DIESEL GENERATOR

For an off-grid energy system, a good alternative for covering peaks in the electric demand, and therefore to serve as a back-up source of energy, is the use of fuel generators. The most widely used fuel generators operate with fossil fuels such as gasoline, diesel or natural gas, although other models exist for biogas or hydrogen fuels. Due to the high availability of diesel fuel and the wide range in rated power models, the type of generator that was used in this thesis is a diesel generator.

A diesel generator is a power generating set consisting of a diesel engine coupled with an electrical synchronous generator (alternator), although models with asynchronous generators also exist. The chemical energy in the diesel fuel is released in the engine and converted into rotational mechanical energy in a shaft which is then transformed into usable electric energy in the alternator.

Diesel generators are available in AC and DC versions. Since the load modeled in this work is a general AC load, an AC generator will be considered for the calculations of the optimal size of the renewable energy system. Under certain circumstances, the AC diesel generator will be used to charge the batteries, in which case a rectifier should be used to convert the AC current into DC current. However, most AC diesel generators include a built-in rectifier for this purpose or they can be mounted by the manufacturer in the worst-case scenario. Other systems and features that mid- to large-size diesel generators usually include are a frequency control system, a voltage regulator, electronic engine controls and fuel controllers to continuously adapt to the current electric demand of the loads.

When selecting a diesel generator, it is important to know which will be its main role in the energy system. In some applications, the diesel generator(s) are the main source of energy of the system whereas in other applications, such as systems including other sources of energy, hospitals or on construction sites, they are mainly used for support. For this reasons, manufacturers usually specify in the generators spec sheet their power range ratings:

- Standby Rating (in kW or KVA): Applicable to emergency generators used as a back-source of energy. Under these rating conditions, no electric demand is sustained for long periods of time.
- Prime Rating (in kW or KVA): Applicable to generators used as the main source of power in the system. This is the maximum power available for an unlimited number of hours.

For the present work, the standby rating will be used since the diesel generator will serve as a secondary/support source of energy for the solar PV panels and the wind turbines.

Unlike solar insolation or wind speed, diesel fuel is not a renewable source of energy and the cost of operating diesel generators should be accounted for throughout the entire project lifetime. Moreover, as it can be seen in Fig. 2.7, the price of diesel fuel does not remain constant with time thus introducing an additional complexity to the calculation of the net present cost (NPC) of the system. A typical fuel consumption curve of a diesel generation is shown in Fig. 3.8.

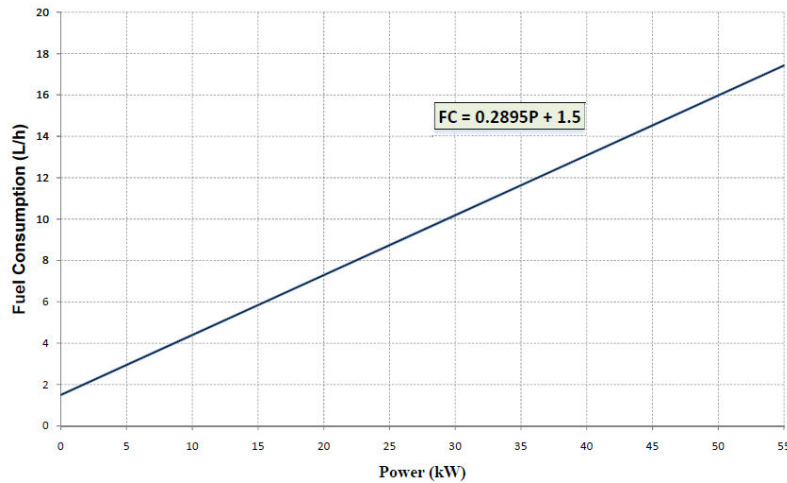


Figure 3.8 Fuel consumption curve of the diesel generator modeled in this thesis.

The fuel consumption equation of a diesel generator is usually given in the following form [22],

$$\dot{m}_{gen} = IC \cdot P_N + S \cdot P_{out} \quad (3.16)$$

where \dot{m}_{gen} is the fuel consumption [l/h], IC is the intercept coefficient which is the no-load fuel consumption divided by the rated capacity [l/h/kW], P_N is the nominal/rated power of the generator [kW], S is the slope of the marginal fuel consumption which is the slope of the fuel consumption curve [l/h/kW], and P_{out} is the actual output power of the generator [kW].

The efficiency of the diesel generator represents the amount of electric energy which is achieved with each liter of diesel fuel. It can be calculated by dividing the output electric power of the generator (P_{out}) by the power in the diesel fuel used by the generator (P_{in}),

$$\eta_{gen} = \frac{P_{out}}{P_{in}}$$

where the power in the diesel fuel, P_{in} , is the product of fuel consumption rate \dot{m} [l/s] by the chemical energy stored in the fuel, usually called the Internal Heat Capacity, IHC [kWh/l]. Therefore, the efficiency of the fuel generator takes the form,

$$\eta_{gen} = \frac{P_{out}}{\dot{m}_{gen}(IHC)_{fuel}} \quad (3.17)$$

The efficiency of a fuel generator can be derived from the fuel consumption curve and the internal heat capacity of the fuel by combining Eq. 3.16 and 3.17.,

$$\eta_{gen} = \frac{1}{IHC \left(S + \frac{P_N}{P_{out}} IC \right)} \quad (3.18)$$

A typical efficiency curve of a diesel generator is showed in Fig. 3.9.

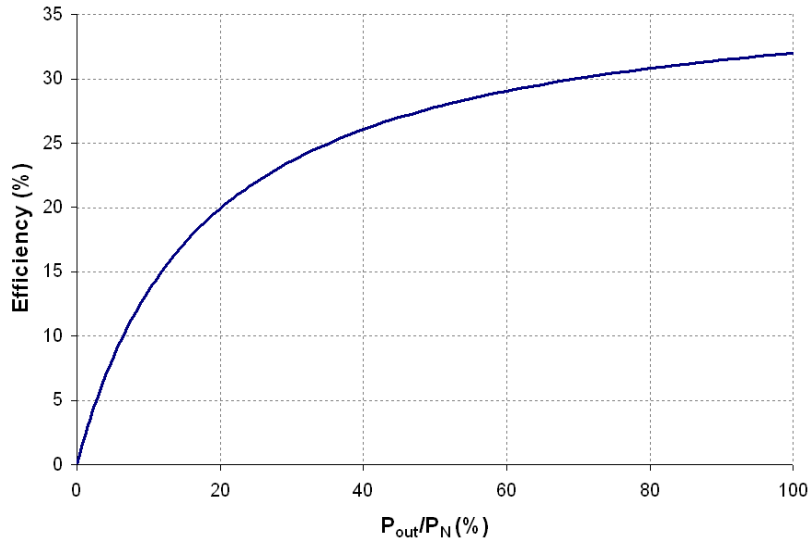


Figure 3.9 Efficiency curve of the diesel generator modeled in this thesis.

This plot shows why is it highly desirable to have the diesel generators working over 70% of their nominal power.

3.4. BATTERIES

Under favorable meteorological conditions, hybrid renewable systems are usually able to produce more energy than that demanded by the loads and thus it would be very desirable to have a method to store the surplus energy for the case when the conditions are not favorable. Several technologies exist for this purpose such as flywheels, water tanks or compressed air, but without any question lead-acid (Pb-acid) batteries are the most commonly used in stand-alone systems.

Lead-acid batteries are chosen for renewable energy systems because of their high reliability, little maintenance, easy installation and their ability to provide electricity directly, without involving any intermediate steps. There are several types of lead-acid batteries depending on the needed applications, but the most appropriate for hybrid systems are the deep-cycle, lead-acid batteries. These batteries can be discharged up to 80%, although their lifetime will suffer significantly.

The lifetime of a battery is usually expressed in number of cycles (N_{cycles}) versus Depth-of-Discharge (DOD). The number of cycles represents how many times a battery may be discharged and recharged before it will no longer take a full charge, and the Depth-of-Discharge is just the percentage that a battery has discharged from its maximum charge. Therefore, the maximum DOD of a lead-acid battery is somewhere around 80%. To show the negative effect of a high DOD on the life expectancy of batteries, a plot of N_{cycles} vs. DOD was provided in Fig. 3.10, which was created using the following equation [22],

$$N_{cycles,i} = CF_i \frac{DOD_i}{100} \quad (3.19)$$

where CF_i are the Cycles to Failure for a given Depth-of-Discharge, DOD_i (%). These two parameters are typically provided by the battery manufacturer in a tabular form.

DOD (%)	CF
10	4,398
20	2,322
30	1,614
40	1,266
50	1,036
60	884
70	774
80	698
90	633
100	600

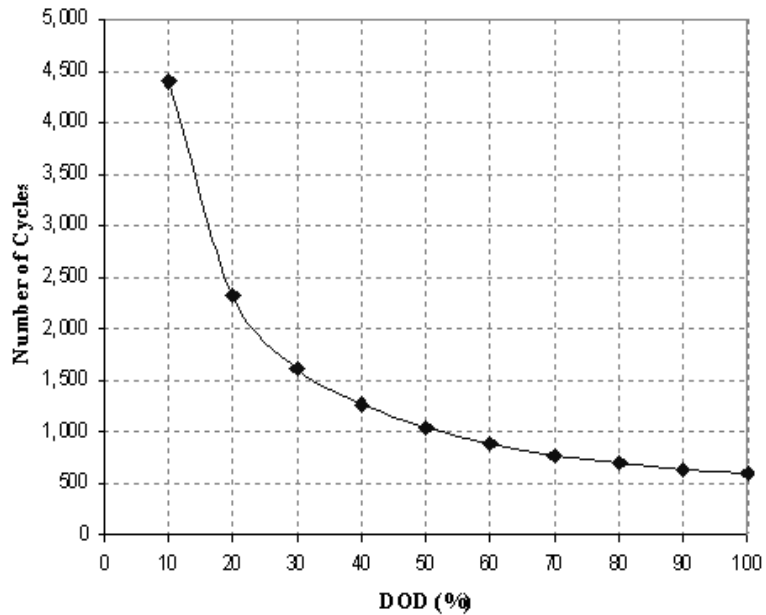


Figure 3.10 Lifetime curve. Effect of the Depth-of-Discharge on a deep-cycle, lead-acid battery lifetime.

There exist several models theoretical that describe the charge and discharge processes of batteries, some of them quite simple since they only use a few parameters of

the battery, and others more complex and difficult to implement, which require a detailed description of the batteries and sometimes certain experimental calculations. The simulation program used in the present work, called HOMER, uses the Kinetic Battery Model which was model in 1993 by Manwell and McGowan [23]. This model represents each battery as two tanks of energy. One tank provides immediately available energy while the energy in the second one (bound energy) cannot be supplied immediately and can only be discharged at a limited rate. In order for HOMER to perform the calculations, the values of the battery capacity for different discharge currents should be provided. This information is usually provided by the battery manufacturer, and can be seen in Fig. 3.11.

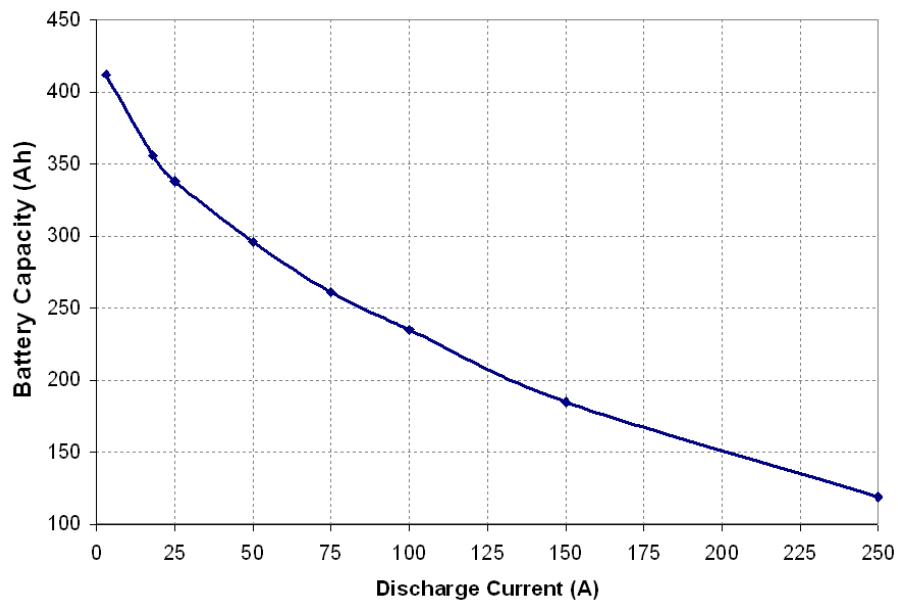


Figure 3.11 Battery capacity curve for a typical deep-cycle, lead-acid battery

3.5. INVERTER

The inverter is a signal conditioning device which converts AC voltage into DC. They are frequently used in hybrid energy systems to convert the DC voltage generated by photovoltaic panels, batteries and some types of wind turbines and generators into AC when part or all of the loads are in AC. This is the case of the present study, in which the

electricity generated in DC by the PV array, the wind turbines and stored in the battery bank needs to be transformed into AC before it can be used by the AC loads (Fig. 1.1).

The working principle of an inverter is quite simple. The DC input voltage is sent to two or more power switching transistors which are connected to a small transformer. By switching these transistors on and off very rapidly, the DC signal seems to alternate resembling to an AC signal. Then this alternating DC signal is passed through the transformer which raises the voltage to the desired output, usually 120 or 240 VAC. Depending on the complexity of the inverter, the quality of the output signal may vary from a square wave to a true sine wave.

The most important parameter to determine the performance of an inverter is its efficiency. The efficiency of an inverter is a measure of how well it converts the DC voltage into AC,

$$\eta_{inv} = \frac{P_{AC}}{P_{DC}} \quad (3.20)$$

The most efficient inverters in the market are the true sine wave inverters, which are designed to output a very realistic sinusoidal AC signal. These inverters have efficiencies around 85 – 95 %, with a world record of 99.03 % claimed by the Fraunhofer Institute for Solar Energy Systems ISE [24].

3.6. PARAMETERS USED IN THE CALCULATIONS

The description of the components of the hybrid system needs to be provided to ensure accurate results in the calculations. The physical properties of solar photovoltaic panels, wind turbines, diesel generators, batteries and inverters are described below. The economic description of these components can be found in Appendix B [19].

Solar Photovoltaic Panels

The following information was obtained by averaging parameters from a large number of silicon-based photovoltaic panels manufacturers ranging from 225 – 275 W. The solar panels modeled in this work will have a rated power of 250 W, which is a very typical value of most panels found in the market. Table 3.1 shows a summary of the parameters used in this work.

Some panels include a built-in inverter such that their output is in AC. However, this is not the common case since most of the PV panels output is in DC. This last option was selected for the panels used in the calculations.

The lifetime of PV panels is usually between 20 and 30 years. Thus, it is a good approximation to select a value of 25 years for their lifetime.

The rated power of the PV panel does not accurately represent the real output power that is delivered to the loads. The reason is that the real-world operating conditions differ from the conditions under which the PV panel was rated. Factors such as soiling of panels, shading, wiring losses or aging influence in the decrease of the output power. The PV derating factor is used to account for these losses. In the absence of data, a default value of 0.9 is commonly used as an estimate of the PV derating factor [25]. This is the value used in this thesis.

Tracking systems are sometimes used to maximize the amount of incident insolation on the solar panels. They track the direction of the sun's rays at all times and orient the PV panels according to that. However, these systems are expensive and thus they will not be considered for the PV array in this work. The most popular approach is to tilt the panels an angle equal to the latitude of the PV array. With this tilt angle the sun's rays strike perpendicular to the panels face at noon during the equinoxes (March 21 and September 21). At other times of the year the sun's rays would be slightly high or low from the normal incidence. However, this angle would still represent a good angle on an average [9]. Therefore, a tilt angle equal to the average latitude of the United States will be used as the slope of the PV panels.

Depending on the particular application, solar panels may be oriented facing east or west of south. For example, for applications which require having most of their energy early in the morning, panels can be mounted facing westward to start collecting energy during the sunrise. The most common case is when the application has its peak energy demand a few hours before or after noon, for which the PV panels need to be oriented facing south. This is the option selected for the present work. The azimuth is defined as the angle towards which the solar panels face. Therefore, the azimuth will be selected to be zero degrees.

Table 3.1 Parameters used in the description of the PV panels

Rated power	250 W
Output current	DC
Lifetime	25 years
Derating factor	90 %
Slope	38°
Azimuth	0° (facing South)
Tracking system	No

Wind Turbines

The model of wind turbine used in this work is a Southwest Whisper 500 [26], rated at 3 kW. It was desired to select a wind turbine in the order of a few kilowatts in order to provide the system with flexibility. In other words, since the loads modeled in the hybrid system are in the range of 10 – 100 kW, a larger turbine in the order of tens of kW or more would not draw significant conclusions; by using a smaller turbine the

amount of wind energy required to optimize the system would be described more accurately. The technical specifications of the Southwest Whisper 500 wind turbine modeled in this thesis are given in Table 3.2.

Table 3.2 Technical specification of the Southwest Whisper 500 wind turbine

Rated power	3 kW
Output current	DC
Lifetime	25 years
Hub height	21.34 m

Among the small wind turbines available in the market, the Southwest Whisper 500 was chosen for two reasons. The first reason is its low ratio of installed cost per kilowatt produced. While the selected wind turbine can be installed at a cost of \$2.5/W, most other wind turbines have installation costs between 2.75 and 3.00 \$/W.

The second reason is its availability to pick winds as low as 3.5 m/s. This feature is particularly important since the lowest annual average wind speed modeled in this work is 4 m/s. Thus, wind speeds below this value are expected and the wind turbine should be capable of collecting them. The power curve of the Southwest Whisper 500 is given in Fig. 3.12.

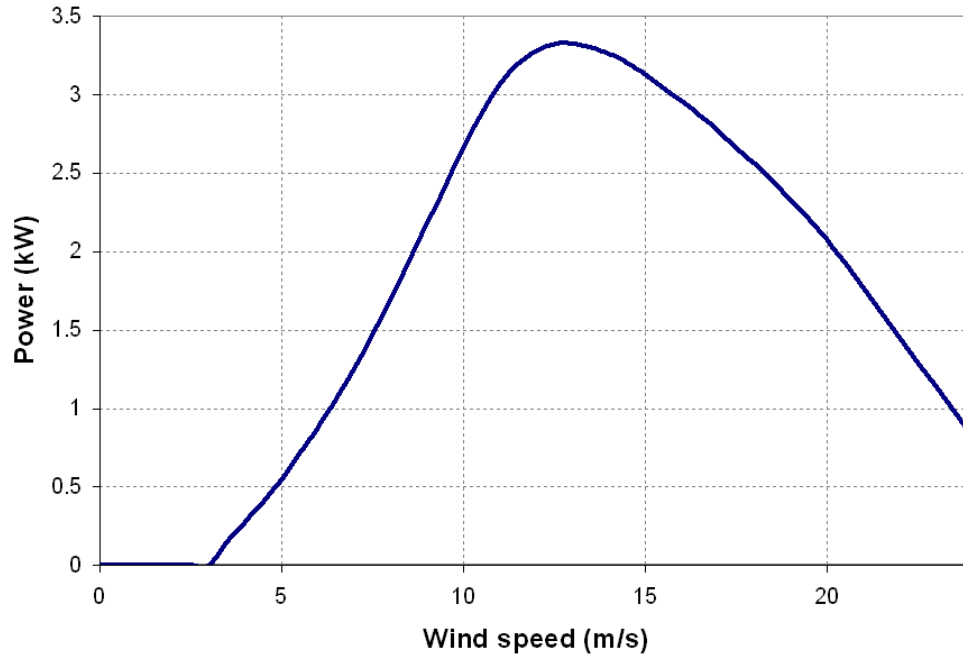


Figure 3.12 Power curve of the Southwest Whisper 500 wind turbine

Diesel Generator

The performance of a fuel generator is defined by its efficiency. It can be derived from Eq. 3.18 from the knowledge of the internal heat capacity of the diesel fuel, the rated capacity of the generator and the slope and intercept coefficient from the fuel consumption curve (Fig. 3.8).

The internal heat capacity of diesel fuel is 43.2 MJ/kg [27]. Since the load was modeled in the range of 10 – 100 kW, the diesel generators was selected to have a rated capacity between 0 and 100 kW to ensure covering the entire electricity demand.

By using the fuel consumption curve of a large number of 10 – 100 kW diesel generators in the market, the values of the slope and intercept coefficient were estimated. A plot of the slope versus the rated power of the diesel generator is given in Fig. 3.13, in which the data has been fitted to a logarithmic curve. The equation displayed in this

figure was used to estimate the slope coefficient of the diesel generators in the present work.

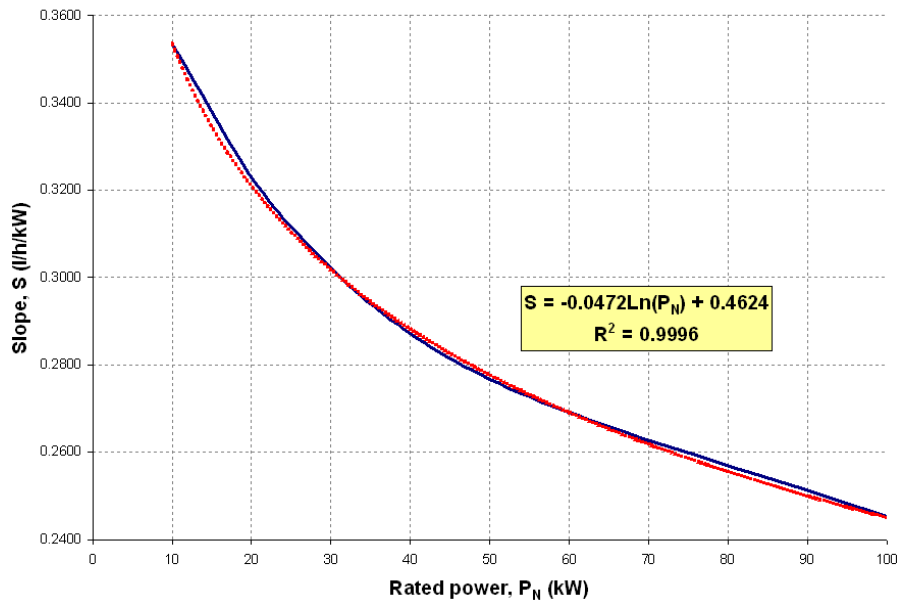


Figure 3.13 Slope curve of the diesel generator

Similarly, the intercept coefficient is plotted versus the rated power of the diesel generator in Fig. 3.14. In this case the data was found to follow a linear trend, which was used to estimate the intercept coefficient of the diesel generators in the calculations.

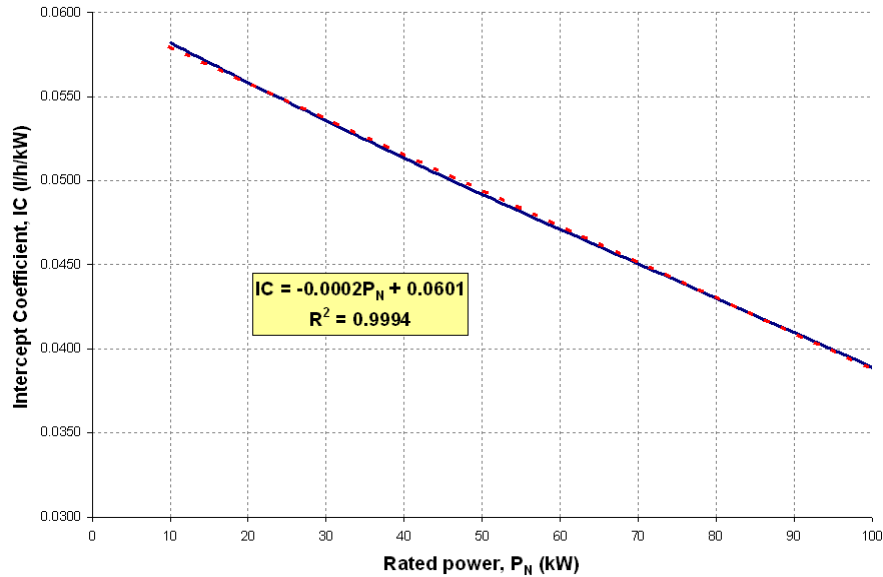


Figure 3.14 Intercept coefficient curve of the diesel generator

Batteries

A lead-acid battery will be used as the storage system for the hybrid system. Among the advantages of this type of batteries are their high reliability, little maintenance and easy installation.

Reliability is one of the most important characteristics of batteries which are to be installed in stand-alone systems. Thus, it is a good practice to select batteries from one of the top brands in the market. For this reason a Trojan L16P battery [28] was selected for this project, which was especially designed for stand-alone renewable energy systems at a cheap price.

The performance of batteries is determined by their lifetime and capacity curves. These curves for the Trojan L16P were obtained from the manufacturer's web page [28], and are given in Fig. 3.10 and Fig. 3.11, respectively. A summary of the most important parameters required to define this battery in HOMER is given in Table 3.3.

Table 3.3 Parameters of the Trojan L16P battery used in this work

Nominal voltage	6 V
Nominal capacity	360 Ah (at 20 hr. rate)
Life expectancy	5 – 10 years
Maximum DOD	80 % (assuming 300 cycles)

Inverter

As discussed in section 3.5, there are several types of inverters depending on the quality of the AC signal produced. A true sine wave type inverter will be modeled in this work for having the higher efficiency.

Since an AC generator will be used as a backup source of energy, the inverter should be able to operate simultaneously with it. Inverters that are not able to operate this way are sometimes called switched inverters.

Most inverters in the market have efficiencies between 0.85 and 0.95, and a lifetime between 10 and 20 years. Thus, a reasonable value for the inverter modeled in this work would be 0.90 and a lifetime of 15 years. The parameters used in the calculations are shown in Table 3.4.

Table 3.4 Parameters of the true sine wave inverter

Efficiency	0.90
Lifetime	15 years
Simultaneous operation with AC generator	Yes

4. DESCRIPTION OF THE ELECTRIC DEMAND

In order to evaluate the performance of the proposed PV/wind/diesel/batteries energy system, it is necessary to model an electric demand which needs to be satisfied during the entire 25 years lifetime project.

According to the U.S. Energy Information Administration [29], the energy consumption in the United States can be divided into four big groups: residential, commercial, industrial and transportation. Most of the energy in the transportation group comes from petroleum (94.5 %) whereas only a small portion of it comes from renewable sources (biomass, 3 %). Besides, it is hard to think of applications in the transportation sector that would fit into the off-grid energy system developed in this thesis. For this reason, the electric demand modeled for the calculations will not be taken into account the data from the transportation sector. Therefore, based on the Annual Energy Review 2008, the energy consumption in the other three sectors is distributed as follows (Fig. 4.1).

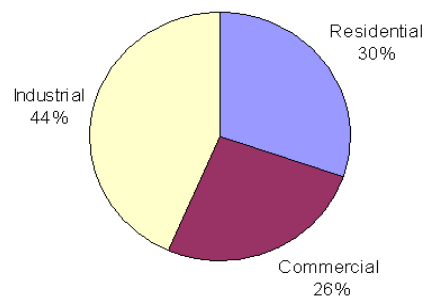


Figure 4.1. Energy consumption by sectors in the United States. Transportation sector not included

For the sake of this work, it would be very interesting to model an electric demand that fits into most part of these three categories. Therefore, some assumptions need to be made:

- 1) An off-grid system would most likely not be beneficial for large industries, in the order of several hundreds of kW's peak power, since the weight of the grid

connection costs in the overall system costs decreases as the system size increases.

- 2) The electric demand of individual households is quite variable and thus is hard to find a model that fits for all of them. But a group of households forming a small community, in the order of several kW's peak power, has an electric demand profile similar to another community since the differences tend to even out as the community size increases.

Therefore, based on these assumptions, an hourly electric demand would be modeled to fit most applications in the commercial sector (building offices, stores and small businesses), small industry and residential communities. As previously discussed, the range of peak power considered would range from several kW's to tenths of kW's. For practical purposes, this range was chosen to be 10 – 100 kW in the present study.

To better understand these numbers consider the average monthly values of electricity consumption in California (Annual Energy Review 2008) in the three sectors mentioned above:

- Residential → Energy consumption = 587 kWh/month = 19.57 kWh/day/person.
- Commercial → Energy consumption = 5,765 kWh/month = 192.17 kWh/day.
- Industrial → Energy consumption = 54,996 kWh/month = 1833.2 kWh/day.

The hourly load profile will be described as in Fig. 4.2 so it matches with the electricity demand of building offices, stores, small businesses and industry and certain small – size communities. For the weekdays, the demand increases quite fast during the first hours of the day (6 – 9 A.M.) because that is when business and stores typically start to operate, reaches the peak power during the working hours (between 9 A.M. and 5 P.M.) and then decreases progressively until it stays in a value of electricity demand needed to maintain the primary systems of the installation. During the weekends, the demand is assumed to be flat and equal to the minimum reached during the weekdays because no activity is regarded during the weekends.

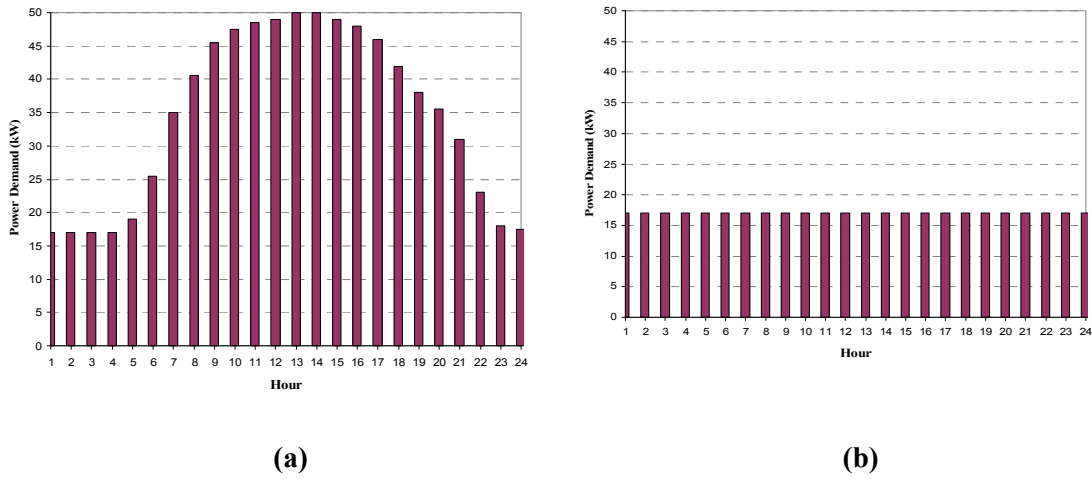


Figure 4.2 Hourly electric demand modeled in this work for weekdays (a) and weekends (b).

The load profile in Fig. 4.2 has a peak power of 50 kW and an average energy daily consumption of 627 kWh/day. Comparing this value to the average energy consumption in California gives an approximate idea of the capabilities of this system (Table 4.1).

Table 4.1 Evaluation of the energy supply capacity for the described 50 kW peak demand load profile in the United States with the same total consumption of 627 kWh/day.

	<i>Actual energy consumption</i>	<i>System capability</i>
<i>Residential</i>	19.57 kWh/day/person	32 people
<i>Commercial</i>	192.17 kWh/day	3 – 4 businesses
<i>Industrial</i>	1833.2 kWh/day	1/3 industry

The AC load profile described herein will be used to model the electricity needs of a hybrid PV/wind/diesel generator/batteries system. Since it is desired to evaluate the

optimum size of this system over a variety of energy demands, the load profile will be scaled proportionally to account for this factor. More specifically, the load profile in Fig. 4.2 will be scaled such that the peak electricity demand is 10, 20, 50 and 100 kW. This will allow studying size scalability factors of the system with varying electricity demands. In practical terms, it will help in the prediction of the optimum system size for different electricity demands other than those studied in this work.

5. THE OPTIMIZATION METHOD

The optimization of an off-grid hybrid power system involves finding the number and size of components that would produce the lowest net present cost over the entire lifetime of the system (typically between 20 and 30 years) while satisfying an specific electric demand at all times.

However, there are several factors that may make this optimization process very complex and time-consuming. Some of these factors are the increased number of components, as compared with systems consisting only of solar PV panels or wind turbines; the variability of the renewable resources with time; the difficulty in predicting the diesel fuel price over the project lifetime; the need for modeling the electric demand in hourly increments for a better approximation; the change of installation and O&M costs with the system size.; the interdependency of components in the overall performance and the large number of parameters that need to be defined.

Due to these factors, the optimal system size was found using HOMER (Hybrid Optimization Model for Electric Renewables), a software developed by the National Renewable Energy Laboratory, NREL. Homer's computational engine is based on an enumerative method that simulates all possible combinations of the hybrid system for every hour of the year and provides the lowest life-cycle cost for those configurations that meet the required loads.

As previously discussed in chapter 1, the hybrid system shown in Fig. 1.1 was optimized. This system may include an array of photovoltaic panels, wind turbines, a diesel generator, a bank of lead-acid batteries and an inverter.

The goal is to optimize this system for several values of solar insolation and wind speed within the United States and for different values of the peak electric demand when the hourly profile follows the pattern described in section 4 of this work. This will allow studying how the optimal size of this system develops with changing insolation, wind speed or electric demand.

The values used in the simulations are given below:

- Solar insolation → 4.5 – 6.5 kWh/m²/day, in 0.5 kWh/m²/day increments.
- Wind speed → 4.0 – 8.0 m/s, in 1 m/s increments.
- Peak electric demand → 10, 20, 50 and 100 kW.

Therefore the number of simulations that need to be performed can be calculated by the product of all possible system configurations:

$$\text{Nr. Simulations} = (\# \text{ of insolation values}) \times (\# \text{ of wind speed values}) \times (\# \text{ of peak demand values}) = 5 \times 5 \times 4 = 100$$

For each of these simulations the flow diagram shown in Fig. 5.1 was used. This process can be broken down into three stages:

- Data entry and initial simulation.
- Initial system refinement and evaluation of preliminary results.
- Iteration of subsequent system refinements and generation of the final solution.

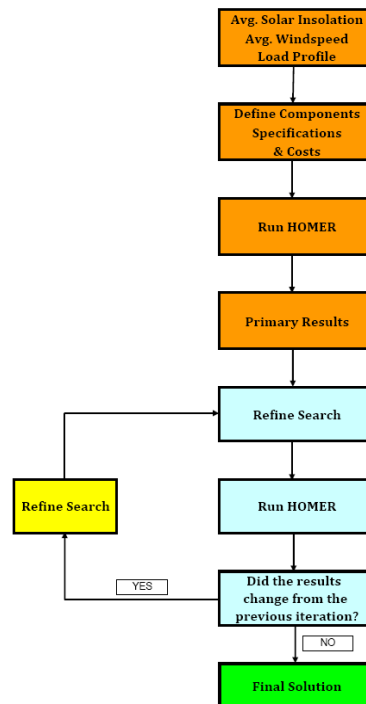


Figure 5.1 Simulation flow diagram used to compute the optimum size of the hybrid renewable system

1st Stage: Data entry and initial simulation

In this initial stage of the simulations, the data of the average monthly renewable resources values and peak electricity demand was inputted. After the simulation of this system configuration is completed, its optimum size would be achieved which represents the number of solar PV panels, wind turbines, batteries, diesel generator size and required inverter capacity needed to minimize the net present cost of the entire 25 years lifetime of this system. The average values of insolation and wind speed are quite dependant on the latitude and longitude of the system location which, for practical purposes, can be found from the “*NASA Surface meteorology and Solar Energy Data Set* [12]

To perform the simulations, a general monthly insolation distribution was created for the United States using the information in the above data base considering different regions in the country. The reasoning under this generalization is that due to the short range of latitude and longitude considered, the monthly distribution geometry of the insolation would not change considerably within the United States. This monthly distribution was then scaled proportionally to the annual insolation values considered in this work (4.5 – 6.5 kWh/m²/day, in 0.5 kWh/m²/day increments).

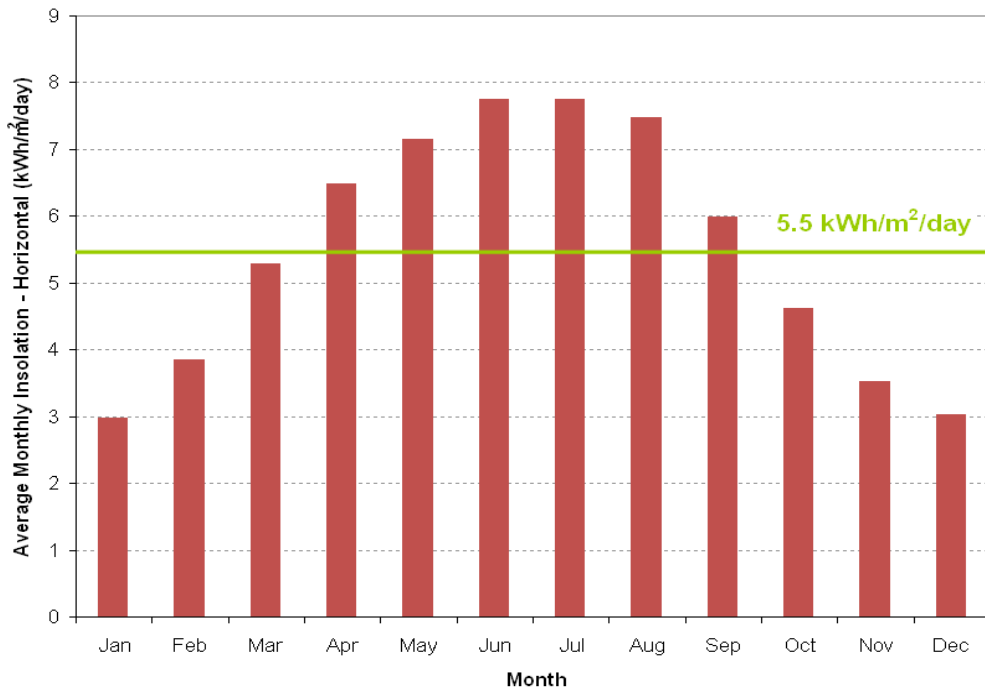


Figure 5.2 Average annual insolation distribution considered in this thesis.

As regards the wind speed distribution, it is quite changeable throughout an entire day and also between consecutive days, although it does not change much in a monthly scale. The parameters required to describe the daily variability of wind speed are provided in section 2.4 whereas the monthly wind speed distribution will be considered to be constant.

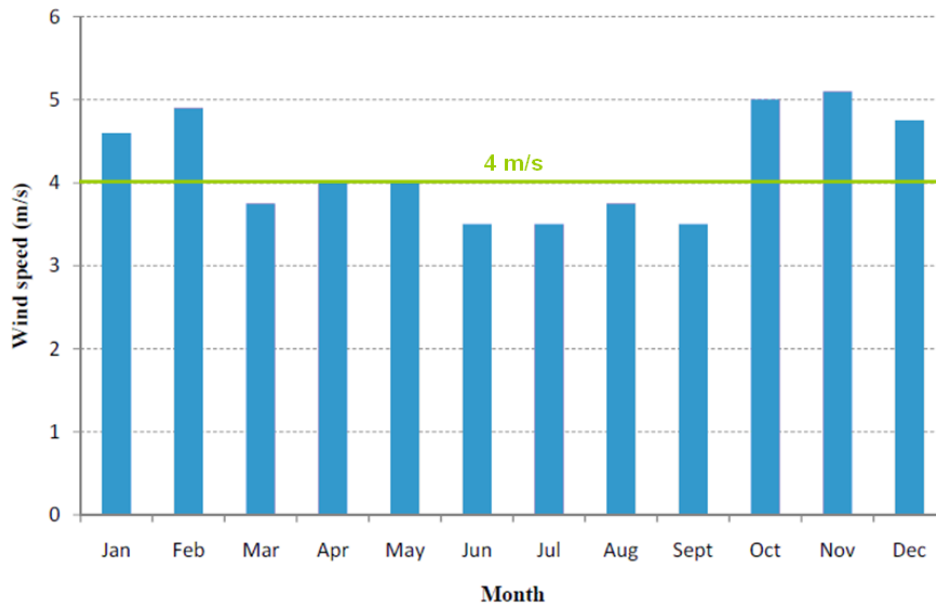


Figure 5.3 Average annual wind speed distribution considered in this thesis.

Next, it is necessary to input the technical specifications of the solar panels, wind turbines, diesel generators, batteries and inverters, as well as their installation, replacement and O&M costs. The technical specifications and parameters required for the simulation in HOMER are given in section 3.6, and the economic description is provided in Appendix B.

At this point, HOMER has all the needed parameters to perform the simulations and an estimate size of the system has to be inputted (this represents the initial solution in the algorithm). Since the optimal size is initially unknown, a range for the possible initial solutions needs to be given.

$$x = (x_1 + x_2 + x_3 + x_4 + x_5)$$

where x_1 is the size of the PV array (kW), x_2 is the number of wind turbines, x_3 is the size of the diesel generator (kW), x_4 is the number of batteries and x_5 is the inverter size (kW).

Also, each of these variables can be modeled as an $n \times 1$ array, with each of the elements in the array representing a possible size for that variable. For example, the array,

$$x_1 = \begin{bmatrix} 0 \\ 10 \\ 30 \\ 65 \end{bmatrix}$$

represents four different PV array sizes, in kW, that HOMER will simulate. This approach can be done for each of the five variables defined in the program, although increasing the size of these arrays will translate into higher simulation times (the simulation time of each feasible system configuration typically takes around 10 seconds). Therefore, it is more efficient to work with smaller arrays, run the program with these values to obtain an approximation of the optimal system size and refine the search for subsequent simulations using these results.

Since the optimal size of the system is initially unknown, in this stage of the optimization method is recommended to use relatively large arrays (around 8 to 10 elements per array) trying to cover a wide spectrum of possible solutions. For example, for the PV array size, if the peak electric demand is 50 kW then a good initial solution would be,

$$x_1 = [0, 10, 20, 30, 40, 50, 60, 70, 80, 90] \text{ kW of the PV array}$$

A similar approximation may be done for the remaining four variables of the system.

2nd Stage: Initial system refinement and evaluation of preliminary results

After the first simulation is completed, an initial but not very accurate approximation of the optimal system size is obtained. This solution might look like:

$x_1 = [0, 10, 20, \mathbf{30}, 40, 50, 60, 70, 80, 90]$	<i>kW of the PV array</i>
$x_2 = [0, 5, 10, \mathbf{15}, 20, 25, 30, 35]$	<i>number of wind turbines</i>
$x_3 = [0, \mathbf{50}]$	<i>kW rated power of generator</i>
$x_4 = [8, 16, 24, 32, 40, 48, \mathbf{56}, 64, 72, 80]$	<i>number of batteries</i>
$x_5 = [40, 43, 46, 49, \mathbf{52}, 55, 58, 61, 64]$	<i>kW of inverter capacity</i>

where the optimum solution is represented in bold. For this initial simulation, HOMER determined the feasibility of all possible system configurations, which in the case shown above is,

$$\text{Nr. of configurations} = (10 \text{ PV array sizes}) \times (8 \text{ wind turbine sizes}) \times (2 \text{ diesel generator sizes}) \times (10 \text{ batteries}) \times (9 \text{ inverter sizes}) = 14,400$$

But not all of these system configurations are feasible. If for example only 1% of these simulations represents feasible configurations and, as previously mentioned, each feasible solution takes about 10 seconds of running time, then the total time to perform this initial simulation would be around 24 minutes. Once all the feasible solutions are found, the net present cost of all of them is calculated over the project's lifecycle, which for this work it was assumed to be 25 years.

By analyzing the above results, a new but more refined solution set can be found by delimiting the possible array of solutions to the closer neighbors at both sides of the optimum solution of the considered array.

$x_1 = [20, 22, 24, 26, \mathbf{28}, 30]$	<i>kW of the PV array</i>
$x_2 = [10, 12, \mathbf{14}, 16, 18, 20]$	<i>number of wind turbines</i>
$x_3 = [0, \mathbf{50}]$	<i>kW rated power of generator</i>
$x_4 = [\mathbf{48}, 50, 52, 54, 56, 58, 60, 62, 64]$	<i>number of batteries</i>
$x_5 = [49, \mathbf{51}, 53, 55]$	<i>kW of inverter capacity</i>

A similar analysis can be done for this simulation. As expected, the number of configurations is reduced to,

$$\text{Nr. of configurations} = (6 \text{ PV array sizes}) \times (6 \text{ wind turbine sizes}) \times (2 \text{ diesel generator sizes}) \times (9 \text{ batteries}) \times (4 \text{ inverter sizes}) = 2,592$$

Now assume that the percentage of feasible configurations increased, say to 4%. Then, the running time is 17 minutes.

This system configuration is not the optimal, but it is very close to it since we reduced the range considerably. The new NPC is calculated and observed to be smaller than the previous one, which is a good sign that the simulations are being carried out successfully. At this point, it would be a good idea to update the PV array installation costs, since they depend on the size of the PV array, before moving on to next stage of the simulations.

3rd Stage: Iteration of subsequent system refinements and generation of the final solution.

In this final stage, the system is refined iteratively in the same manner than in the previous stage until the final solution is found. Because we are very close to the optimum, for each of these iterations the PV array installation costs need to be updated or otherwise some precision will be lost.

The final solution is achieved when the range in each of the arrays cannot be further reduced. Even though technically some variables (like the PV array size) could be refined to a different order of magnitude, a precision of one unit will be regarded as good enough for the sake of this work.

The final solution might look like,

$x_1 = [26, 27, 28, \mathbf{29}, 30]$	<i>kW of the PV array</i>
$x_2 = [12, \mathbf{13}, 14, 15, 16]$	<i>number of wind turbines</i>
$x_3 = [0, \mathbf{50}]$	<i>kW rated power of generator</i>
$x_4 = [45, \mathbf{46}, 47, 48, 49, 50]$	<i>number of batteries</i>
$x_5 = [49, 50, \mathbf{51}, 52, 53]$	<i>kW of inverter capacity</i>

The number of configurations is then,

$$\text{Nr. of configurations} = (5 \text{ PV array sizes}) \times (5 \text{ wind turbine sizes}) \times (2 \text{ diesel generator sizes}) \times (6 \text{ batteries}) \times (5 \text{ inverter sizes}) = 1,500$$

for a running time of 10 minutes

The method proposed in this section will be applied iteratively until the optimum results for each of the system combinations are obtained. The time consumed for each combination can be drastically reduced if the results from previous simulations are considered before setting up the arrays for each component's size. In most of the cases, a small change in one variable, such as the wind speed or the insolation values, would produce small variations in the optimum system size. Thus, the results from the previous simulation would typically be a good starting point to set up the arrays. This approach was followed in the present work, resulting in a great amount of time saved.

6. GENERATION AND ANALYSIS OF RESULTS

The optimization method described in Ch. 5 was applied to obtain the optimum size and lifetime cost of the system for the given values of insolation, wind speed values, and different electric demands (Fig. 6.1).

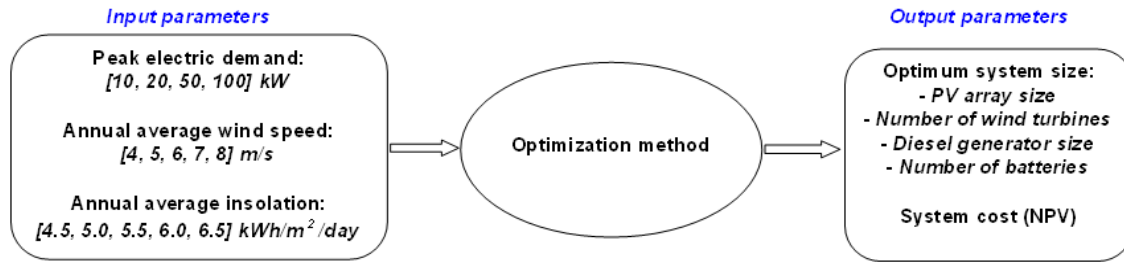


Figure 6.1 Diagram of the optimization technique followed in the generation of results.

After each simulation is completed, HOMER displays a window of the optimum system configuration for the given input parameters and a summary of other important economic and performance results (Fig. 6.2).

	PV (kW)	w500	G50 (kW)	L16P	Conv. (kW)	Initial Capital	Operating Cost (\$/yr)	Total NPC	COE (\$/kWh)	Ren. Frac.	Diesel (L)	G50 (hrs)	Batt. Li. (yr)
	1	31	50	94	55	\$ 376,421	44,549	\$ 945,910	0.323	0.71	35,680	3,494	5.4
		30	50	96	55	\$ 372,823	45,083	\$ 949,132	0.324	0.70	35,864	3,499	5.2

Figure 6.2 The results window displayed in HOMER after each simulation.

In the example shown in Fig. 6.2, the two possible system configurations to satisfy the electric demand are given in two separate rows. However, the optimal configuration (lower net present value, NPV) is given in the top row and will consist of zero PV panels, 31 wind turbines, a 50 kW diesel generator, 94 batteries and a 55 kW converter. Three other economic results are given along with the NPV: the initial cost of the system, the annual operating cost and the cost of electricity (COE). The last four columns represent the fraction of renewable energy used, the annual volume of diesel fuel that needs to be

purchased, the hours per year the diesel generator should work and the calculated battery lifetime. The last row represents another feasible system configuration including a 1 kW array of PV panels.

6.1. SYSTEM SIZE DEPENDENCE ON THE INSOLATION INTENSITY

Due to the large amount of results generated, and since the analysis pertaining to a given peak electricity demand also applies to the other electricity demands, only part of it will be shown and discussed in this section. The results for the remaining peak electricity demands were observed to have a similar behavior and are given in Appendix C.

To analyze the dependence of the optimal system size with the insolation intensity, the results for the 50 kW peak electricity demand, which lies in the midpoint of the considered range, are given in Table 6.1 below.

Table 6.1 Optimization results for the 50 kW peak demand system. Results sorted by insolation values for each wind speed.

50 kW peak demand						
Insolation (kWh/m ² /day)	Windspeed (m/s)	PV panels (kW)	Wind Turbines	Generator (kW)	Batteries	Inverter (kW)
4.5	4	24	1	40	24	19
4.5	5	4	32	40	54	54
4.5	6	0	32	40	70	55
4.5	7	0	30	50	118	55
4.5	8	0	26	40	84	55
5.0	4	36	9	30	46	31
5.0	5	27	26	30	44	54
5.0	6	3	31	40	58	55
5.0	7	0	27	45	76	55
5.0	8	0	26	40	84	55
5.5	4	60	3	30	26	55
5.5	5	32	24	30	42	55
5.5	6	22	26	30	46	55
5.5	7	0	28	40	68	55
5.5	8	0	26	40	84	55
6.0	4	60	2	30	26	55
6.0	5	40	20	30	42	55
6.0	6	25	25	30	40	55
6.0	7	16	24	30	48	55
6.0	8	0	26	40	62	55
6.5	4	59	1	30	28	55
6.5	5	43	18	30	42	55
6.5	6	24	25	30	40	55
6.5	7	17	24	30	46	55
6.5	8	10	24	30	48	55

To facilitate the visualization of this dependence, the results are sorted in increasing order of insolation intensity for each value of wind speed between 4 and 8 m/s.

As one can easily expect, the size of the PV array for a fixed wind speed increases with increasing insolation. A plot of this dependency is shown in Fig. 6.3. Notice that the curves in this plot do not exhibit a perfectly linear trend because of the highly nonlinear nature of the system. Nonlinearities arise mainly from the random variability of the resources and the performance of the renewable components of the system. As seen in Ch. 2, the amount of both insolation and wind speed is highly variable throughout a year. Thus, it is impossible to find linear models to accurately describe the renewable resources. Additionally, the power produced by the components of the hybrid system does not exhibit a linear trend with the amount of resources received. This can be observed in the I-V curve of a solar panel, Fig. 3.4, or in the power curve of the wind turbine, Fig. 3.12. These two effects combined cause a lack of proportionality between the five cases seen in Fig. 6.3.

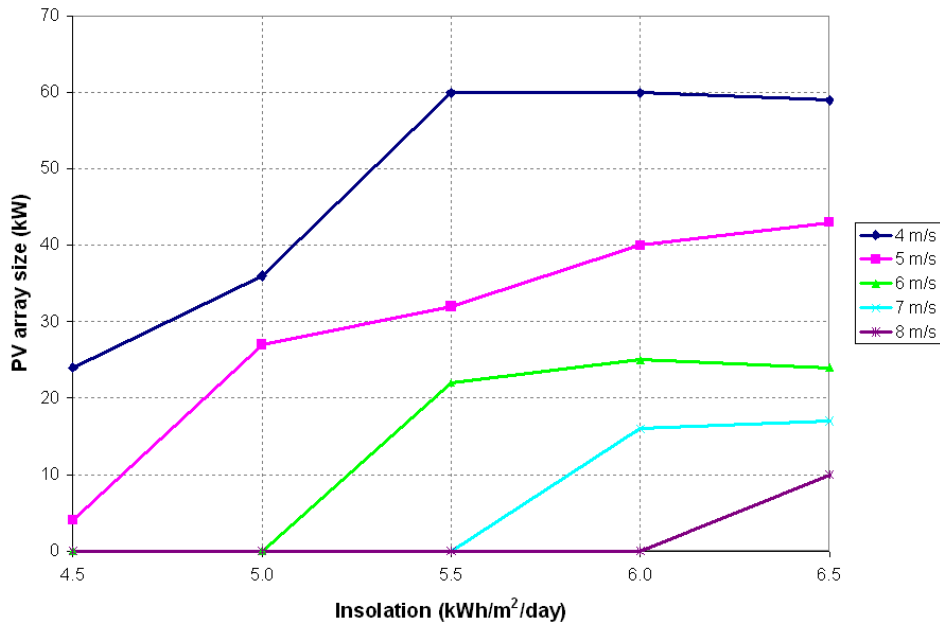


Figure 6.3 PV array size versus insolation intensity for different wind speeds and for a 50 kW peak electricity demand.

More importantly is to analyze how the PV array size increases with increasing wind speed. When stronger winds are available, the importance of solar panels is shadowed by the wind turbines (Fig. 6.4). By studying Fig. 6.3 and Fig. 6.4 together it is clear that when weak winds of 4 m/s are present, the weight of the PV array in the system is very significant as compared to the importance of wind turbines, whereas in strong winds environments (7 – 8 m/s) wind turbines are the predominant renewable energy component. In these cases, only when the insolation reaches a relatively high value then the solar panels start to be considered in the optimum system.

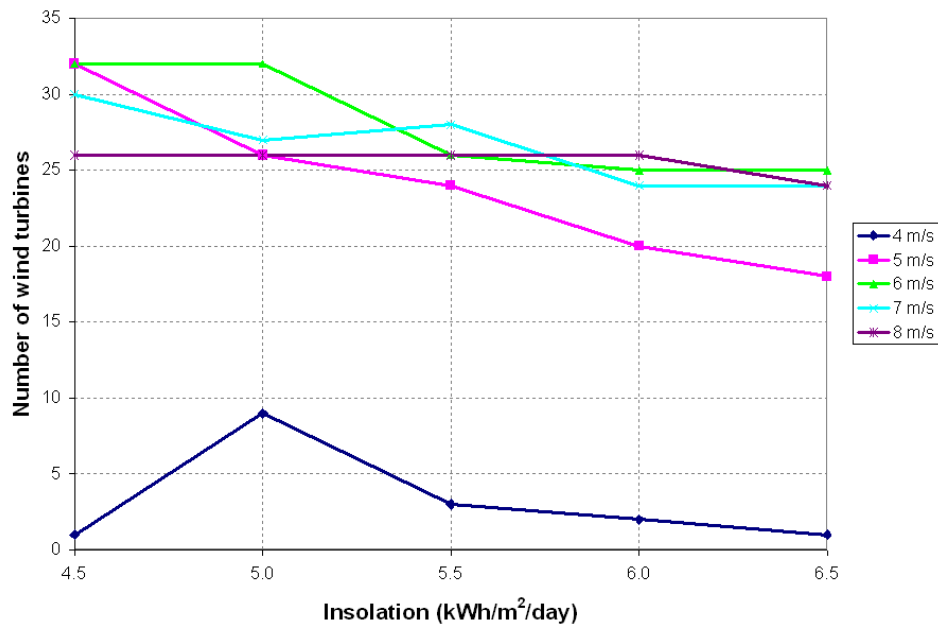


Figure 6.4 Number of wind turbines versus insolation values for different wind speeds and for a 50 kW peak electricity demand.

A special attention should be paid to the 4 m/s case in Fig. 6.4 since it does not seem to follow the trend of the other four curves. The reason is that the wind turbine selected for this work has a cut-in wind speed of 3.5 m/s and it will not start working below this wind speed value. The technical specifications of the wind turbine used in this work were given in Section 3.6. If the average wind speed is 4 m/s, only a small portion of the energy in the wind will be converted into electricity in the wind turbine, and not in a very effective manner. Increasing the average wind speed to 5 m/s and above enables

the wind turbine to work more efficiently and collect a bigger portion of the wind energy, thus making the use of wind turbines a good alternative.

Over the limiting wind speed value of 4 m/s, the optimum system includes a larger number of wind turbines as shown in Fig. 6.4. Two different trends are observed in the range of 5-8 m/s: first, under low insolation values between 4.5 and 5.5 kWh/m²/day the contribution of wind turbines decreases as wind speed increases. Second, between 5.5 and 6.5 kWh/m²/day the importance of wind turbines becomes higher with increasing wind speed. These two behaviors are explained by looking at the power curve of the wind turbine modeled in this work, Fig. 3.12. Under higher wind speeds, the wind turbine is capable of generating more energy than with weaker wind speeds. Thus, although at low insolation values the number of wind turbines is smaller with higher wind speeds, these turbines generate a larger amount of energy. The actual amount of energy generated by the wind turbines for each case will be studied in section 6.4 in this chapter. In other words, as wind speed increases, a smaller number of wind turbines is required to produce a bigger amount of energy. As the insolation increases, the contribution of PV panels in the system becomes more important, as seen in Fig. 6.3. This explains the decaying trend of the number of wind turbines as the insolation increases.

A final result is obtained by analyzing the system size in the presence of very high (or very low) solar radiation and wind speed. When very strong winds and very high insolation are present at a particular location, it is more likely that the optimum system will consist of mostly wind turbines. This result can be extracted by analyzing the 8 m/s curve with 6.5 kWh/m²/day together in Fig. 6.3 and Fig. 6.4. The reverse result is also true: when low insolation values and low wind speeds are available, the system will have a higher proportion of solar panels than wind turbines. Therefore, solar panels seem to be a better alternative for renewable systems installed at locations with very poor solar and wind resources, whereas wind turbines are the best solution for locations having high values of insolation and wind speed.

From the results in Table 6.1 it is difficult to analyze the role of the diesel generator in the overall system. The calculated optimum size of the generator, which ranges between 30 and 50 kW, does not provide enough information on its annual energy

production. The reason is that the time the generator is being operated should be accounted for in the calculation of the annual energy production. An extensive analysis of this fact will be carried out in section 6.4, where the annual energy production of each component is studied.

By looking simultaneously at the optimum generator and inverter size, an estimate of the generator usage can be obtained. The optimum inverter size shown in Table 6.1 is given in kW of DC power. Recall that the electricity demand has a peak in AC of 50 kW and the inverter was assumed to be 90 % efficient. Thus, in order to satisfy this demand exclusively with the DC components, according to Eq. 3.19 the inverter size should be,

$$P_{DC} = P_{AC} / \eta_{inv} = (50 \text{ kW}) \times 0.9 \approx 55 \text{ kW}$$

This means that the systems in Table 6.1 with an inverter rated at 55 kW make an optimum usage of the renewable resources and the batteries. In this case, the diesel generator is being used only as a backup energy source. On the other hand, there are a few cases with an optimum inverter size less than 55 kW, for which an opposite reasoning can be applied. If a smaller inverter is required then a smaller portion of the energy is delivered by the DC components. In fact, this only happens when the insolation and wind speed values take very small values. Under these conditions solar panels and wind turbines do not work efficiently. Thus, a larger portion of the energy should come in AC from the diesel generator to meet the electricity demand explaining why a smaller inverter is needed.

Finally, from the results given in Table 6.1 it is observed that the number of batteries increases as the average wind speed increases or the insolation intensity decreases, although the latter case is not so clear (Fig. 6.5).

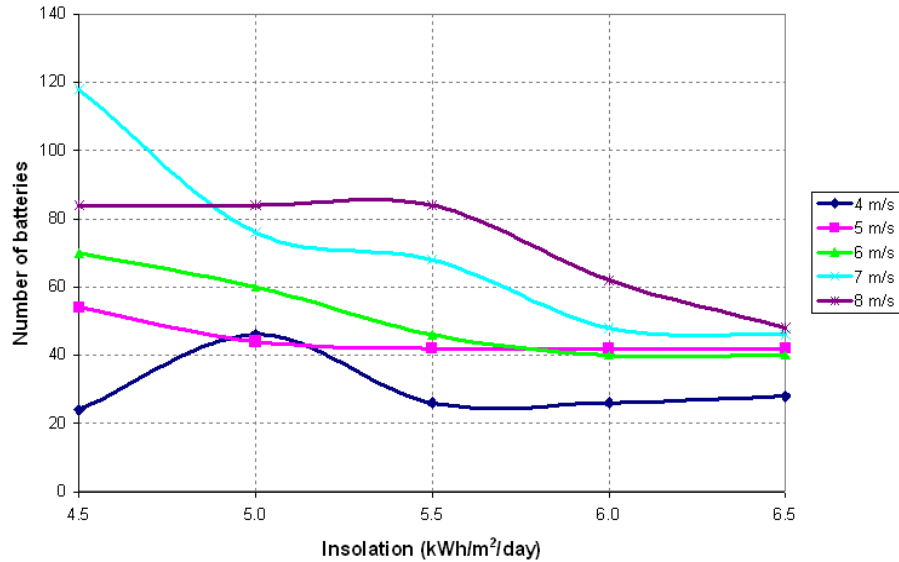


Figure 6.5 Number of batteries versus wind speed for different insolation values and for a 50 kW peak electricity demand.

The availability of stronger winds at a particular location translates into having a more reliable source of energy and thus, the dependence on the diesel generator becomes smaller. Therefore, more energy is generated with the wind turbines and less with the generator, so this larger amount of energy needs to be stored in more batteries. The dependence of the number of batteries with the insolation is not so clear, although a slight reduction of the number of batteries is observed when the insolation intensity increases. Unlike the wind speed distribution which does not show great fluctuations throughout an entire day, the distribution of solar radiation experiences abrupt changes between the day and the night. Hence, in the case of low insolation values, the diesel generator gains more weight in the overall system which can be used to supply energy, charge the batteries or both.

The optimum size of the diesel generator shown in Table 6.1 only provides information about the maximum amount of electricity that it will eventually need to generate. Most importantly is to study when the generator will be used as either a backup source of energy or as one of the main energy generation components of the system. For this analysis, the amount of energy produced by the generator needs to be studied

together with the optimum inverter size. The size of the inverter is a very good indicator of the generator usage in the system. When small inverters are required in the system, little energy is generated in DC and, thus, most of the energy is produced by the AC diesel generator. The reverse result is also true: large inverters means little energy produced by the AC generator and more by PV panels and wind turbines. This analysis will be carried out extensively in section 6.4 of this chapter

6.2. SYSTEM SIZE DEPENDENCE ON THE WIND SPEED INTENSITY

The next step is to study the effect of the wind speed over the optimal system size keeping the insolation values fixed. By using again the results from the 50 kW peak electricity demand case, the previous results will be validated as well as new others obtained. The results for the remaining peak electricity demands were observed to have a similar behavior and are given in Appendix C.

Table 6.2 shows the same results than in Table 6.1 but re-arranged to show the dependence of the 50 kW peak demand system size with the considered wind speed range for every (fixed) value of solar radiation.

Table 6.2 Optimization results for the 50 kW peak demand system. Results shorted by wind speed values for each insolation intensity value.

50 kW peak demand						
Insolation (kWh/m ² /day)	Windspeed (m/s)	PV panels (kW)	Wind Turbines	Generator (kW)	Batteries	Inverter (kW)
4.5	4	24	1	40	24	19
5.0	4	36	9	30	46	31
5.5	4	60	3	30	26	55
6.0	4	60	2	30	26	55
6.5	4	59	1	30	28	55
4.5	5	4	32	40	54	54
5.0	5	27	26	30	44	54
5.5	5	32	24	30	42	55
6.0	5	40	20	30	42	55
6.5	5	43	18	30	42	55
4.5	6	0	32	40	70	55
5.0	6	3	31	40	58	55
5.5	6	22	26	30	46	55
6.0	6	25	25	30	40	55
6.5	6	24	25	30	40	55
4.5	7	0	30	50	118	55
5.0	7	0	27	45	76	55
5.5	7	0	28	40	68	55
6.0	7	16	24	30	48	55
6.5	7	17	24	30	46	55
4.5	8	0	26	40	84	55
5.0	8	0	26	40	84	55
5.5	8	0	26	40	84	55
6.0	8	0	26	40	62	55
6.5	8	10	24	30	48	55

Looking separately at each of the five sets of insolation – wind speed values it is very noticeable that, as the average wind speed value increases, so does the number of wind turbines whereas the size of the PV array decreases. Since more wind energy becomes available to the system, it turns out to be more efficient to generate the electricity with wind turbines and, therefore, less solar panels are required.

This result is shown graphically in Fig. 6.6 and Fig. 6.7, where the influence of the wind speed is graphed versus the PV array size and the number of wind turbines, respectively. The negative slope in each of the five curves in Fig. 6.6 represents that as the wind speed increases, the PV array size decreases.

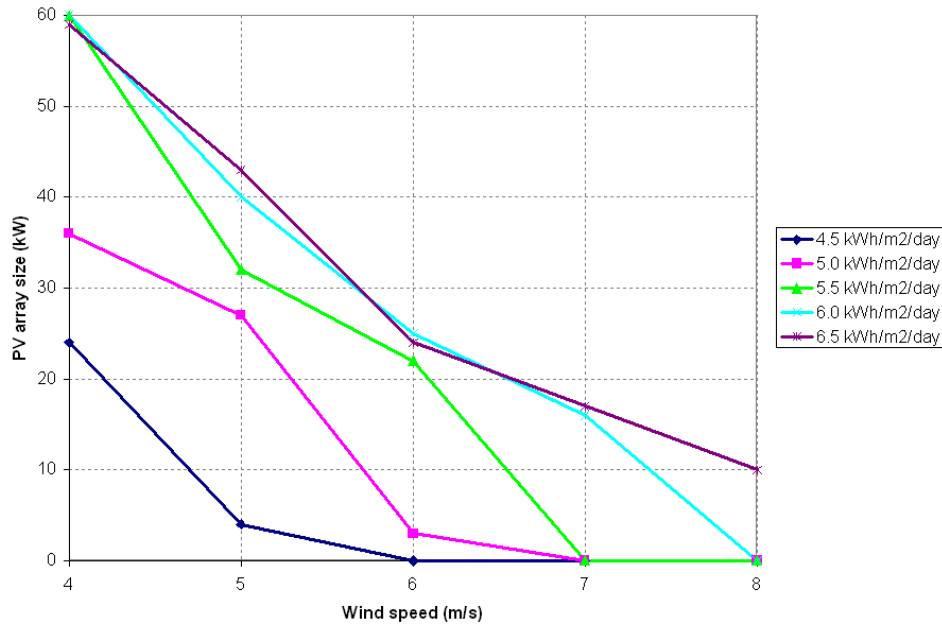


Figure 6.6 PV array size versus wind speed for different insolation values and for a 50 kW peak electricity demand.

As mentioned above, an increase in the wind speed (for a fixed insolation value) results in an increased number of wind turbines. By studying Fig. 6.6 and Fig. 6.7 together, one can draw important conclusions about how the optimum system size changes with varying insolation. Since PV panels do not perform well under low

insolation values, the size of the PV array is expected to be small. Thus, the energy needs to be supplied by a larger number of wind turbines. This effect is very apparent in the 4.5 and 5.0 kWh/m²/day cases shown in both figures. On the other side, high insolation values translate into a larger amount of energy collected by the PV panels, explaining why a larger PV array is required in the optimum system, as seen in Fig. 6.6 for high insolation values. Since more energy is supplied by the PV panels, less wind turbines are needed (Fig. 6.7).

Furthermore, when Fig 6.4 was discussed the number of wind turbines was found to be very small in the presence of low wind speeds. This result can be corroborated when looking at the curves in Fig. 6.7 in the range of 4 – 5 m/s, where the wind turbines selected for this study do not seem to work efficiently under 3.5 m/s winds.

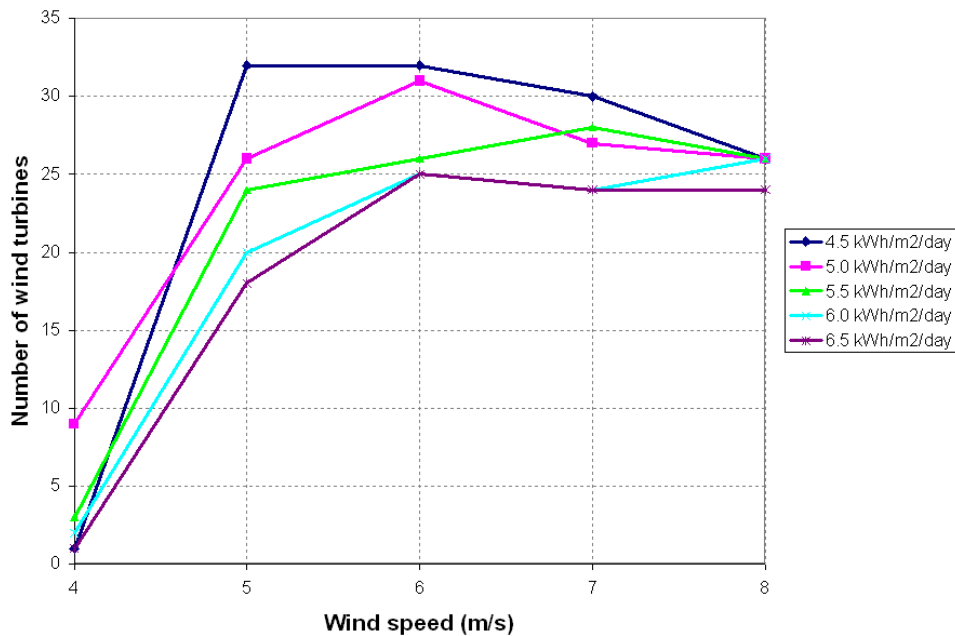


Figure 6.7 Number of wind turbines versus wind speed for different insolation values and for a 50 kW peak electricity demand.

In this case, the results of the optimum inverter size provide much more useful information on the generator usage. It helps to identify the breaking point over which the

diesel generator is being used only as a backup source of energy. Table 6.2 shows that when the insolation is below $5.0 \text{ kWh/m}^2/\text{day}$ and the wind speed is below 4 m/s , the inverter has a rated power below 55 kW . As discussed in section 6.1, this is a sign that diesel generator is being used as one of the main sources of energy for the system.

However, as seen in Fig. 6.4, with winds below 4 m/s the energy must be supplied by other components other than the wind turbines. With insolation values below $5.5 \text{ kWh/m}^2/\text{day}$ the optimum system configuration includes solar panels and a diesel generator as the main sources of energy. Over $5.5 \text{ kWh/m}^2/\text{day}$, the only component delivering a large amount of energy to the system is the PV array; in this case the diesel generator is used as backup and a few wind turbines are included to generate electricity during occasional wind gusts.

6.3. SYSTEM SIZE DEPENDENCE ON THE ELECTRICITY DEMAND

So far the analysis has been performed for a fixed peak electricity demand of 50 kW . It would be very interesting to analyze how the system size changes along the considered range of electricity demands (recall $10 - 100 \text{ kW}$) keeping fixed either the wind speed or the insolation value.

6.3.1 RESULTS FOR A FIXED WIND SPEED

First, consider the optimization results obtained with HOMER for a 6 m/s wind speed for different values of peak electricity demand and insolation intensity (Table 6.3). This wind speed value was chosen as the reference point for lying in the middle point of the considered range of wind speeds, although the results for other wind speeds share a similar trend. A table containing the optimization results for different wind speeds can be found in Appendix C at the end of this work.

Table 6.3 Optimization results for a 6 m/s fixed wind speed. Results sorted by peak electricity demand for each insolation intensity value.

Wind speed 6m/s						
Peak Demand (kW)	Insolation (kWh/m ² /day)	PV panels (kW)	Wind Turbines	Generator (kW)	Batteries	Inverter (kW)
10.0	4.5	0	8	10	54	11
20.0	4.5	1	15	15	116	23
50.0	4.5	0	32	40	70	55
100.0	4.5	0	56	80	104	110
10.0	5.0	2	7	10	56	11
20.0	5.0	1	13	15	38	22
50.0	5.0	0	32	40	60	55
100.0	5.0	0	56	80	104	110
10.0	5.5	4	6	10	60	11
20.0	5.5	11	10	10	28	22
50.0	5.5	22	26	30	46	55
100.0	5.5	37	47	65	78	110
10.0	6.0	8	6	5	102	11
20.0	6.0	11	11	10	30	22
50.0	6.0	25	25	30	40	55
100.0	6.0	39	46	65	78	110
10.0	6.5	10	5	10	76	11
20.0	6.5	11	11	15	88	23
50.0	6.5	24	25	30	40	54
100.0	6.5	48	45	60	64	110

A quick look at the results reveals that solar panels are not a good option for locations with insolation below 5.0 kWh/m²/day. Thereafter, the required size of the PV array increases almost linearly with increasing peak demand, which can be seen in Fig. 6.8. This result is very important since this value of insolation represents the limit under which the use of PV panels is not a feasible option for this system, no matter what the electricity demand is.

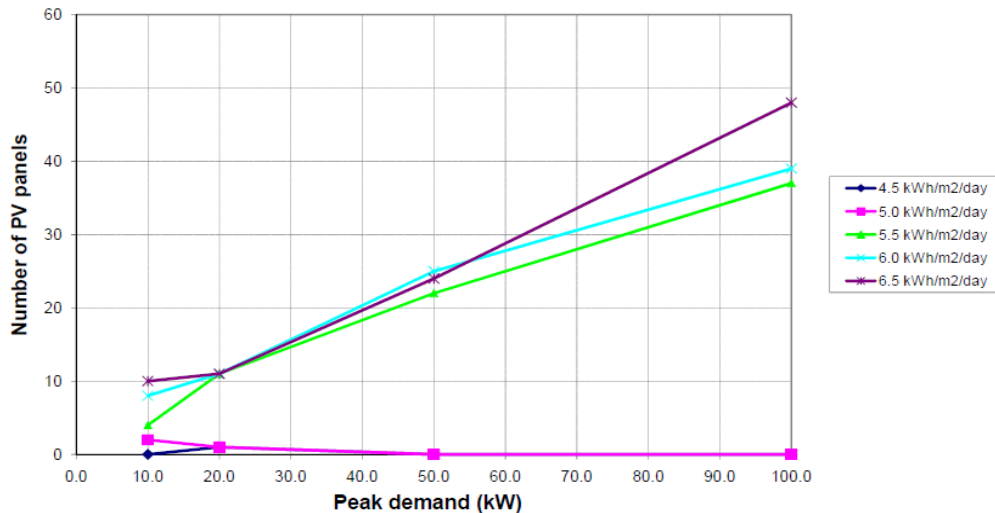


Figure 6.8 PV array size versus peak electricity demand for different insolation values and for a 6 m/s wind speed location.

A plot of the number of wind turbines versus the peak electricity demand (Fig. 6.9) reveals that for an average wind speed of 6 m/s the use of wind turbines is justified for the entire range of insolation intensity, since solar radiation is not a factor in the performance of wind turbines. The curves exhibit a linear proportionality, noticing that for high insolation values the curves are shifted down by a small factor meaning that part of the energy demand will also be supplied by solar panels since the insolation intensity reached the breaking point mentioned before over which the solar panels represent a feasible alternative to the system.

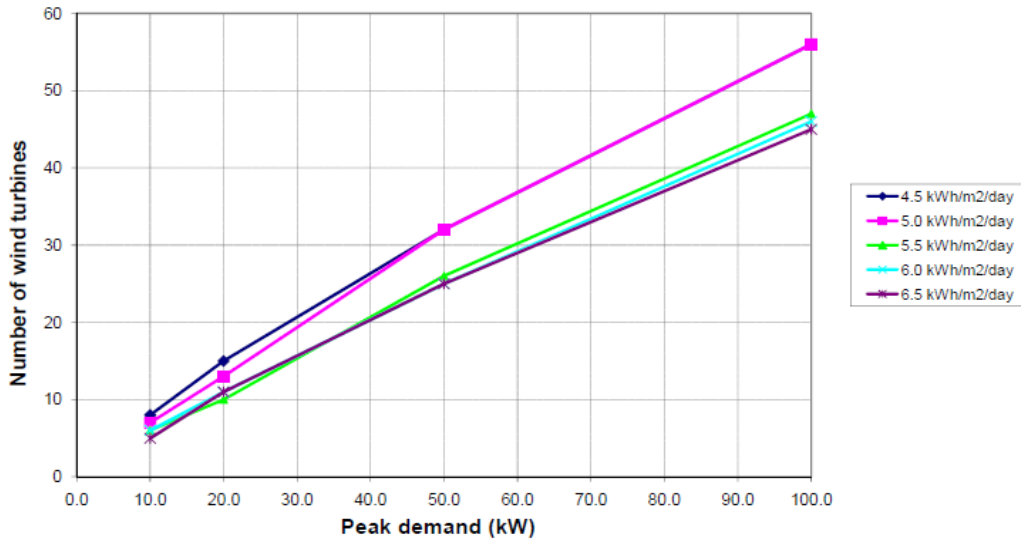


Figure 6.9 Number of wind turbines versus peak electricity demand for different insolation values and for a 6 m/s wind speed location.

Therefore, below an insolation intensity value of 5.0 kWh/m²/day the energy demand will be covered mostly by wind turbines and the diesel generator. On the other hand, when the insolation value is above 5.0 kWh/m²/day then the electricity demand is covered by a combination of wind turbines, solar panels and a diesel generator.

According to the results in Table 6.3, the inverter size for each system configuration is optimized such that it will convert the maximum amount of DC power into AC. In other words, the diesel generator will be used exclusively as a backup source of energy for the system. The amount of energy produced by the generator for each

system configuration can be estimated from the results in Table 6.3. This can be done by assuming that larger generators are used to produce higher amounts of energy. Additionally, an accurate study of the amount of annual energy produced by the generator for each system configuration is given in section 6.4. The plot in Fig. 6.10 shows the optimum generator size versus the considered electricity demand range for different insolation values.

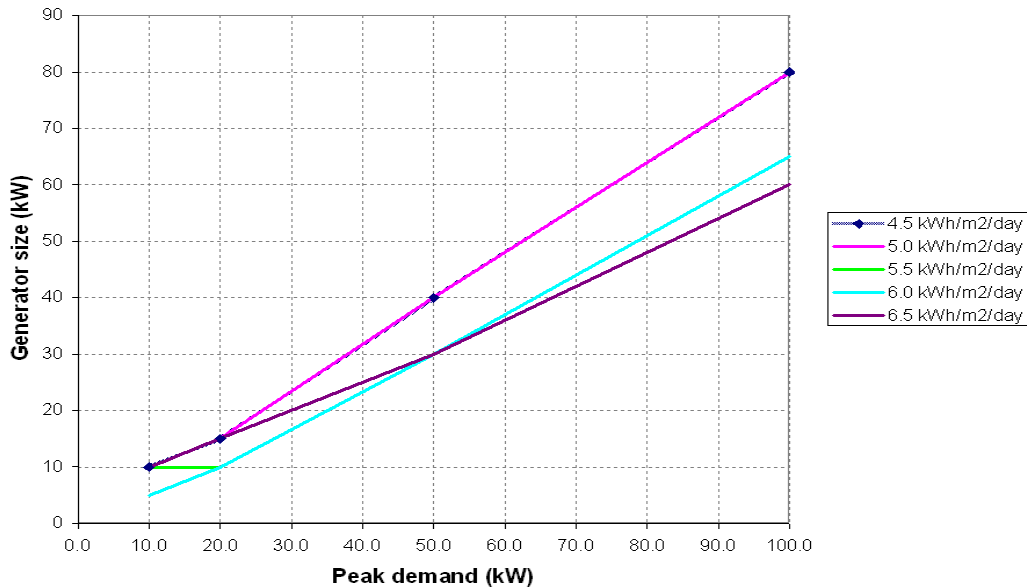


Figure 6.10 Generator size versus peak electricity demand for different insolation values and for a 6 m/s wind speed location.

As it can be seen, for low insolation values below 5.0 kWh/m²/day the size of the generator is around 20 to 25 percent larger than for high values of insolation. Since PV panels do not perform well below this insolation value (Fig. 6.8), the energy required to satisfy the electricity demand should come from somewhere else. Part of this energy will be produced by the wind turbines, as average wind speeds of 6 m/s were found to be beneficial for this type of wind turbine. However, there may be periods of winds below 3.5 m/s for which the wind turbines do not produce electricity. In this case, and when the insolation is over 5.0 kWh/m²/day, both PV panels and the diesel generator provide insufficient energy left by the turbines. On the other hand, below 5.0 kWh/m²/day no PV panels are present in the optimum system, so the energy gap should be filled only by the

diesel generator. This fact explains why the diesel generator should be larger in systems with small insolation values.

The next step is to analyze the fraction of energy produced by each component for different peak electricity demands. Even though Fig. 6.8 through Fig. 6.10 gave an approximate idea to this problem, an extensive study will be performed in Section 6.3.

6.3.2 RESULTS FOR A FIXED INSOLATION INTENSITY

For a 5.5 kWh/m²/day fixed insolation intensity value lying in the middle point of the considered range, the optimization results are showed in Table 6.4 shorted by peak electricity demand for each of the five wind speeds considered in this thesis.

Table 6.4 Optimization results for a 5.5 kWh/m²/day fixed insolation value. Results shorted by peak electricity demand for each wind speed.

Insolation 5.5 kWh/m ² /day						
Peak Demand (kW)	Wind speed (m/s)	PV panels (kW)	Wind Turbines	Generator (kW)	Batteries	Inverter (kW)
10.0	4	12	3	5	14	11
20.0	4	23	6	10	20	22
50.0	4	60	3	30	26	55
100.0	4	72	1	65	42	105
10.0	5	12	6	15	120	11
20.0	5	16	10	10	22	22
50.0	5	32	24	30	42	55
100.0	5	72	36	55	68	105
10.0	6	4	6	10	60	11
20.0	6	11	10	10	28	22
50.0	6	22	26	30	46	55
100.0	6	37	47	65	78	110
10.0	7	0	7	10	54	11
20.0	7	0	14	25	92	23
50.0	7	0	28	40	68	55
100.0	7	0	53	80	100	110
10.0	8	0	7	10	84	11
20.0	8	0	12	20	78	23
50.0	8	0	26	40	84	55
100.0	8	0	49	75	96	110

The most significant results from this table are the lack of photovoltaic panels in the optimum system in environments with strong winds over 7 m/s and the small number of wind turbines for 4 m/s wind speeds. The large number of PV panels in the lack of strong winds is explained by a need in delivering energy to the loads, and since wind

turbines do not perform well in small winds then the energy demand needs to be supplied with more solar panels.

From the previous section it was observed that only when the insolation intensity exceeds 5.0 kWh/m²/day the PV panels gain importance in the optimum system for a wind speed of 6 m/s. For a slightly higher insolation intensity of 5.5 kWh/m²/day and 6 m/s wind speed, an increase in the size of the PV array would be expected, as it can be observed in Fig. 6.11.

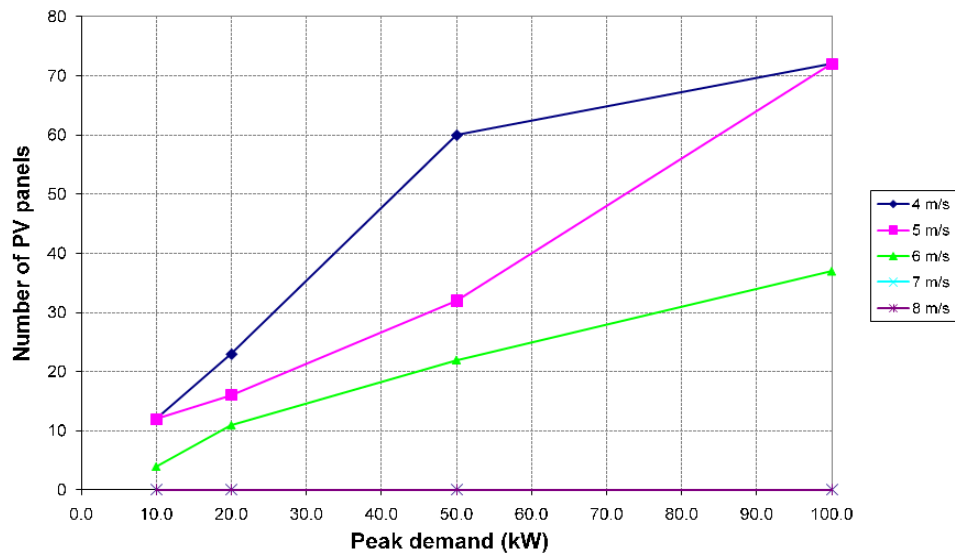


Figure 6.11 PV array size versus peak electricity demand for different wind speeds and for a 5.5 kWh/m²/day insolation intensity.

A plot given in Fig. 6.12 of the peak electricity demand versus the size of the wind turbine park shows that the results for a 50 kW demand (Fig. 6.4) also apply to the entire range of electricity demands; the wind turbines used in this work do not perform well under 4 m/s wind speeds, and the electricity demand is covered by solar panels and the diesel generator which also works as one of the primary sources of energy of the system.

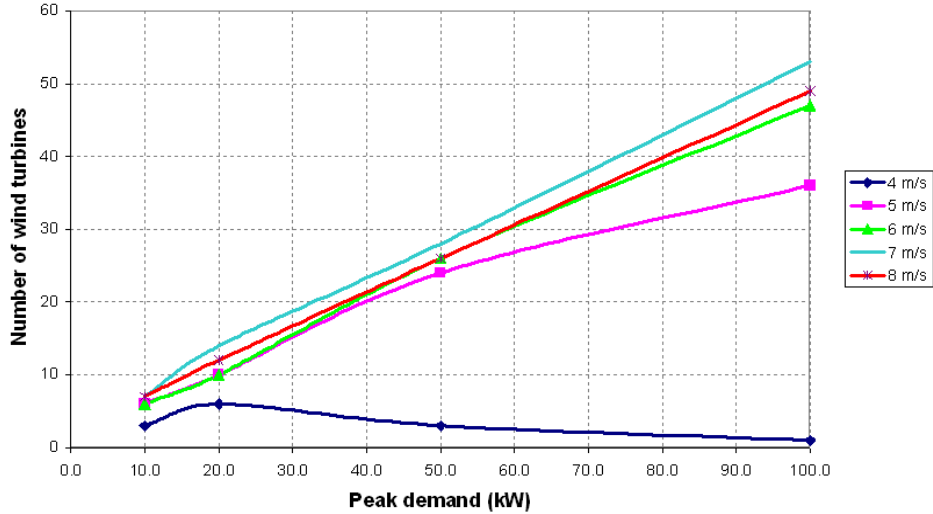


Figure 6.12 Number of wind turbines versus peak electricity demand for different insolation values and for a 6 m/s wind speed.

However, when the wind speed is between 5 m/s and 6 m/s the optimal system consist of both wind turbines and solar panels, although the ratio of PV panels to wind turbines is larger for the 5 m/s case since the solar radiation represents a more dominant energy generating mechanism than the wind speed. Over 7 m/s the system is completely dominated by the wind turbines. From the results for 7 and 8 m/s in Table 6.4 and the linear trend of these two systems displayed in Fig. 6.12 it seems clear that a great increase in the average annual wind speed will not translate into a significant change in the size of the wind turbine park. This suggests that under these high wind speeds the turbines appear to be working close to their maximum efficiency and therefore wind energy represents the dominant energy generation mechanism for this system.

6.4. ANNUAL ENERGY PRODUCTION BY EACH COMPONENT

In the previous sections of the current chapter, the analysis showed that a different combination of PV panels, wind turbines and a diesel generator can be used to generate electricity. As discussed, this combination displays a high dependency on the availability of renewable resources. The size of the PV array and the wind park gives an approximate idea about the amount of energy produced by each component. This system also includes

a backup diesel generator, so its role in the production of energy in the overall system should be also studied. To better understand how these three components contribute to the overall system, first the amount of annual energy generated by each of them needs to be calculated. HOMER does this by simulating the system for each of the 8,760 hours of the year. The results of this simulation are shown in Table 6.4 for the 50 kW peak electricity demand system previously studied. A similar analysis can be done for the remaining peak electricity demands in the considered range. The optimization results for these other cases were observed to have a similar trend and are given in Appendix C.

Moreover, the knowledge of the amount of annual energy produced by each component leads to the total annual energy production of the system. Since the annual energy demand is also known, the battery usage can also be estimated by calculating the surplus of energy produced which, in turn, is sent to the battery bank.

To understand how HOMER calculates the annual energy produced by each component, consider the case of the diesel generator. Table 6.2 and Table 6.3 showed the calculated optimum size of the diesel generator. Notice that the optimum size is between 30 and 50 kW, depending on the availability of insolation and wind speed. The amount of energy produced by the generator can be calculated from this value and the efficiency curve of the generator, given in Fig. 3.9. Since the energy from the generator is different for each of the 8,760 hours of the year, this calculation needs to be performed 8,760 times and added together to obtain the annual energy production. A similar calculation needs to be done for the amount of energy produced by the PV array and the wind turbines.

Table 6.4 Annual energy production of each component for the 50 kW peak demand system. Results sorted to show their dependency on the availability of renewable resources.

50 kW peak demand						
Insolation kWh/m ² /day	Wind speed m/s	PV MWh/yr	Wind MWh/yr	PV + Wind MWh/yr	Generator MWh/yr	Total MWh/yr
4.5	4	41	3	44	191	235
4.5	5	7	161	168	121	289
4.5	6	0	241	241	96	337
4.5	7	0	301	301	74	375
4.5	8	0	319	319	65	384
5.0	4	70	25	95	154	249
5.0	5	52	131	183	105	288
5.0	6	6	234	240	94	334
5.0	7	0	271	271	81	352
5.0	8	0	319	319	65	384
5.5	4	130	8	138	128	267
5.5	5	69	121	190	99	289
5.5	6	48	196	244	83	326
5.5	7	0	281	281	80	361
5.5	8	0	319	319	65	384
6.0	4	143	6	149	123	272
6.0	5	95	101	196	93	289
6.0	6	60	189	248	79	327
6.0	7	38	241	279	71	350
6.0	8	0	319	319	66	385
6.5	4	154	3	157	120	277
6.5	5	112	91	203	90	293
6.5	6	63	189	251	78	329
6.5	7	44	241	285	68	353
6.5	8	26	294	320	61	381

First, the dependency of the amount of energy produced by each component versus the available average wind speed needs to be studied. This is shown in Fig. 6.13 for a location having an average insolation of 5.5 kWh/m²/day. The selection of this value allows the comparison with the results discussed in section 6.2 and section 6.3, in which the size of the system was analyzed for the same insolation value.

As it can be seen, the energy generated by the wind turbines increases with the wind speed. In Fig. 6.7 it was observed that in stronger winds more turbines are required in the optimum system. The reason is that the output power of the wind turbine increases in the same manner between 4 and 8 m/s according to its power curve (Fig. 3.12). Therefore, more energy is being generated by each wind turbine and thus, it becomes beneficial to install more wind turbines in the system. Since more energy is being produced by the wind turbines, less energy is required from the PV panels. This result

validates the observations in Fig. 6.6, in which the size of the PV array decreased with increasing wind speed.

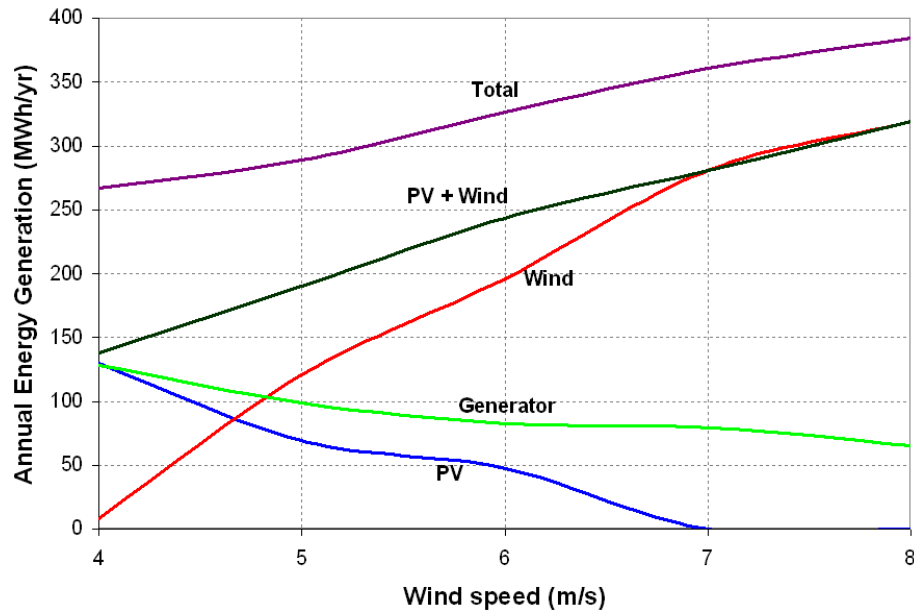


Figure 6.13 Annual energy generation versus availability of wind speed. Results shown for a 50 kW peak demand system under an average insolation of 5.5 kWh/m²/day.

To a bigger or smaller extent, wind is available throughout the entire day. Thus, a larger number of wind turbines in the system guarantees a higher reliability of the energy supply. This fact explains the reduction of the amount of energy demanded from the backup generator as the wind speed increases, shown in Fig. 6.13. To help visualize this result quantitatively and percentagewise, the bar diagram in Fig. 6.14 can be used.

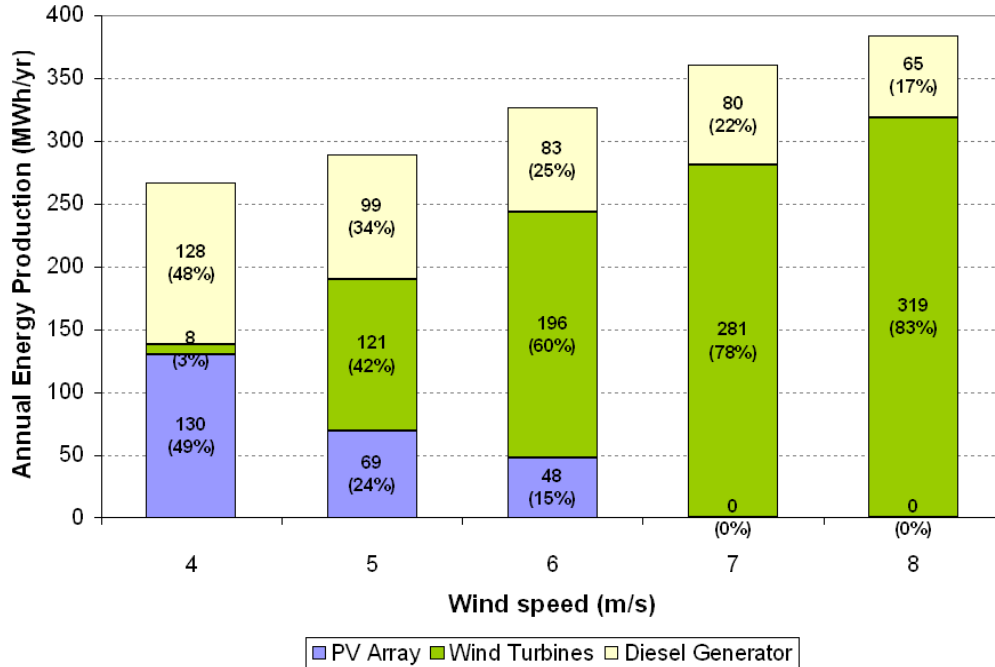


Figure 6.14 Quantitative and percentage of annual energy production by component versus availability of wind. Results shown for a 50 kW peak demand system with an average insolation of 5.5 kWh/m²/day.

In section 4, the average daily energy consumption of the AC loads was calculated to be 627 kWh/day, which is equivalent to an annual energy consumption of approximately 229 MWh/yr in AC. The energy generated by the system in each of the cases shown above is higher than this value. This means that the surplus of energy generated, corrected by the inverter's efficiency, is stored in the batteries for a later use. For example, in the 4 m/s case shown in Fig. 6.14 the diesel generator produces 128 MWh/yr of energy in AC. If all the energy from the generator is assumed to be consumed instantaneously at the loads, then the remaining energy, 101 MWh/yr in AC, needs to be delivered by the PV array and the wind turbines. This is equivalent to 112 MWh/yr in DC since the inverter was modeled with an efficiency of 90%. From Fig. 6.14 the combined amount of energy generated by solar panels and wind turbines is 138 MWh/yr in DC. Thus, the difference between this value and the amount of energy demanded from the renewable components represents the energy that is stored in the

batteries. This value was calculated to be 26 MWh/yr for the 4 m/s case. A plot of the calculated values for the other wind speeds and insolation values is given in Fig. 6.15.

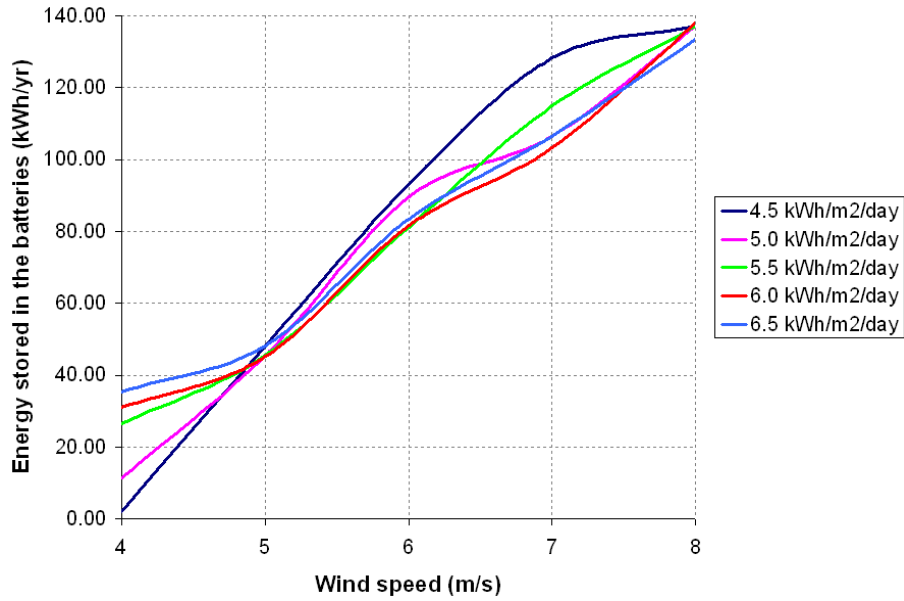


Figure 6.15 Annual energy stored in the batteries versus wind speed values.

The results in Fig. 6.15 support the previous discussion. As the average wind speed increases, more energy is generated by the wind turbines and less by the diesel generator. Consequently, less energy becomes directly available from the generator. Thus, the wind turbines need to generate most of the energy to satisfy the electricity demand. Since they generate electricity only when the wind is available, part of the energy will be used instantaneously at the loads, and a surplus will be generated and stored in the batteries for when wind is not available.

A similar analysis and discussion can be made by evaluating the results in Table 6.4 over the range of insolation values. In this case, the average wind speed will be fixed to a value of 6 m/s in order to allow for the comparison with the results in section 6.1 and 6.3. A plot of the amount of annual energy generated by each component of the system is shown in Fig. 6.16 over the considered range of insolation values.

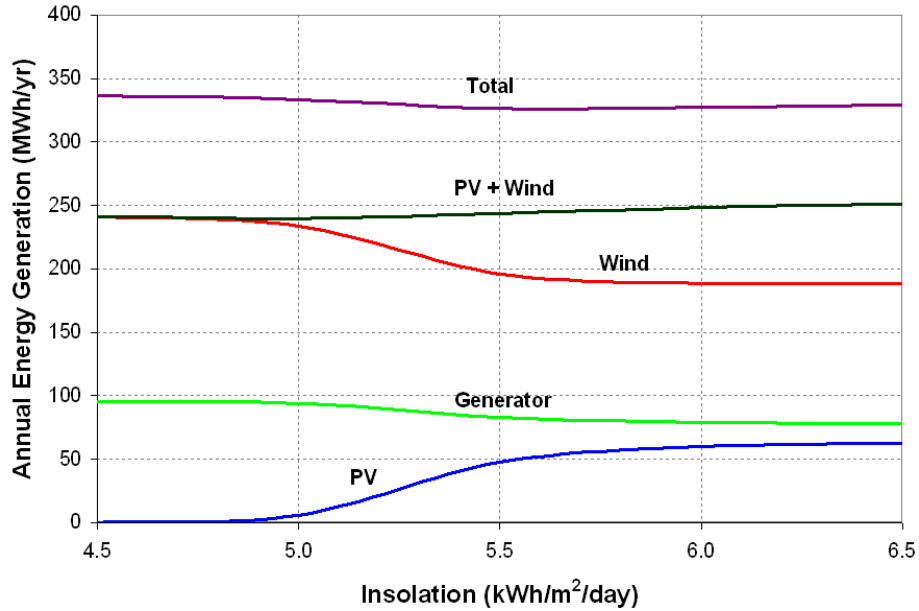


Figure 6.16 Annual energy generation versus the available insolation. Results shown for a 50 kW peak demand system under an average wind speed of 6 m/s.

It was observed in Fig. 6.3 that the size of the PV array increased with increasing values of insolation, whereas the number of wind turbines decreased, as shown in Fig. 6.4. The same trend is experienced in terms of the energy production; the contribution of solar panels to the system increases and that of the wind turbines decreases with increasing values of insolation. However, as it was studied in section 6.1, the energy production from the wind remains higher than that from the sun over the entire range of insolation values.

An important result from Fig. 6.3 is that the annual energy produced by the diesel generator remains somewhat constant along the insolation range. This differs from the previous case (Fig. 6.13) in which the energy from the generator decreased with higher wind speed values. The reason is that an increase in the energy from the PV array does not guarantee a higher reliability of the energy supply. Unlike wind turbines, PV panels work exclusively during the daytime and thus, a backup source of energy is still required. The quantitative and percentage-wise importance of each component in the system is given in the bar diagram in Fig. 6.17.

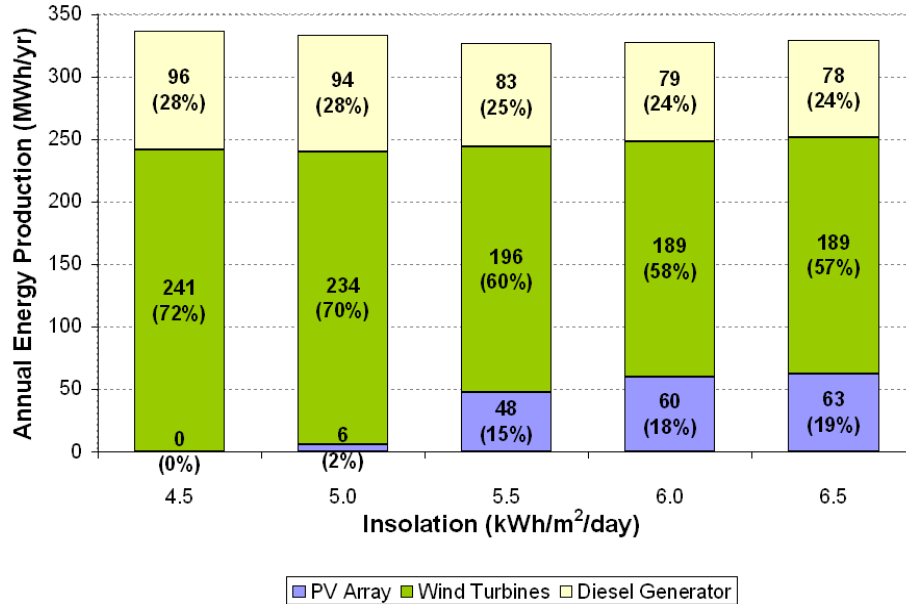


Figure 6.17 Quantitative and percentage of annual energy production by component versus availability of insolation. Results shown for a 50 kW peak demand system with an average wind speed of 6 m/s.

Since the amount of energy produced by the generator remains practically constant for the whole range of insolation values as seen in Fig. 6.17, so does the amount of annual energy generated by the renewable components. In other words, the same amount of annual energy needs to be stored in the battery bank. This has been calculated using the same method than for the case of a fixed insolation value, and plotted in Fig. 6.18.

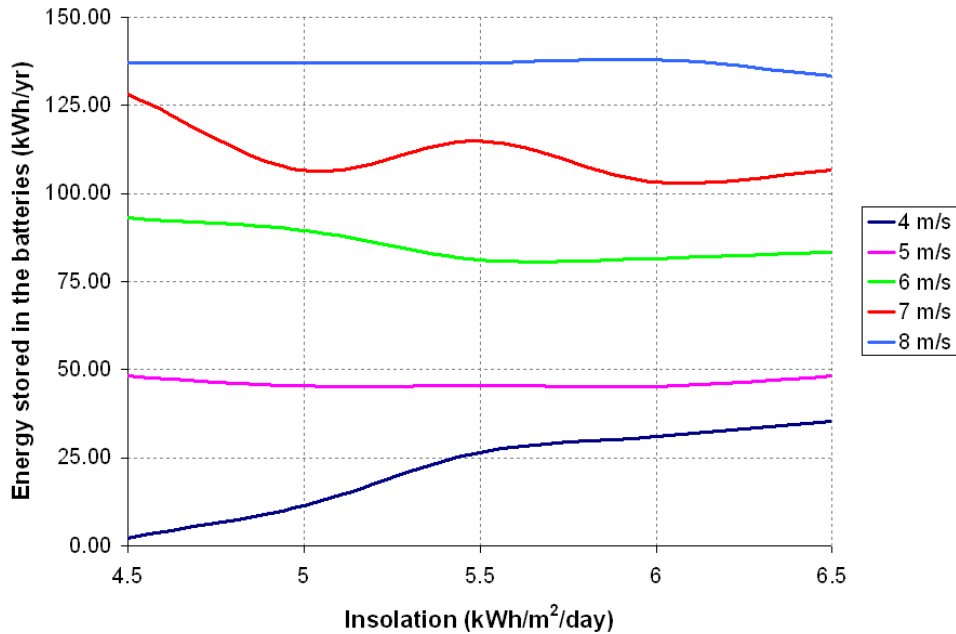


Figure 6.18 Annual energy stored in the batteries versus insolation values.

The 4 m/s case in this figure follows a different trend since no wind turbines are present in the system for the same reason discussed in section 6.1. In this case, the number of PV panels increases as the insolation increases because they become more efficient. This allows generating an increasing surplus of energy that can be stored in more batteries, explaining the growth in the 4 m/s curve in Fig. 6.18.

Wind turbines and PV panels represent in most of the cases the main energy generation components of the system. Thus, the relationship between the amount of annual energy generated by the PV panels and the wind turbines should be investigated. Moreover, this relationship is highly dependent on the amount of available resources at a particular site, as it has been studied in this section. In general, as the wind speed increases, so does the amount of energy generated by an increasing number of wind turbines in the system. Thus, less solar panels are needed and the required energy from the PV array decreases. This relationship is shown in Fig. 6.19.

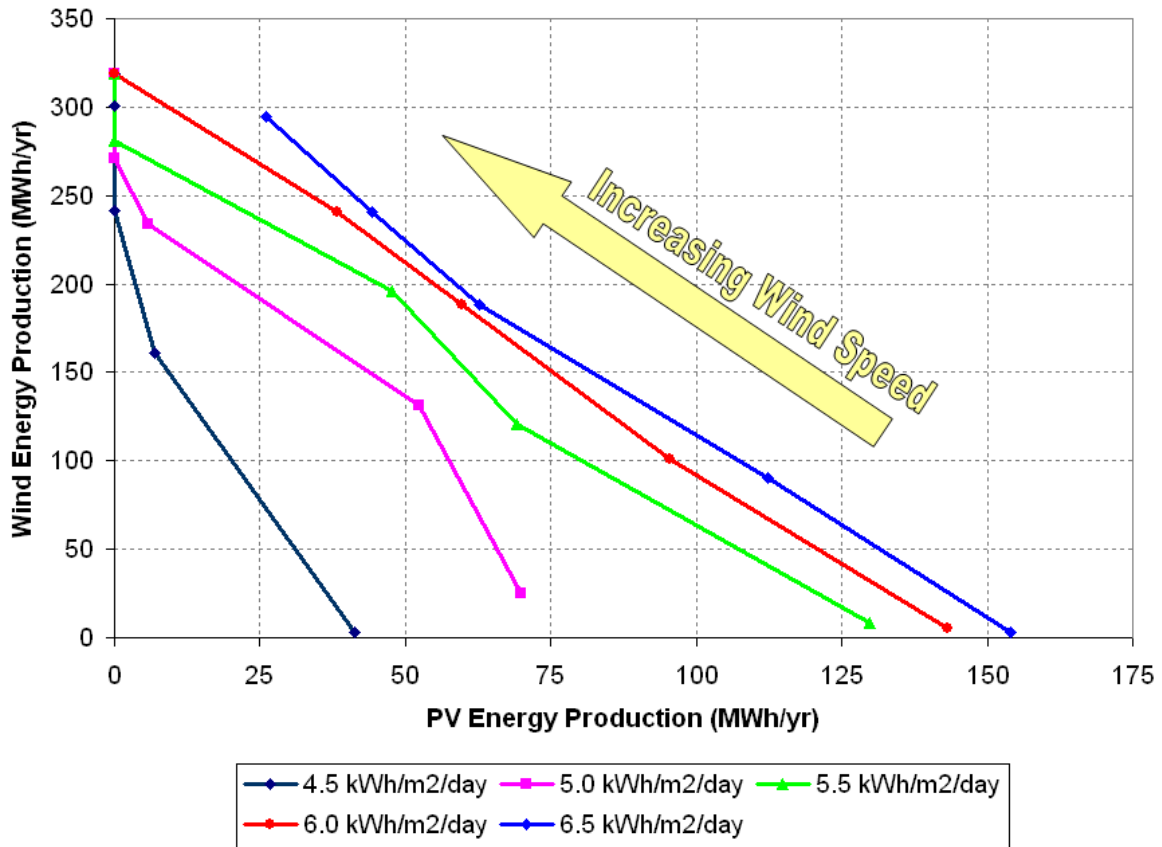


Figure 6.19 Relationship between the annual energy generated by wind turbines and solar panels as a function of the amount of available resources.

The opposite statement is also true: increasing the amount of insolation makes the PV panels work more efficiently. This translates into a larger portion of the total energy of the system to be produced by the PV array. Consequently, less energy is demanded from the wind turbines to meet the electricity demand.

6.5. SYSTEM SIZE COST & COST OF ELECTRICITY PRODUCED BY THE SYSTEM

For each combination of peak electricity demand, insolation intensity and wind speed the optimal system configuration was found. This optimal configuration is

characterized by a certain number of components of a certain size that minimizes the lifecycle costs, also known as the net present value (NPV), while being able to satisfy the given electricity demand.

After each simulation is completed, HOMER provides the best system configuration together with its NPV. The problem of minimizing the NPV is very complex because of the large number of variables considered, the variability of the operating costs with the system usage, the lifetime of each component and the uncertainty in the availability of the energy resources which in turn affects the performance of the overall system. Thus, the software does minimize the NPV and instead calculates which system configurations can meet the given demand and then simulates those systems over their entire lifetime to calculate the NPV.

For this reason, the calculation of the minimum NPV of a hybrid PV/Wind/Diesel/Battery system is out of the scope of this work. However, the results provided by HOMER can be used to get an approximate idea of what the lifecycle costs of this system are and draw some significant conclusions. These results are given in Table 6.5.

Table 6.5 Relevant costs of the 50 kW peak electricity demand system versus the amount of available resources.

50 kW peak demand			
Insolation (kWh/m ² /day)	Windspeed (m/s)	NPV (\$)	Initial Costs (\$)
4.5	4	1,189,905	159,523
4.5	5	1,076,048	389,983
4.5	6	922,478	376,263
4.5	7	824,894	374,762
4.5	8	713,618	325,618
5.0	4	1,168,778	302,525
5.0	5	1,057,053	438,395
5.0	6	921,804	378,131
5.0	7	809,725	391,978
5.0	8	713,618	325,618
5.5	4	1,117,966	363,958
5.5	5	1,034,835	442,769
5.5	6	913,878	417,083
5.5	7	802,457	338,952
5.5	8	713,618	325,618
6.0	4	1,079,357	354,377
6.0	5	1,011,896	441,171
6.0	6	899,534	419,784
6.0	7	800,325	371,440
6.0	8	714,378	318,732
6.5	4	1,049,413	341,819
6.5	5	991,412	435,727
6.5	6	888,354	414,316
6.5	7	792,736	375,508
6.5	8	711,165	342,945

By using the data in Table 6.5 and plotting the NPV of each optimum system configuration over their respective wind speed and insolation values, Fig. 6.20 was obtained.

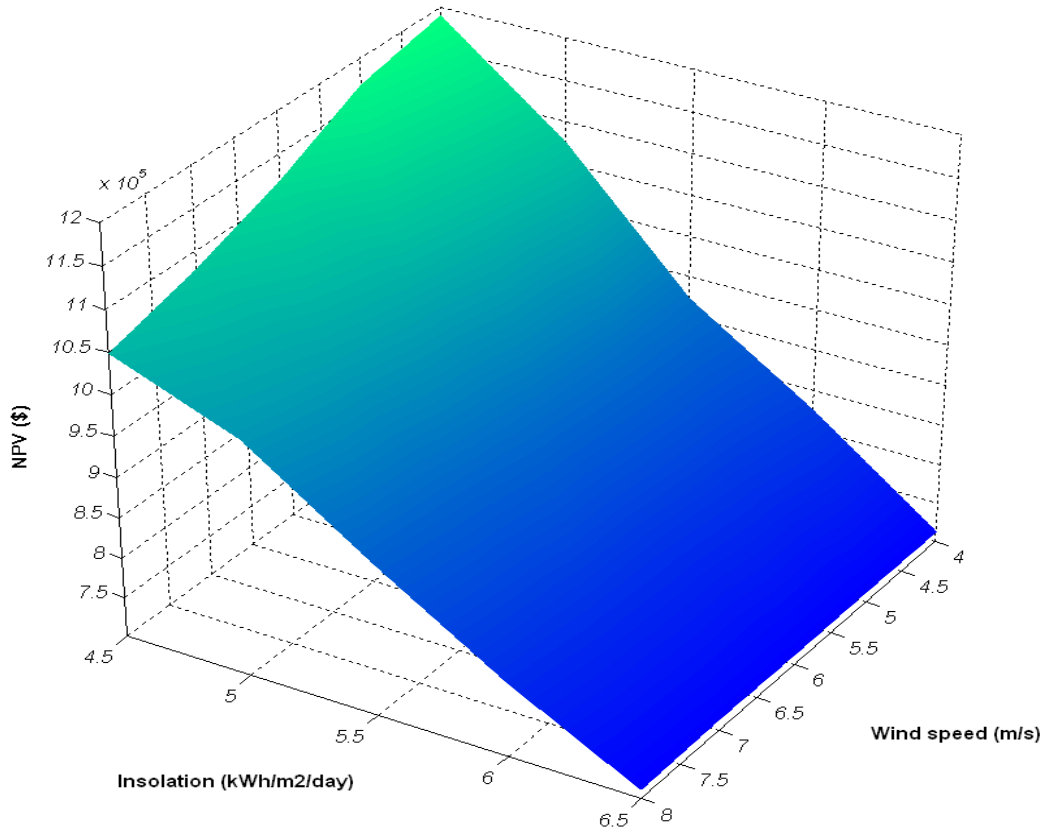


Figure 6.20 Net present value dependence on the amount of renewable resources available for the 50 kW peak electricity demand system.

As it was expected, an increase in either the wind speed or the insolation intensity translates into lower lifecycle costs because less solar panels and/or wind turbines are required to satisfy the electricity demand since they can operate more efficiently. Furthermore, the backup diesel generator is then used for emergency situations only and not as the main source of energy, thus reducing the amount of diesel fuel that needs to be purchased.

More interesting is the linear trend that the change in either the wind speed or the insolation values has on the NPV. By keeping fixed the value of insolation or wind speed,

an almost perfectly linear relation of the other two variables is observed. For instance, starting from the topmost point in Fig. 6.20 and moving down the 4 m/s plane, a reduction of the NPV is seen when the solar insolation increases from 4.5 to 6.5 kWh/m²/day. A similar relation can be observed when keeping fixed the value of insolation and varying the wind speed.

Systems installed in the surroundings of very low wind speeds and insolation values have the highest lifecycle costs, as shown in Fig. 6.20. However, the effect on the initial costs is the opposite as it can be seen in Fig. 6.21. As discussed in the previous sections, most of the systems with a wind speed intensity below 5 m/s and insolation values below 5 kWh/m²/day have a high dependency on the diesel generator. The optimum system was observed to have a low number of wind turbines and PV panels and, thus, the initial costs turns out to be very low. The drawback lies in that the diesel generator needs to be run for more hours per year to satisfy the electricity demand, which translates into higher annual O&M costs. Over the 25 years lifetime of the system, this fact will produce very high costs. This is the reason why these systems do not represent a good economical option.

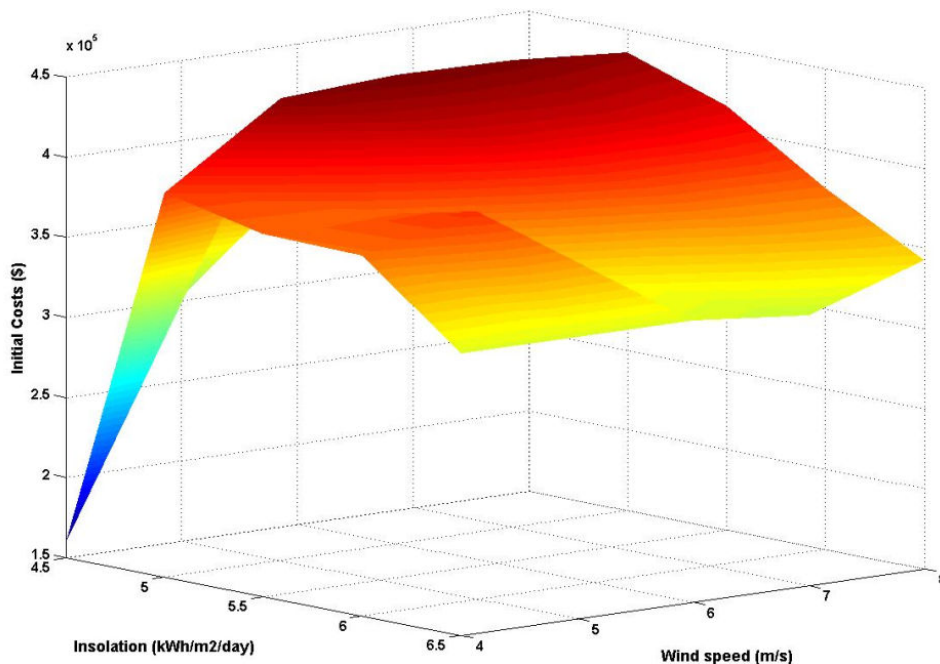


Figure 6.21 Initial costs dependence on the amount of renewable resources available for the 50 kW peak electricity demand system.

Over the critical values of 5 m/s wind speed and 5 kWh/m²/day insolation, the initial costs of the system display the expected trend. As either the wind speed or the insolation increases the initial costs of the system decrease. This is due to an increase in the efficiency of the solar panels and the wind turbines. In order to satisfy the electricity demand fewer components are needed and, thus, the initial costs of the installation drops as shown in Fig. 6.21.

In summary, the size, energy requirements and costs of a PV/wind/diesel generator/batteries were studied over the entire range of available wind speed and insolation values in the United States. A general AC load between 10 and 100 kW was model to assess the performance of each component of the system. The optimization results obtained with HOMER were studied and analyzed by changing the insolation, wind speed and/or peak electricity demand in the system. Overall the results were as expected, although a few deviations were observed and discussed. The analytical method described herein could be used for other types of energy generation systems and different electricity demands.

7. CONCLUSIONS

In this work the optimum size of a hybrid renewable energy system was investigated over all the possible values of insolation and wind speed in the United States. The system under study was comprised of an array of PV panels, a set of wind turbines, a diesel generator, a bank of lead-acid batteries and an inverter. In order to analyze the dependency of the system size on the amount of energy demanded by the loads, an AC electricity demand ranging from 10 to 100 kW was modeled. An iterative optimization method was developed in HOMER which provided not only the optimum size of the system, but also valuable information on its initial and lifecycle costs, and the energy generated by each component.

As expected, an increase in either solar insolation or wind speed caused the system to become more dependent on the PV array or the wind turbines park, respectively. A larger amount of solar radiation enables the PV panels to work more efficiently and, thus, increase their energy output. According to the operating principles of PV panels, the increase in insolation has an almost linear dependence with the energy generated by them. In terms of the optimum system size, this translates into a larger PV array with increasing insolation intensity.

The case of the wind turbines displayed a different behavior, which allowed drawing a very important result. The availability of stronger winds in the system causes a bigger portion of the energy to be produced by the wind turbines. However, this is achieved by a decrease in the number of wind turbines, in contrast to the PV case. Since the power in the wind grows with the cube of the wind speed, a smaller number of wind turbines can be used to produce the same or more amount of energy with stronger winds. Thus, less wind turbines will be present in the optimum system as the wind speed increases.

By analyzing the optimum system configuration under very high or very low amount of renewable resources, a trend was found for the diesel generator, the batteries and the inverter. The results for the lowest insolation and wind speed values (4.5 kWh/m²/day and 4 m/s, respectively) showed that neither the PV panels nor the wind turbines are capable of producing a great amount of energy. A small inverter size

revealed that most of the energy was delivered in AC. Since both renewable components were modeled in DC for this work, a big portion of the energy was delivered by the AC diesel generator, which works as the main source of energy of the system. The diesel generator produces electricity only when demanded by the loads. Therefore, when the generator is being used extensively, very little energy needs to be stored in the batteries for a later use. This explains the small size of the battery bank in the optimum system.

This limiting case of insolation and wind speed provided another important result. Under very poor conditions, PV panels are preferred over wind turbines in the optimum system. Although the efficiency of PV panels increase with increasing values of insolation, they are still capable of producing some energy. This fact is also true for wind turbines; as wind speed increases, they can generate more electricity. However, the 4 m/s wind speed case represents a special case for the wind turbines modeled in this work. They have a cut-in wind speed of 3.5 m/s and, thus, will not start generating electricity below this value. The benefit of installing these wind turbines under 4 m/s wind speeds or below is then very small. Because of this reason, more PV panels than wind turbines are present in the optimum system, although the diesel generator remains as the main source of energy for the system, as explained above.

In contrast to the very low insolation and wind speed case, it was found that when a suitable value of wind speed (around 7 m/s) is reached, the system becomes highly dependent on the wind turbines. A small amount of PV panels is required to cover periods of high electricity demand during the daytime, and a diesel generator is used only as back-up. As wind speed increases, a larger battery bank is needed since a larger portion of the energy produced by the wind turbines is not consumed instantaneously. When both the insolation and wind speed values are small, PV panels and wind turbines do not perform well. In this case, the diesel generator becomes the main source of energy for the system.

Next, the optimal system size was studied along the considered range of peak electric demands for two different cases, a fixed wind speed of 6 m/s and a fixed insolation intensity of 5.5 kWh/m²/day. For the first case, the results revealed a threshold under which the efficiency of solar panels makes them unsuitable to be used in the

optimal system. This value was found to be close to 5.0 kWh/m²/day for this particular case. Under this value of insolation, all the electric demand is fully covered by the wind turbines and the back-up diesel generator whereas over 5.0 kWh/m²/day solar panels become efficient as to be considered in the optimal system configuration thus requiring less wind turbines to satisfy the demand. In the second case, part of the previous results were corroborated: over the 5.0 kWh/m²/day threshold solar panels take part in the generation of electricity and wind turbines do not work efficiently under 4 m/s winds for any of the considered peak electricity demand values.

Finally, using the economic results of the system provided by HOMER, an estimate of its optimal lifecycle and initial costs was provided. As either the insolation intensity or the wind speed increases, the usage of the diesel generator decreases significantly. The biggest portion of the lifecycle costs of the system is due to the diesel fuel that needs to be purchased to run the generator. Consequently, as either insolation or wind speed increases, the lifecycle costs decrease as well since a smaller amount of diesel fuel needs to be purchased. This decrease was observed to follow an almost linear trend with the values of insolation and wind speed.

The initial costs followed a slightly different trend. In the lack of strong insolation and wind speed values, just a few PV panels and wind turbines need to be installed, since the diesel generator will be the main source of energy for the system. Thus, the initial costs are very small for this case. Once the PV panels and wind turbines become a good alternative for the optimum system, the initial costs increase significantly since more renewable components need to be purchased. However, as either insolation or wind speed keeps increasing, the renewable components work more efficiently. In other words, less PV panels and wind turbines are required in most of the cases and a smaller diesel generator needs to be installed. Thus, a decrease in the initial costs was observed as the amount of renewable resources increased.

In summary, a method to evaluate the optimum size, energy requirements and costs of a hybrid renewable system was presented in this work. It was found that the selection of the wind turbines to be installed in the system is more critical than the PV panels. Wind turbines condition the overall trend of the system, setting the breaking point

at which the diesel generator is used as either a back-up source of energy or as one of the main energy components for the system.

REFERENCES

- [1] Davidson P. “Off the grid or on, solar and wind power gain; Incentives, savings push more families to renewable energy”. USA Today. 13 Apr. 2006.
- [2] National Renewable Energy Laboratory, NREL. Dynamic Maps, GIS Data, & Analysis Tools. June 15, 2010. (<http://www.nrel.gov/gis/wind.html>)
- [3] National Renewable Energy Laboratory, NREL. Hybrid Optimization Model for Electric Renewables (HOMER). Homer Energy, 2010. (<http://homerenergy.com/>)
- [4] Messenger R.A. & Ventre J. (2003). “Photovoltaic Systems Engineering”. 2nd Ed. CRC Press.
- [5] National Renewable Energy Laboratory, NREL. “Simple Model of the Atmospheric Radiative Transfer of Sunshine SMARTS” (2010). (<http://www.nrel.gov/rredc/smarts>).
- [6] Gueymard C.A. “The sun's total and spectral irradiance for solar energy applications and solar radiation models”, Volume 76, Issue 4, April 2004, Pages 423-453.
- [7] Wenham S.R., Green M.A., Watt M.E. & Corkish R. (2007) “Applied Photovoltaics”. 2nd Ed., Earthscan. ARC Center for Advanced Silicon Photovoltaics and Photonics.
- [8] Duffie, J.A. & Beckman, W.A. (1991). “Solar Engineering of Thermal Processes” 2nd edition, Wiley, New York, NY.
- [9] Masters G.M. “Renewable and Efficient Electric Power Systems” (2004). 1st Ed., John Wiley & Sons, Inc. ISBN 0-471-28060-7.
- [10] Erbs, D.G., Klein, S.A. & Duffie, J.A. (1982). “Estimation of the diffuse radiation fraction for hourly, daily, and monthly-average global radiation”, Solar Energy, vol. 28, issue 4, p. 293 -302.
- [11] American Society of Heating, Refrigerating and Air-Conditioning, ASHRAE. (2005). “2005 ASHRAE Handbook: Fundamentals – SI Units”. ASHRAE.

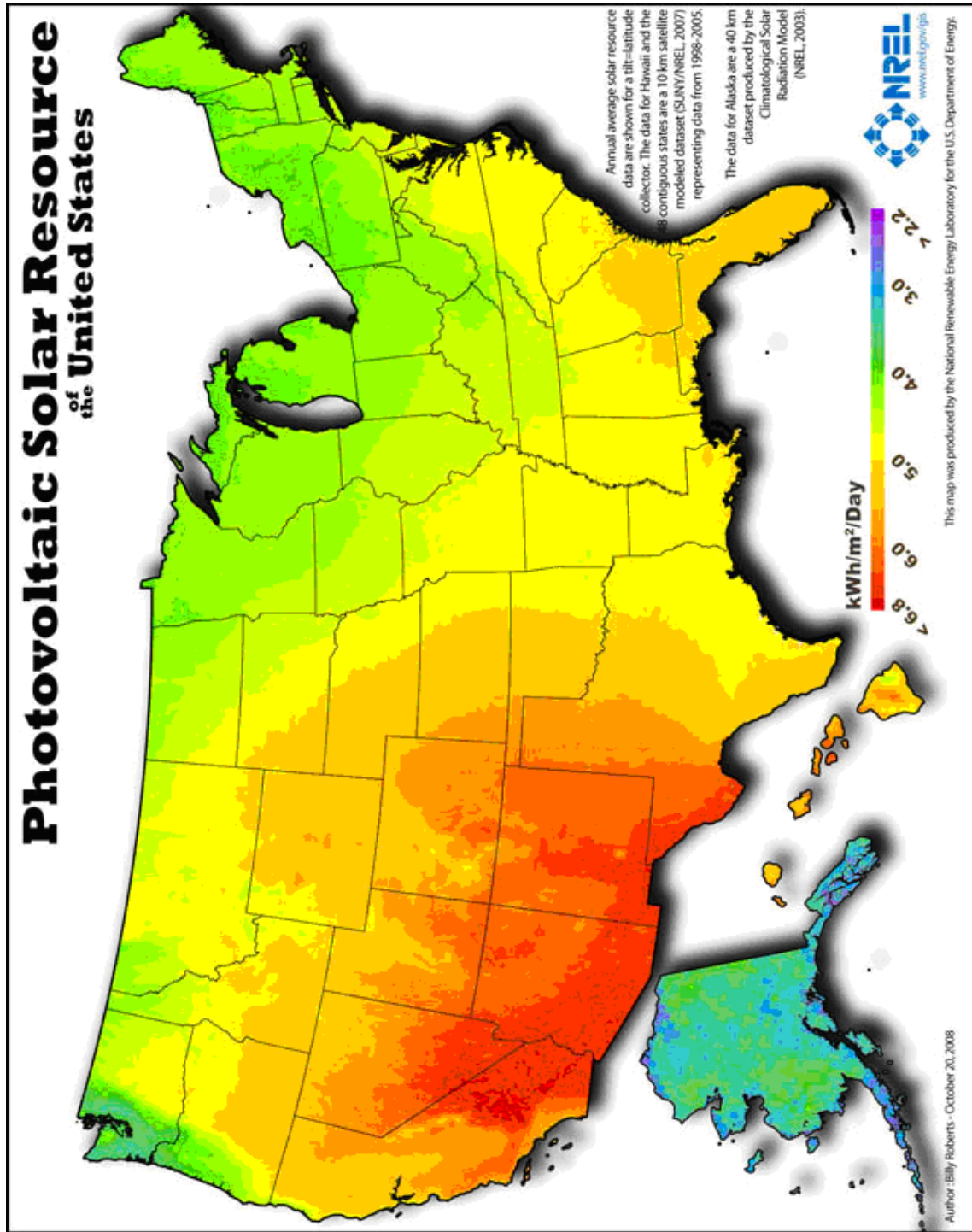
- [12] NASA & the Atmospheric Science Data Center (2008). "Surface meteorology and Solar Energy Data Set". (<http://eosweb.larc.nasa.gov/sse/RETScreen>).
- [13] Burton T., Sharpe D., Jenkins N. & Bossanyi E (2001). "Wind Energy Handbook" 1st Ed., John Wiley & Sons, Inc.
- [14] National Solar Radiation Data Base. Typical Meteorological Year 3 data sets, TMY3. National Renewable Energy Laboratory, NREL. Electric's System Center (2008).
- [15] Stevens, M.J.M. & Smulders, P.T. "The estimation of the parameters of the Weibull wind speed distribution for wind energy utilization purposes", Wind Engineering, Vol. 3, Nr. 2, 132-145. 1979.
- [16] U.S. Energy Information Administration, EIA. Annual Energy Outlook 2010. Dec. 2009. (<http://www.eia.doe.gov/oiaf/forecasting.html>)
- [17] Becquerel, A. E. (1839). "Mémoire sur les effets électriques produits sous l'influence des rayons solaires". Comptes Rendus 9: 561–567.
- [18] Luque, A. & Hegedus, S. "Handbook of Photovoltaic Science and Engineering" (2003). 1st Ed., John Wiley & Sons, Ltd. ISBN 0-471-49196-9.
- [19] Solarbuzz (2010). "2010 Global PV Industry Report" - Fast Solar Energy Facts (<http://www.solarbuzz.com/fastfactsindustry.htm>)
- [20] Shockley, W. & Queisser, H.J. "Detailed Balance of Efficiency of p-n Junction Solar Cells". Journal of Applied Physics, Vol. 32, Nr. 3, March 1961.
- [21] Betz, A. "Das Maximum der theoretischen möglichen Ausnutzung des Windes durch Windmotoren". Zeitschrift für das gesamte Turbinewesen, Sept. 1920.
- [22] Dufo-Lopez, R. "Dimensionado y Control Optimos de Sistemas Híbridos Aplicando Algoritmos Evolutivos", tesis doctoral. Universidad de Zaragoza, Spain. Department of Electrical Engineering. April 2007.
-

- [23] Manwell, J.F. & McGowan J.G. “Lead acid battery storage model for hybrid energy systems”. Renewable Energy Research Laboratory, University of Massachusetts. Solar Energy, Vol. 50, Issue 5, 399-405. May 1993
- [24] Fraunhofer Institute for Solar Energy Systems ISE. Annual Report 2009. Apr. 1, 2010.
- [25] National Renewable Energy Laboratory, NREL. Renewable Resource Data Center. PV Watts Version 1 Calculator. Feb. 5, 2010.
<http://www.nrel.gov/rredc/pvwatts/version1.html>
- [26] Southwest Windpower. Whisper 500.
http://www.windenergy.com/products/whisper_500.htm
- [27] The Engineering Toolbox. (<http://www.engineeringtoolbox.com>)
- [28] Trojan Battery Company. (www.trojanbattery.com/Products)
- [29] U.S. Energy Information Administration, EIA. Office of Energy Markets and End Use. U.S. Department of Energy. “Annual Energy Review 2008”, report No. DOE/EIA-0384. Jan. 2009. (<http://www.eia.doe.gov/aer/pdf/aer.pdf>)

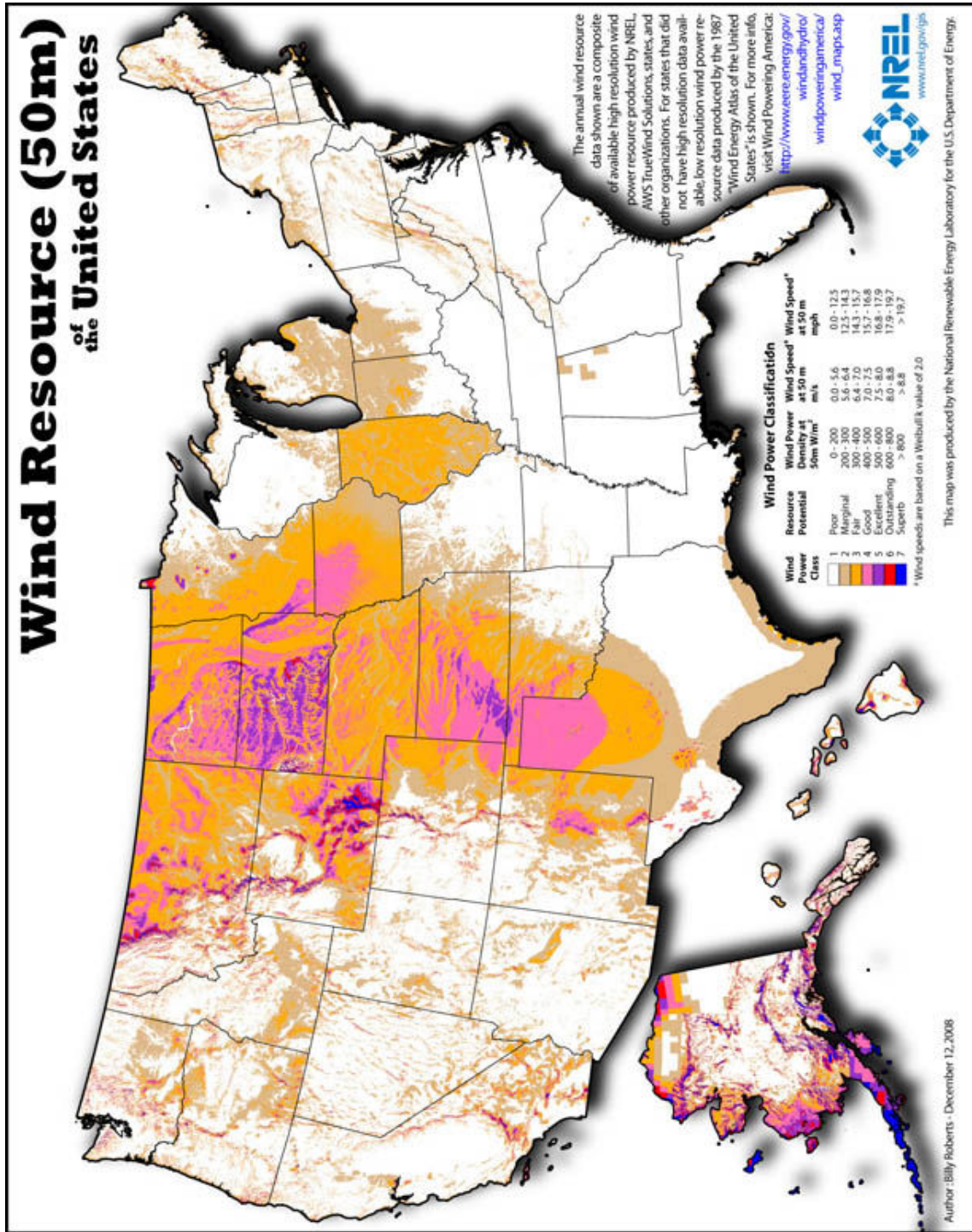
APPENDIX A

U.S. SOLAR AND WIND RESOURCE MAPS

APPENDIX A



APPENDIX A



APPENDIX A

The solar resource

Jan	2.4	2.7	3.0	3.2	3.5
Feb	3.2	3.5	3.9	4.2	4.6
Mar	4.3	4.8	5.3	5.8	6.2
Apr	5.3	5.9	6.5	7.1	7.7
May	5.9	6.5	7.2	7.8	8.5
Jun	6.3	7.1	7.8	8.5	9.2
Jul	6.3	7.1	7.8	8.5	9.2
Aug	6.1	6.8	7.5	8.2	8.8
Sep	4.9	5.5	6.0	6.5	7.1
Oct	3.8	4.2	4.6	5.0	5.5
Nov	2.9	3.2	3.5	3.8	4.2
Dec	2.5	2.8	3.0	3.3	3.6
Avg	4.5	5.0	5.5	6.0	6.5

Table A.1. Monthly and annual average insolation values used in this work, in kWh/m²/day

The wind resource

Jan	4	5	6	7	8
Feb	4	5	6	7	8
Mar	4	5	6	7	8
Apr	4	5	6	7	8
May	4	5	6	7	8
Jun	4	5	6	7	8
Jul	4	5	6	7	8
Aug	4	5	6	7	8
Sep	4	5	6	7	8
Oct	4	5	6	7	8
Nov	4	5	6	7	8
Dec	4	5	6	7	8
Avg	4	5	6	7	8

Table A.2. Monthly and annual average wind speed values used in this work, in m/s

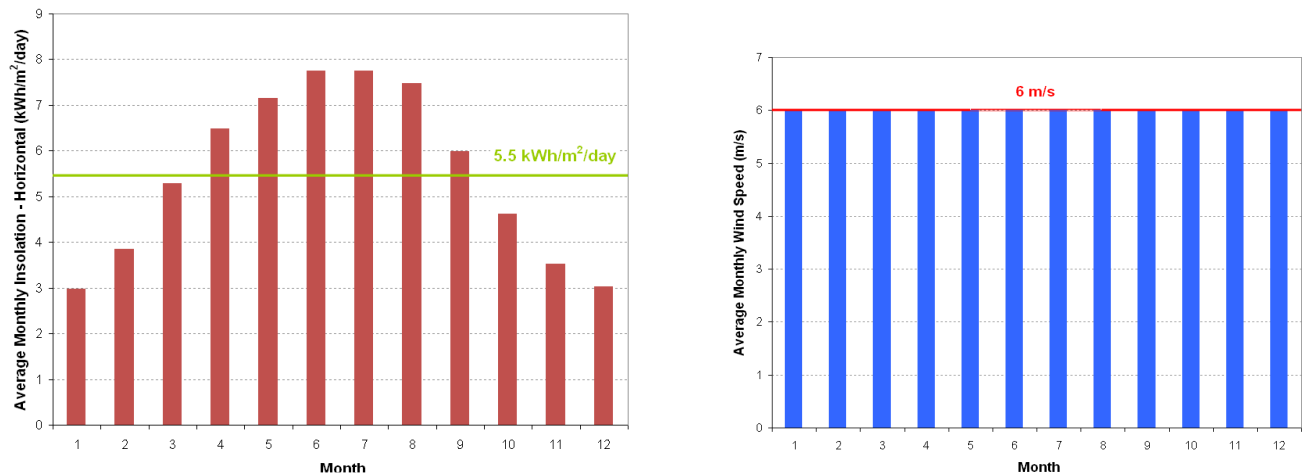


Figure A.1. Examples of the insolation and wind speed distributions used in this work

APPENDIX B

ECONOMIC DESCRIPTION OF THE COMPONENTS

APPENDIX B

The capital, replacement and operation & maintenance (O&M) costs were defined in the present work for each component. The capital cost represents the initial price that should be paid to purchase and install each component. The replacement cost represents the price of purchasing a new component, assuming that the installation cost will not need to be covered again. The O&M cost represents the annual money spent in operating and maintaining the component.

B.1 SOLAR PANELS

Capital Cost (\$)	Replacement Cost (\$)	O&M Cost
Figure B.1	625	Figure B.2

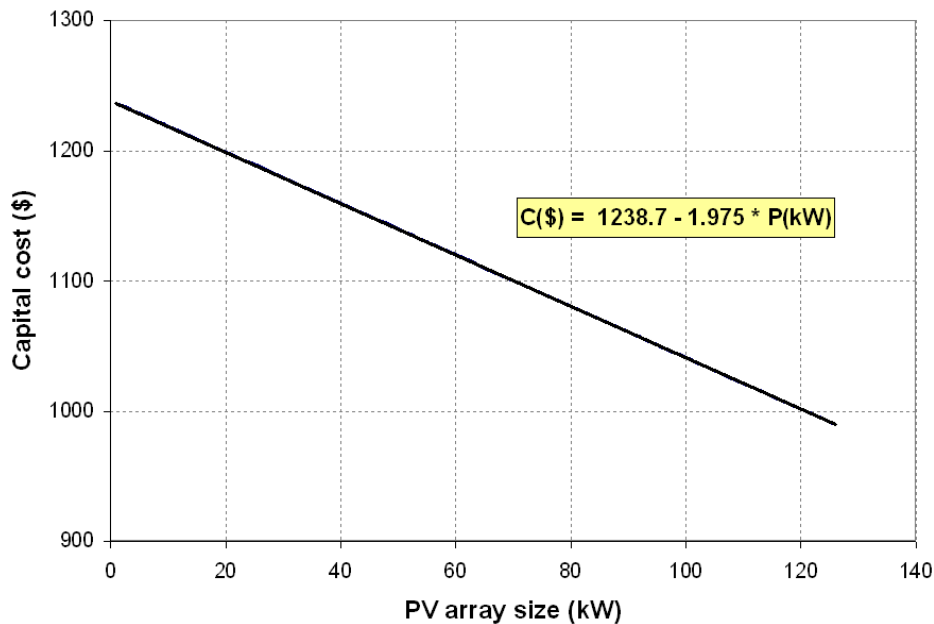


Figure B.1. Capital cost dependence on the PV array size.

APPENDIX B

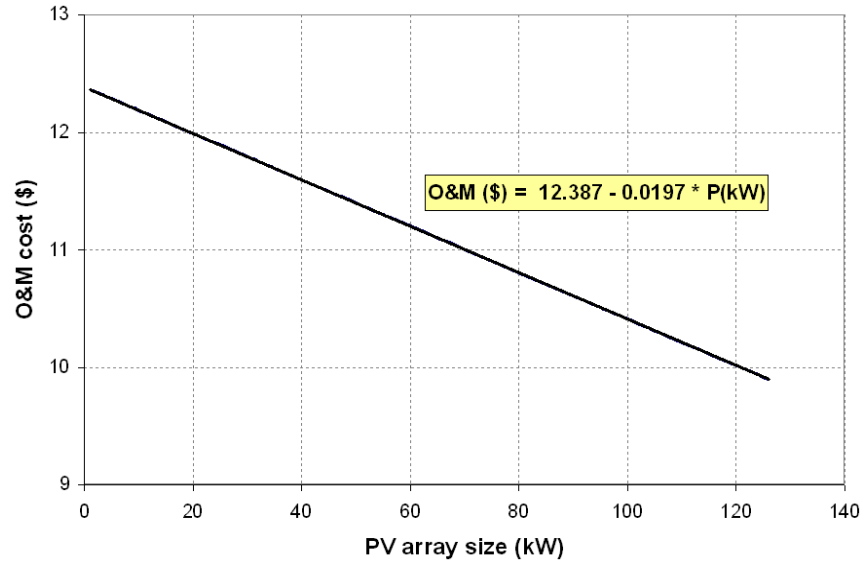


Figure B.2. O&M cost dependence on the PV array size.

B.2 WIND TURBINES

Capital Cost (\$)	Replacement Cost (\$)	O&M Cost
9,171	7,654	0

B.3 DIESEL GENERATOR

Capital Cost (\$)	Replacement Cost (\$)	O&M Cost
Figure B.3	Figure B.3	Figure B.4

APPENDIX B

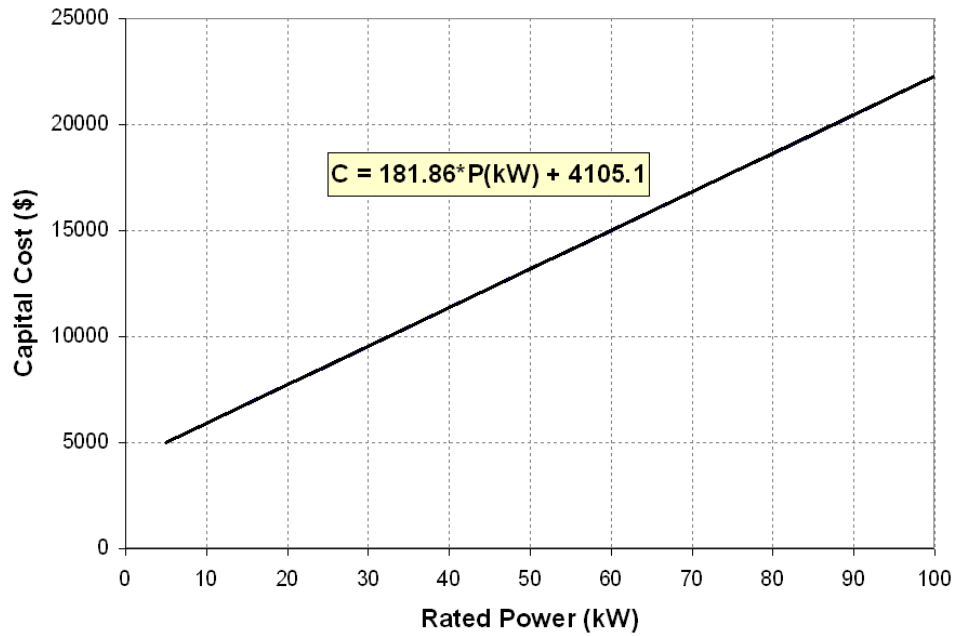


Figure B.3. Capital cost dependence on the size of the diesel generator

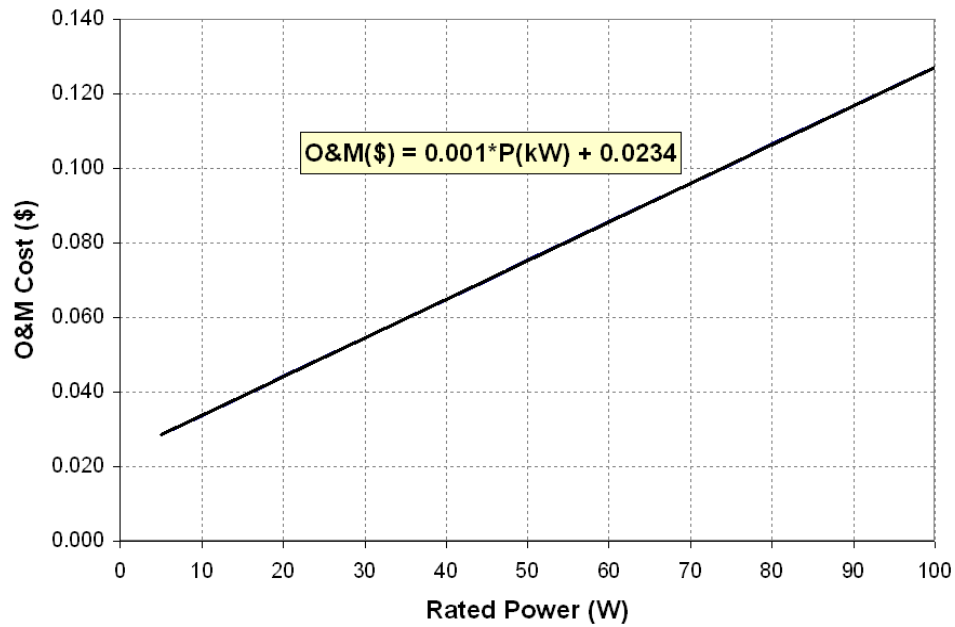


Figure B.4. O&M cost dependence on the size of the diesel generator

APPENDIX B

B.4 BATTERIES

Capital Cost (\$)	Replacement Cost (\$)	O&M Cost
626	626	10

B.5 INVERTER

Capital Cost (\$)	Replacement Cost (\$)	O&M Cost
Figure B.5	Figure B.5	0

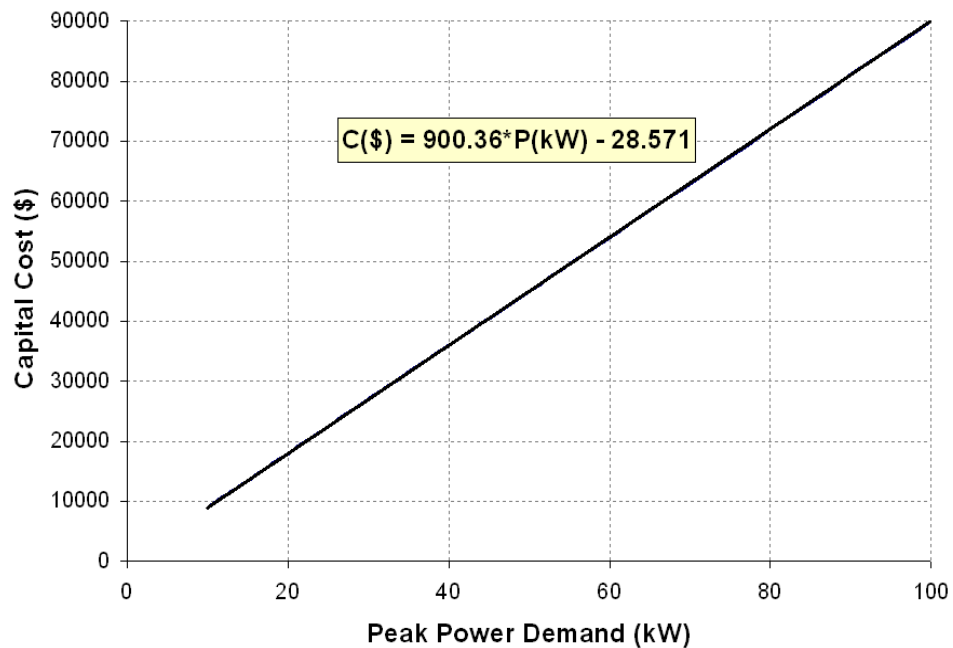


Figure B.5. Inverter's capital cost dependence on the peak electricity demand.

APPENDIX C

OPTIMIZATION RESULTS

APPENDIX C

- 10 kW Peak Electricity Demand

Insolation (kWh/m ² /day)	Windspeed (m/s)	10 kW Peak Demand						NPV (\$)	Initial Costs (\$)
		PV Panels Size (kW)	Number of Wind Turbines	Generator Size (kW)	Number of Batteries	Inverter Size (kW)			
4.5	4	11	4	5	16	11	296,578	110,099	
4.5	5	4	8	10	68	11	261,757	130,204	
4.5	6	0	8	10	54	11	219,010	106,094	
4.5	7	0	7	10	122	11	191,288	118,207	
4.5	8	0	7	10	84	11	167,601	106,313	
5.0	4	11	4	5	14	11	286,177	109,470	
5.0	5	12	7	5	88	11	255,867	164,918	
5.0	6	2	7	10	56	11	218,084	107,429	
5.0	7	0	7	10	122	11	191,288	118,207	
5.0	8	0	7	10	84	11	167,601	106,313	
5.5	4	12	3	5	14	11	275,930	105,074	
5.5	5	12	6	15	120	11	250,455	167,637	
5.5	6	4	6	10	60	11	217,351	109,322	
5.5	7	0	7	10	54	11	189,598	96,923	
5.5	8	0	7	10	84	11	167,601	106,313	
6.0	4	17	4	5	110	11	267,992	167,918	
6.0	5	14	5	5	92	11	237,051	157,326	
6.0	6	8	6	5	102	11	208,995	140,942	
6.0	7	5	6	5	82	11	185,204	120,127	
6.0	8	4	6	5	78	11	165,273	113,991	
6.5	4	19	2	5	110	11	256,603	158,917	
6.5	5	13	5	5	82	11	230,055	149,456	
6.5	6	10	5	10	76	11	207,078	134,223	
6.5	7	7	5	5	94	11	182,697	124,431	
6.5	8	4	5	5	84	11	163,491	106,698	

Figure C.5. Optimization results of the 10 kW peak electricity demand system.

APPENDIX C

- 20 kW Peak Electricity Demand

Insolation (kWh/m ² /day)	Windspeed (m/s)	20 kW peak demand						NPV (\$)	Initial Costs (\$)
		PV Panels Size (kW)	Number of Wind Turbines	Generator Size (kW)	Number of Batteries	Inverter Size (kW)			
4.5	5	6	13	15	28	22	474,163	184,063	
4.5	6	0	13	15	94	23	352,517	206,354	
4.5	7	0	13	15	94	23	352,517	176,178	
4.5	8	0	11	15	86	23	310,375	155,332	
5.0	4	24	6	10	22	22	526,923	201,996	
5.0	5	8	13	15	32	22	468,787	195,003	
5.0	6	1	13	15	38	22	409,601	162,697	
5.0	7	0	13	15	100	23	352,710	164,131	
5.0	8	0	11	15	86	23	310,375	155,332	
5.5	4	23	6	10	20	22	507,622	196,787	
5.5	5	16	10	10	22	22	456,486	201,571	
5.5	6	11	10	10	28	23	404,168	179,743	
5.5	7	0	14	25	92	23	361,995	186,542	
5.5	8	0	12	20	78	23	313,351	162,908	
6.0	4	23	5	10	18	20	490,677	189,990	
6.0	5	16	10	10	22	22	446,053	201,571	
6.0	6	11	11	10	30	22	396,477	189,540	
6.0	7	3	12	15	104	23	351,303	184,930	
6.0	8	0	11	15	86	23	310,375	155,332	
6.5	4	22	4	10	18	22	477,778	173,220	
6.5	5	18	9	10	102	22	446,406	226,812	
6.5	6	11	11	15	88	23	396,520	209,503	
6.5	7	6	15	15	82	23	348,748	183,523	
6.5	8	0	11	15	86	23	310,375	155,332	

Figure C.6. Optimization results of the 20 kW peak electricity demand system.

APPENDIX C

- 50 kW Peak Electricity Demand

50 kW peak demand

Insolation (kWh/m ² /day)	Windspeed (m/s)	PV Panels Size (kW)	Number of Wind Turbines	Generator Size (kW)	Number of Batteries	Inverter Size (kW)	NPV (\$)	Initial Costs (\$)
4.5	5	4	32	40	54	54	1,076,048	389,983
4.5	6	0	32	40	70	55	922,478	376,263
4.5	7	0	30	50	118	55	824,894	374,762
4.5	8	0	26	40	84	55	713,618	325,618
5.0	4	36	9	30	46	31	1,168,778	302,525
5.0	5	27	26	30	44	54	1,057,053	438,395
5.0	6	3	31	40	58	55	921,804	378,131
5.0	7	0	27	45	76	55	809,725	391,978
5.0	8	0	26	40	84	55	713,618	325,618
5.5	4	60	3	30	26	55	1,117,966	363,958
5.5	5	32	24	30	42	55	1,034,836	442,769
5.5	6	22	26	30	46	55	913,878	417,083
5.5	7	0	28	40	68	55	802,457	338,952
5.5	8	0	26	40	84	55	713,618	325,618
6.0	4	60	2	30	26	55	1,079,357	364,377
6.0	5	40	20	30	42	55	1,011,896	441,171
6.0	6	25	25	30	40	55	899,534	419,784
6.0	7	16	24	30	48	55	800,325	371,440
6.0	8	0	26	40	62	55	714,378	318,732
6.5	4	59	1	30	28	55	1,049,413	341,819
6.5	5	43	18	30	42	55	991,412	436,727
6.5	6	24	25	30	40	55	888,354	414,316
6.5	7	17	24	30	46	55	792,736	375,508
6.5	8	10	24	30	48	55	711,165	342,945

Figure C.7. Optimization results of the 50 kW peak electricity demand system..

APPENDIX C

- *100 kW Peak Electricity Demand*

Insolation (kWh/m ² /day)	Windspeed (m/s)	100 kW peak demand						NPV (\$)	Initial Costs (\$)
		PV Panels Size (kW)	Number of Wind Turbines	Generator Size (kW)	Number of Batteries	Inverter Size (kW)			
4.5	5	11	52	75	90	102	1,949,364	667,895	
4.5	6	0	56	80	104	110	1,695,946	663,782	
4.5	7	0	53	80	100	110	1,477,661	635,017	
4.5	8	0	49	75	96	110	1,314,265	596,172	
5.0	4	50	0	75	36	38	2,055,419	281,913	
5.0	5	44	46	65	76	102	1,944,826	756,088	
5.0	6	0	56	80	104	110	1,695,946	663,782	
5.0	7	0	53	80	100	110	1,477,661	635,702	
5.0	8	0	49	75	96	110	1,314,265	596,172	
5.5	4	72	1	65	42	57	2,008,528	125,414	
5.5	5	72	36	55	68	105	1,909,754	775,825	
5.5	6	37	47	65	78	110	1,693,353	742,883	
5.5	7	0	53	80	100	110	1,477,661	635,017	
5.5	8	0	49	75	96	110	1,314,265	596,172	
6.0	4	69	0	65	26	57	1,960,786	379,621	
6.0	5	84	34	55	64	108	1,856,815	803,597	
6.0	6	39	46	65	78	110	1,671,718	742,420	
6.0	7	0	53	80	100	110	1,477,661	635,017	
6.0	8	0	49	75	96	110	1,314,265	596,172	
6.5	4	118	2	55	62	110	1,890,141	625,498	
6.5	5	87	33	60	64	110	1,815,088	807,949	
6.5	6	48	45	60	64	110	1,650,403	769,493	
6.5	7	8	53	75	88	110	1,476,924	669,483	
6.5	8	0	49	75	96	110	1,314,265	596,172	

Figure C.8. Optimization results of the 100 kW peak electricity demand system.